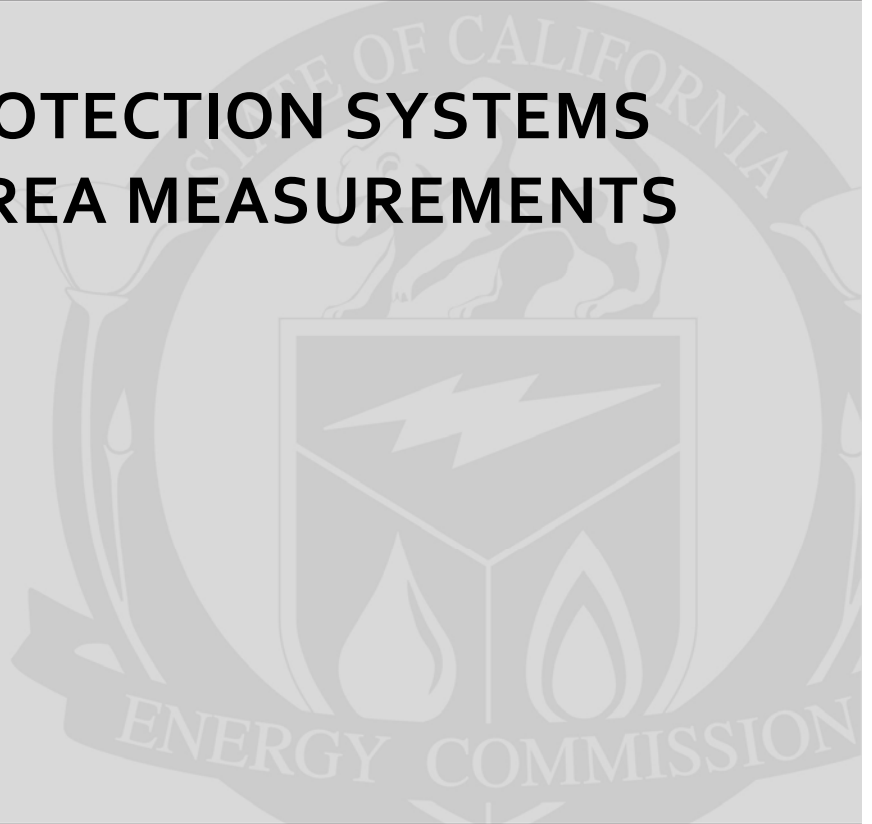


**Energy Research and Development Division
FINAL PROJECT REPORT**

**ADVANCED PROTECTION SYSTEMS
USING WIDE AREA MEASUREMENTS**



Prepared for: California Energy Commission
Prepared by: Virginia Polytechnic Institute and State University



SEPTEMBER 2010
CEC-500-2013-078

PREPARED BY:

Primary Author(s):

Virgilio Centeno
James Thorp
Arun Phadke

Virginia Polytechnic Institute and State University
302 Whittemore Hall
Blacksburg, VA 24061
www.vt.edu

Contract Number: 500-02-004

Prepared for:

California Energy Commission

Steve Ghadiri
Contract Manager

Fernando Pina
Office Manager
Energy Systems Research Office

Laurie ten Hope
Deputy Director
ENERGY RESEARCH AND DEVELOPMENT DIVISION

Robert P. Oglesby
Executive Director

DISCLAIMER

This report was prepared as the result of work sponsored by the California Energy Commission. It does not necessarily represent the views of the Energy Commission, its employees or the State of California. The Energy Commission, the State of California, its employees, contractors and subcontractors make no warranty, express or implied, and assume no legal liability for the information in this report; nor does any party represent that the uses of this information will not infringe upon privately owned rights. This report has not been approved or disapproved by the California Energy Commission nor has the California Energy Commission passed upon the accuracy or adequacy of the information in this report.

ACKNOWLEDGEMENTS

The research team would like to especially thank the California Energy Commission for funding this research project. The research team would also like to express its appreciation for the valuable guidance and advice received from Vahid Madani (PG&E) throughout this project. The team also acknowledges the support of Phil Overholt (DOE) for providing funding for the acquisition of the PSLF software. The input received from the other members of the advisory team: Bharat Bhargava (SCE), Farrokh Habibiashrafi (SCE), Damir Novosel (Quanta Technology), and Armando Salazar (SCE) was of great value for the successful completion of this project. This project report would have not been possible without the administrative guidance and patience of Larry Miller (CIEE).

PREFACE

The California Energy Commission Energy Research and Development Division supports public interest energy research and development that will help improve the quality of life in California by bringing environmentally safe, affordable, and reliable energy services and products to the marketplace.

The Energy Research and Development Division conducts public interest research, development, and demonstration (RD&D) projects to benefit California.

The Energy Research and Development Division strives to conduct the most promising public interest energy research by partnering with RD&D entities, including individuals, businesses, utilities, and public or private research institutions.

Energy Research and Development Division funding efforts are focused on the following RD&D program areas:

- Buildings End-Use Energy Efficiency
- Energy Innovations Small Grants
- Energy-Related Environmental Research
- Energy Systems Integration
- Environmentally Preferred Advanced Generation
- Industrial/Agricultural/Water End-Use Energy Efficiency
- Renewable Energy Technologies
- Transportation

Advanced Protection Systems using Wide Area Measurements is the final report for the Real-Time System Operations project (Contract Number 500-02-004 MR-054) conducted by Virginia Polytechnic Institute. The information from this project contributes to the Energy Research and Development Division's Transmission Program.

When the source of a table, figure or photo is not otherwise credited, it is the work of the author of the report.

For more information about the Energy Research and Development Division, please visit the Energy Commission's website at www.energy.ca.gov/research/ or contact the Energy Commission at 916-327-1551.

ABSTRACT

This project's goal was using a wide area measurement system to improve supervision of California's grid power protection system. A wide area measurement system consists of advanced measurement technology, information tools, and operational infrastructure that facilitate understanding and managing large power systems. A wide area measurement system can be used as stand-alone infrastructure that complements the grid's conventional supervisory control and data acquisition system. As a complementary system, a wide area measurement system is expressly designed to enhance the operator's real-time "situational awareness." Wide area measurement can also be a solution to grid stress through real-time, synchronous measurements of multiple remote measurement points on the grid.

This project developed three enhancement techniques for the California protection system – a system that protects electrical power systems from faults – that take advantage of wide area measurements. All three applications can enhance the protection system operation when wide area information is available and can revert to normal operation if a wide area measurement system is not operational.

The first technique determined where an insecure relaying operation would be detrimental to power system viability during stressed system conditions and where a relay-voting scheme would enhance the protection system's operation. The research team created a decision tree using wide area measurement at key locations to determine when the California system is in stressed conditions and the relay-voting scheme should be activated.

The second technique determined where wide area measurement data and the existing protection system database can be used to determine when the relay characteristics are in danger of being encroached upon during normal operation and where the wide area measurements could be used to alarm for these conditions.

The third technique determined the required location of wide area measurement devices and developed a technique for predicting the existence of out-of-step conditions using wide-area measurements.

Keywords: Wide area measurement, synchrophasor, adaptive protection, blackouts, transmission systems, smart grid, load encroachment, out-of-step relaying

Please use the following citation for this report:

Centeno, Virgilio, James Thorp, Arun Pahdke, Emanuel Bernabeu, Andrew Arana, Francisco Velez, Dawei Fan, Kate Vance. (Virginia Polytechnic Institute and State University). 2010. *Final Report Advanced Protection Systems Using Wide Area Measurements*. California Energy Commission. Publication number: CEC-500-2013-078.

TABLE OF CONTENTS

ACKNOWLEDGEMENTS	i
PREFACE	i
ABSTRACT	ii
TABLE OF CONTENTS.....	iii
LIST OF FIGURES	vii
LIST OF TABLES	viii
EXECUTIVE SUMMARY	1
Introduction	1
Project Purpose.....	1
Project Results.....	1
Project Benefits	2
CHAPTER 1: Introduction.....	3
1.1 Overall Technical Objective	3
1.2 Benefits of the Research.....	4
1.3 Relationship to PIER Goals	5
1.4 Goals of the Project	5
1.5 Background	5
1.5.1 First Task: Online Adjustment of Protection System’s Security-Dependability	6
1.5.2 Second Task: Real-Time Alarms for Encroachment of Relay Trip Characteristics	7
1.5.3 Third Task: Adaptive Out-of-Step Protection on Critical Tie-Lines	8
CHAPTER 2: Model Validation	10
2.1 Introduction	10
2.2 Model Translation.....	10
2.3 Initial Reduced Model	11
2.4 Validation of Initial Reduced Model	12
2.4.1 Steady State Analysis.....	12

2.4.2 Dynamic Analysis	15
2.4.2.1 Case 1. Malin – Round Mountain Fault	16
2.4.2.2 Case 2. Diablo Generation Drop	18
2.4.2.3 Case 3. Sunset G Generation Drop	20
2.5 Model Improvement.....	21
CHAPTER 3: Online Adjustment of the Protection System’s Security-Dependability Balance	25
3.1 Introduction	25
3.2 Relay Critical Locations.....	26
3.2.1 Determining the Location of Critical Relays	26
3.2.1.1 Static Index.....	27
3.2.1.2 The Dynamic Index.....	30
3.2.1.3 The Critical Locations.....	35
3.3 Adaptive Voting Scheme and PMU Locations	37
3.3.1 Methodology.....	37
3.3.2 Data Mining and PMU Placement.....	38
3.4 Performance Evaluation and Functional Specifications	40
3.4.1 Heavy Winter Model	40
3.4.2 Heavy Summer Model	41
3.4.3 Functional Specification	43
3.4.3.1 PMU Minimum Specification.....	44
3.4.3.2 Data Concentrator Specifications.....	45
3.4.3.3 Decision Computer Specifications.....	45
CHAPTER 4: Real-Time Alarms for Encroachment of Relay Trip Characteristics	46
4.1 Introduction	46
4.1.1 Determination of Critical Protection System Locations.....	46
4.1.2 Relay System Database.....	47
4.1.3 Wide Area Measurement-Based Critical Relay Condition Monitoring	47
4.1.4 Countermeasures	48

4.2	Relay-Critical Locations and Characteristics.....	48
4.2.1	Critical Locations for Real-Time Alarms for Encroachment of Relay Trip Characteristics	48
4.2.1.1	Static Index.....	49
4.2.1.2	The Dynamic Index.....	52
4.2.1.3	Critical Relay Locations.....	57
4.2.1.4	PMU Locations	58
4.2.2	Documentation of Relay Types and Characteristics to Be Included in Relay Database	58
4.2.2.1	Alarms of Distance Relays	59
4.2.2.2	Alarms of Loss-of-Excitation Relays.....	59
4.2.2.3	Alarms for Out-of-Step Relays	59
4.3	Relay Encroachment System	60
4.3.1	Introduction	60
4.3.2	Identifying Crucial Alarms	62
4.3.3	Determining Countermeasures for Alarms.....	63
4.3.4	Functional Operation.....	63
4.3.4.1	PMU Minimum Specification	64
4.3.4.2	Data Concentrator Specifications.....	64
4.3.4.3	Encroachment Alarm Computer Specifications	65
CHAPTER 5: Adaptive Out-of-Step Protection on Critical Tie-Lines		66
5.1	Introduction	66
5.1.1	Traditional Out-of-Step Relays	66
5.1.2	Problems With Traditional Out-of-Step Relays	67
5.1.3	Selection of Study System Base Case.....	67
5.1.4	Determination of Coherent Groups of Machine	68
5.1.5	Predicting the Out-of-Step Condition From Real-Time Data	68
5.2	Adaptive Out-of-Step Protection	68
5.2.1	Introduction	68
5.2.2	List of PMU Location for Observing Rotor Angle Swings.....	68

5.2.2.1 Simulations.....	69
5.2.2.2 Critical Cases	69
5.2.2.3 Critical Cases Discussions.....	69
5.2.3 PMU Location List	71
5.2.4 Additional PMU Angle Issues.....	71
5.2.4.1 Voltage Angle “UNWRAPPING”	72
5.2.4.2 Rotor Angles and PMU Voltage Angle.....	73
5.2.5 Proposed Techniques for Determining Machine Coherency.....	74
5.2.6 Techniques for Performing Swing Prediction Algorithms With PMU Data	78
5.2.6.1 Autoregressive Model Order 3 – AR(3)	78
5.2.6.2 Considerations.....	79
5.2.7 Tripping Decisions.....	79
5.2.7.1 PG&E-SCE Tripping Decision.....	80
5.3 Performance Evaluation and Functional Specifications	80
5.3.1 Performance Evaluation.....	80
5.3.1.1 Unstable Cases.....	81
5.3.1.2 Stable Cases.....	84
5.3.2 Functional Specifications	85
5.3.2.1 PMU Minimum Specification	86
5.3.2.2 Data Concentrator Specifications.....	88
5.3.2.3 Out-of-Step Computer Specifications.....	88
CHAPTER 6: Conclusions	90
6.1 Model Validation	90
6.2 Online Adjustment of the Protection System’s Security-Dependability Balance	91
6.3 Real-Time Alarms for Encroachment of Relay Trip Characteristics.....	92
6.4 Adaptive Out-of-Step Protection on Critical Tie-Lines	94
APPENDIX A: Detailed Decision Trees for the Heavy Winter and Heavy Summer Cases	A-1
APPENDIX B: Simulation Cases.....	B-1
APPENDIX C: Rankings Using ISGA.....	C-1

LIST OF FIGURES

Figure 1.1: Adjustment of Dependability-Security Balance Under Stressed System Conditions....	6
Figure 1.2: Traditional Out-of-Step Relay Parameters Using Reactance Type Relays and Timers.	8
Figure 2.1: One Machine Equivalent of WECC System	11
Figure 2.2: WECC Model – Malin Bus.....	16
Figure 2.3: California Model – Malin Bus.....	17
Figure 2.4: Voltage Plot Comparison for Case 1	17
Figure 2.5: WECC and Californian Model – Diablo	18
Figure 2.6: Frequency Plots Comparison for Case 2	19
Figure 2.7: Voltage Magnitude Plots Comparison for Case 2.....	20
Figure 2.8: Voltage Magnitude Plots Comparison for Case 2.....	21
Figure 2.9: Two Machine Equivalent Non-California WECC System	21
Figure 2.10: Comparative Voltage Responses for the Sunset Generation Drop Case	22
Figure 2.11: Comparative Frequency Responses for the Sunset Generation Drop Case	23
Figure 2.12: Comparative Voltage Responses for the Table Mt-Vaca Dixon Line Trip	23
Figure 2.13: Comparative Frequency Response for the Table Mt-Vaca Dixon Line Trip	24
Figure 3.1: Adjustment of Dependability-Security Balance Under Stressed System Conditions..	26
Figure 3.2: Methodology to Identify the Critical Locations of the Power System	27
Figure 3.3: Static Index Flow Diagram	27
Figure 3.4: Sample Hidden Failure and Regions of Vulnerability	28
Figure 3.5: Flow Diagram of the Dynamic Index	30
Figure 3.6: Generator Rotor Angles of Study Case 350 – ISGA Score: 6721.....	33
Figure 3.7: Generator Rotor Angles of Study Case Number 237 – ISGA Score: 4316.....	33
Figure 3.8: Generator Rotor Angles of Study Case Number 269 – ISGA Score: 9.76.....	34
Figure 3.9: Generator Rotor Angles of Study Case Number 115 – ISGA Score: 7.72.....	34
Figure 3.10: Schematic: 500 Kv Buses and Lines in California.....	35
Figure 3.11: Methodology to Develop the Voting Scheme.....	37
Figure 3.12: Sample Data Input to CART Data Mining Software	38
Figure 3.13: CART First Splitting Node	39
Figure 3.14: Decision Tree Schematic	39
Figure 3.15: Functional Overview of the Security – Dependability Adaptive Scheme	43
Figure 4.1: Methodology to Identify the Critical Locations of the Power System	48
Figure 4.2: Static Index Flow Diagram	49
Figure 4.3: Sample Hidden Failure and Regions of Vulnerability	50
Figure 4.4: Flow Diagram of the Dynamic Index	52
Figure 4.5: Generator Rotor Angles of Study Case Number 350. ISGA Score: 6721.....	55
Figure 4.6: Generator Rotor Angles of Study Case Number 237. ISGA Score: 4316.....	55
Figure 4.7: Generator Rotor Angles of Study Case Number 269. ISGA Score: 9.76.....	56

Figure 4.8: Generator Rotor Angles of Study Case Number 115. ISGA Score: 7.72.....	56
Figure 4.9: Schematic: 500 kV Buses and Lines in California.....	57
Figure 4.10: Diagram of Protective Devices on Path 15 and Path 26	58
Figure 4.11: OOS Swing at Captain Jack – Olinda.....	61
Figure 4.12: OOS Swing at Captain Jack – Olinda with Maxwell - Tracy Out-of-Service	62
Figure 4.13: Functional Overview of the Real-Time Alarms for Encroachment Scheme.....	64
Figure 5.1: Traditional Out-of-Step Relay.....	66
Figure 5.2: Rotor Angles for Breaker Failure at Vincent 500kv	70
Figure 5.3: a) Rotor Angles for Area 30 b) Rotor Angles for Southern California	70
Figure 5.4: Wrapped Voltage Angle Due to Frequency Deviation	71
Figure 5.5: a) Sample Wrapped Angle Plot b) Sample Unwrapped Angle Plot	72
Figure 5.6: a) Rotor Angles, Lugo Breaker Failure b) Color-Coded Coherent Groups for Same Failure	73
Figure 5.7: a) Wrapped PMU Voltage Angles b) Unwrapped PMU Voltage Angles	74
Figure 5.8: Flow Chart of Proposed Coherency Identification Algorithm.....	76
Figure 5.9: Growing Window Sample.....	77
Figure 5.10: Sliding Window Sample. Window size 0.5 Seconds	77
Figure 5.11: Swing Determination Points	84
Figure 5.12: Swing Detection Algorithm for Stable Case 10	84
Figure 5.13: Swing Detection Algorithm for Stable Case 11	85
Figure 5.14: Functional Overview of the Adaptive Out-of-Step Scheme	86
Figure 5.15: a) Wrapped Angle at 240 b) Unwrapped Angle at 240 Samples/Sec Samples/Sec.....	87
Figure 5.16: A) Wrapped Angle at 12 Samples/Sec. B) Unwrapped Angle at 12 Samples/Sec	87
Figure 5.17: A) Wrapped Angle at 30 Samples/Sec. B) Unwrapped Angle at 30 Samples/Sec.....	88
Figure A.1: Selected Decision Tree for Heavy Winter Model. Misclassification Rate = 0.99% ...	A-1
Figure A.2: Decision Tree for Heavy Summer Model.....	A-2

LIST OF TABLES

Table 2.1: Initial Conditions at Path 15 Buses	13
Table 2.2: Malin – Round Mountain #2 Line Trip.....	13
Table 2.3: Generation Drop at Diablo (1150 MW)	14
Table 2.4: Generation Drop at Sunset G (225 MW)	14
Table 2.5: Tesla – Los Banos 500kV Line Trip	15
Table 3.1: List of Cases Derived for Figure 3.4.....	29
Table 3.2: Static Index Settings	30
Table 3.3: ISGA Score of Four Different Cases.....	32
Table 3.4: The Critical Locations (Path 15 and Path 26).....	36
Table 3.5: PMU Placement for the Adaptive Relay Scheme.....	40

Table 3.6: Out of Sample Test: Generator Outage	41
Table 3.7: Out of Sample Test: Load Outage	41
Table 3.8: Out of Sample Test: 230 kV Lines Outage.....	41
Table 3.9: Out of Sample test: 500 kV Lines.....	41
Table 3.10: Heavy Summer Out-of-Sample Test: Generator Outage	42
Table 3.11: Heavy Summer Out-of-Sample Test: Load Outage.....	42
Table 3.12: Heavy Summer Out-of-Sample Test: 230 kV Lines Outage	42
Table 3.13: Heavy Summer Out-of-Sample Test: 500 kV Lines	42
Table 3.14: Splitting Attributes of the Heavy Winter Decision Tree.....	44
Table 3.15: List of Surrogates for Heavy Winter Case	44
Table 3.16: Splitting Attributes of the Heavy Summer Decision Tree.....	44
Table 3.17: List of Surrogates for the Heavy Summer Case	45
 Table 4.1: List of Cases Derived for Figure 4.3.....	 50
Table 4.2: Static Index Settings	51
Table 4. 3: ISGA Score of Four Different Cases.....	54
 Table 5.1: Summary of Performance Evaluation	 83
 Table B.1: Simulation Cases on Paths 15 and 26	 B-1
 Table C.1: Set of acses Studied With the Dynamic Index	 C-1
Table C.2: Ranking of Cases Along Path 15 and 26 Using the ISGA	C-6
 Table D.1: List of Buses of Base System Model for Adaptive Protection	 D-1

EXECUTIVE SUMMARY

Introduction

Recent system blackouts throughout the world have shown how critical a reliable power system is to modern societies. They have also demonstrated the enormous economic and societal damage that a major blackout can cause. These unexpected system failures occur when power protection systems – systems that deal with protecting electrical power systems from faults – operate in an unanticipated fashion. In recent years, innovations in power protection systems have led to new approaches for protection systems supervision. These approaches can reduce the likelihood of catastrophic failures in the power grid and limit the regions of the power system affected by such events. They can also improve the speed of power system restoration.

This research project analyzed, developed, and evaluated power protection technologies in California. A phasor measurement unit (PMU), or synchrophasor, is one such technology. This device measures the electrical waves on an electricity grid using a common time source for synchronization. Time synchronization allows for synchronized real-time measurements of multiple remote measurement points on the grid. Synchrophasors therefore provide real-time information about the performance of electrical transmission systems. The protection systems can be modified in real time based on the state of the power system variables information through monitoring and supervision. Synchrophasors are considered one of the most important power engineering measuring devices for future power systems.

Project Purpose

The goal of this project was to use real-time synchronized phasor measurement data to improve power protection system supervision. This project used a wide area measure system (WAMS), which consists of advanced measurement technology, information tools, and operational infrastructure that facilitate understanding and managing the increasingly complex behavior of large power systems. In its present form, a WAMS can be used as stand-alone infrastructure that complements the grid's conventional supervisory control and data acquisition (SCADA) system. As a complementary system, a WAMS is expressly designed to enhance the operator's real-time "situational awareness." By using real-time wide area measurements, protection system planners can determine the best protection measures and settings for critically located relaying systems, which are designed to calculate operating conditions on an electrical circuit and trip circuit breakers when a fault is detected. The project also focused on developing and evaluating the operational performance of protection system enhancement tools to meet California Independent System Operator (CAISO) specifications. This effort was conducted in close cooperation with the California Independent System Operator (CAISO), Pacific Gas and Electric (PG&E), and Southern California Edison (SCE).

Project Results

The research team developed a wide area measurement-based decision tree to determine when the system was in stressed conditions. It also developed a method for using real-time wide area measurement data and the existing protection system database to determine which of the relay characteristics were in danger of being encroached upon during a catastrophic event. In

addition, this project implemented a wide-area measurements technique that provided a more appropriate out-of-step decision process in the power system. A group of generators going “out of step” with the rest of the power system often leads to a complete system collapse. Whether the system will be stable or unstable must be determined before appropriate control actions can be taken to bring the power system to a steady state. Out-of-step relays perform this detection and take appropriate tripping and blocking decisions to keep the system stable.

This research showed that correct assessments of the prevailing power system state can reduce the likelihood of false protection systems trips. In addition, the protection systems can adapt and adjust during stressed conditions, becoming more secure. Finally, this research showed that intelligent relaying systems at key California power facilities will enhance the power protection system. Specifically, intelligent relaying systems can help show where maintenance and calibration checks are needed in the system as well as improve power transfer capabilities.

Project Benefits

This project helped meet the California Energy Commission Public Interest Energy Research (PIER) goals of improving the reliability, quality, and energy cost/value of California’s electricity.

CHAPTER 1:

Introduction

The 2003 blackout in North America and other recent system blackouts throughout the world have shown how critical a reliable power system is to modern societies, and the enormous economic and societal damage a blackout can cause. It has been noted that during the cascading phenomena which lead to blackouts, some protection systems operate in an unanticipated fashion and such operations are often an important contributing factor in the sequence of events leading to cascading outages. Considering the very large number of relaying systems in existence (by a rough estimate over 5 million on the North American Power Grid), it is to be expected that some of these unanticipated operations are due to defective relays. This has been documented as “the hidden-failure phenomenon in protection systems”. Other contributing factors to catastrophic failures are unexpected power system configurations which have not been foreseen when protection systems were set, errors in setting and calibration of relays, or undiscovered design flaws in the protection systems.

In recent years, innovations in the field of power system protection, power system operation and power system devices have made possible new proactive approaches to the supervision of protection systems so that the likelihood of catastrophic failures of the power grid are significantly reduced, the regions of the power system affected by such events are limited, and the power system restoration process can be sped up. This project aim was to research, develop and evaluate the use of these technologies in the California system to monitor, supervise, and modify the protection systems in real-time based upon the information about the state of the power system provided by the phasor measurements. Three aspects of the protection system supervision and control were selected for research, because they address principal concerns regarding protection system responses, and are inter-related and complementary in their scope. Such measures are within the capabilities of technology available today, and when successfully applied can reduce the frequency and intensity of power system blackouts.

This R&D effort was conducted in close cooperation with PG&E, CAISO and SCE. The study system selected was from the California power grid, and the results of the research is aimed to provide proofs-of-concept of the proposed project, as well as complete functional specifications for implementing these ideas on the California system. It is expected that when fully tested by the utilities the results of the research can be directly integrated into the Energy Management Systems of the California Utilities.

1.1 Overall Technical Objective

The technical objective of this project was to use real-time synchronized phasor measurement data to provide improved protection system supervision to make it adaptive to prevailing system state. By using real-time wide area measurements, it is possible to determine optimum protection policies and settings for critically located relaying systems. In particular, adaptive

adjustment of dependability and security, alarming on potential load encroachment, and more intelligent out-of-step relaying tasks will be developed.

This three year Research Development and Demonstration (RD&D) project aimed to:

- Determine key locations on the California electric power system where an insecure relaying operation during stressed system conditions would be detrimental to the viability of the power system.
- Develop a method for using real-time wide area measurement data and the existing protection system data base to determine which of the relay characteristics are in danger of being encroached upon during a catastrophic event and to develop appropriate countermeasures.
- Improve existing out-of-step relay operations. Out-of-step relays are traditionally set based upon transient stability studies performed for assumed base case and contingency conditions. However, in practice the power system is quite different from that assumed in the base case, and the actual complex sequence of events which occurs is often not considered in the study phase. At key locations on the California grid where out-of-step blocking and tripping functions are utilized, the technique developed in this project use wide-area measurements to provide a more appropriate out-of-step decision.

The project was carried out in close cooperation with protection engineers from PG&E and SCE. The system models, relay system data, and representative contingencies considered were developed with the help and close interaction of the utility engineers.

1.2 Benefits of the Research

The principal achievements of this research are to reduce the likelihood of false trips by protection systems based upon a correct assessment of the prevailing power system state. The three areas where benefits were achieved with are:

- Adaptive adjustment of protection systems to become more secure during stressed system conditions,
- On-line estimation of vulnerability of relay characteristics to prevailing loads, swings or other system conditions, and
- Intelligent out-of-step relaying at key facilities.

In addition, by providing real-time assessment of relay settings vis-à-vis the prevailing system conditions it is possible to pin-point where maintenance and calibration checks are needed and thus eliminate the need for extensive engineering reviews of relay settings for the entire system. Also, since out-of-step conditions were assessed based upon actual prevailing system conditions, the possibility of improved power transfer capability exists where previously calculated limits to transfer capability were based upon pre-calculated instability limits of the system.

1.3 Relationship to PIER Goals

This project meets the following PIER Goals:

- Improving the reliability and quality of California's electricity, and
- Improving the energy cost/value of California's electricity.

1.4 Goals of the Project

The goals of this Work Authorization are to:

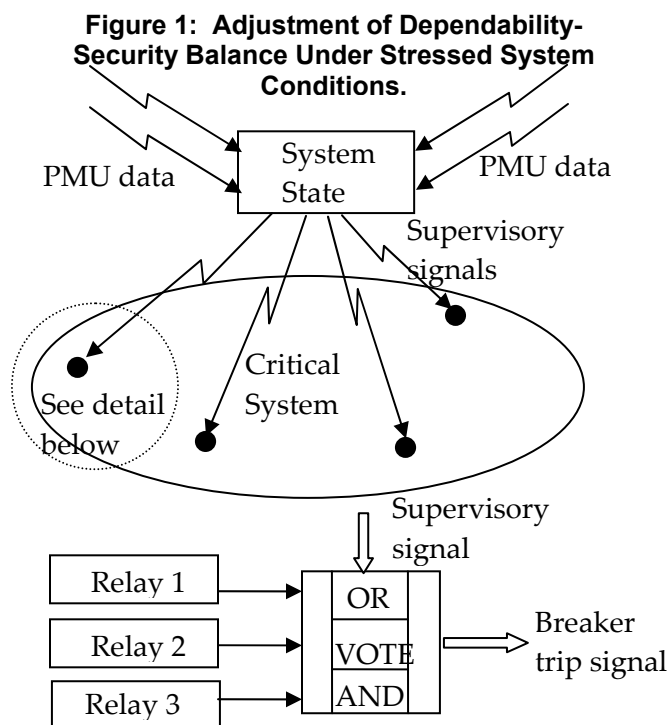
- Develop and evaluate the operational performance of these 3 protection system enhancement tools to meet California Independent System Operator (CA ISO) specifications,
- Initiate the transfer of these prototypes to a CAISO vendor for implementation as production-grade operating tools, and
- Communicate research results to PG&E, CAISO and other entities involved in TRP program.

1.5 Background

The modern wide area measurement system is based upon synchronized phasor measurements which provide time-tagged positive sequence voltage and current data from selected system buses and lines where phasor measurement units (PMUs) have been installed. This technology, pioneered by the research team at Virginia Tech, has seen wide-scale acceptance throughout the world as the measurement system of choice for improved protection, monitoring, and control of power systems. Virginia Tech was also been a leader in developing the concept of 'Adaptive Relaying'. This concept seeks to adjust protection system characteristics automatically to make it more attuned to the prevailing power system state. There are many protection system characteristics which are selected based upon assumed power system state, and as the system undergoes changes, particularly during catastrophic events, the protection system settings are often inappropriate. This leads to over-trips, often contributing to cascading phenomena which may lead to system islanding and blackouts.

This research project identified three protection systems tasks which would benefit from the use of real time wide area measurements to make the protection system adapt to the prevailing power system state. A detailed plan was created and implemented to organize these research projects with close cooperation with participating California Utilities to formulate, test, and demonstrate the efficacy of these ideas on practical utility systems. Each project was organized in three stages of approximately one year duration to facilitate smooth conduct of the work at Virginia Tech with close oversight by the TAG appointed by the Project Manager at PIER. The TAG team was made up of engineers from California Utilities, such as PG&E and SCE.

1.5.1 First Task: Online Adjustment of Protection System's Security-Dependability



Source: VA Tech, 2010

The existing protection system was designed to be dependable at the cost of somewhat reduced security. It should be recognized that a relay has two failure modes. It can trip when it should not trip (a false trip) or it can fail to trip when it should trip. The two types of reliability have been designated as “security” and “dependability” by protection engineers. Dependability is defined as the measure of the certainty that the relays will operate correctly for all faults for which they are designed to operate, while security is the measure of the certainty that the relays will not operate incorrectly. The existing protection systems with their multiple zones of protection and redundant systems are biased toward dependability, for example, a fault is always cleared by some relays. There are typically multiple

primary protection systems often relying on different principles (one might depend on communications while another uses only local information) and multiple backup systems that trip (with some time delay) if all primary systems fail to trip. The result is a system that virtually always clears the fault but as a consequence permits larger numbers of false trips. High dependability is recognized as being a desirable protection principle when the power system is in a normal “healthy” state, and high speed fault clearing is highly desirable to avoid instabilities in the network. The consequent price paid in occasional false trip is an acceptable risk under “system normal” conditions. However, when the system is highly stressed false trips exacerbate disturbances and lead to cascading events.

An attractive solution is to “adapt” the security - dependability balance in response to changing system conditions as determined by real-time phasor measurements. The concept of “Adaptive Relaying” accepts that relays may need to change their characteristics to suit the prevailing power system conditions. With the advent of digital relays the concept of responding to system changes took on a new dimension. Digital relays have two important characteristics that make them vital to the adaptive relaying concept. Their functions are determined through software and they have a communication capability, which can be used to alter the software in response to higher-level supervisory software or under the commands from a remote control center.

The ability to change a relay characteristic or setting, on the fly, as it were, raised serious questions about reliability and responsibility. Adaptive relaying with digital relays was

introduced on a major scale in 1987 [1-2]. One of the driving forces that led to the introduction of adaptive relaying was the change in the power industry wherein the margins of operation were being reduced due to environmental and economic restraints and the emphasis on operation for economic advantage.

With three primary digital protection systems it is possible to implement an adaptive security – dependability scheme by using voting logic. (See Figure 1.1) The conventional arrangement is that if any of the three relays sees a fault then the breaker is tripped. A more secure decision would be made by requiring that two of the three relays see a fault before the trip signal is sent to the breaker. The benefit is in avoiding cascading and creating a more reliable system. The price paid for this increased security under “stressed” system conditions is that there is a somewhat reduced dependability, which is acceptable. The advantage of the adaptive voting scheme is that the actual relays are not modified but only the tripping logic responds to system conditions.

1.5.2 Second Task: Real-Time Alarms for Encroachment of Relay Trip Characteristics

One of the lessons learned from a study of past blackouts is that many relays have settings which, when originally specified, were appropriate for all assumed system conditions and contingencies but which, because of the changes in power system conditions over the years are no longer viable. Some examples of such settings which depend upon assumed system conditions are back-up zones of distance relays, certain overcurrent relays, out-of-step relays and loss-of-field relays. Consider the loadability of a back-up zone of a distance relay. When it is set, it is checked for adequacy for assumed peak loading conditions, credible contingencies, and certain failure modes of the primary relaying system. As power systems change in time, it is not always possible to revise the relay settings either because of a manpower shortage, or due to oversight on the part of the protection engineer. Some system changes may be a result of unforeseen contingencies which depress system voltages beyond normal expectations. In any case, as system conditions change, a setting once thought to be safe is actually being encroached upon by prevailing loading and voltage conditions. Since these are quasi-steady-state phenomena, if they lead to an encroachment of the relay trip characteristic they would lead to an inappropriate trip of the relay and may well start a cascading process. Indeed, the catastrophic blackout of 1965 in eastern North America was precipitated by exactly such an event.

Although hidden failures in protection systems have been identified as contributing factors to cascading phenomena, the scenario considered in this research project does not depend upon there being a hidden failure. Indeed, the emphasis here is on normally functioning relays, whose settings are inappropriate for prevailing system conditions, and unless corrective actions are taken, would increase the probability of cascading outages if a triggering event (such as a natural fault) occurred.

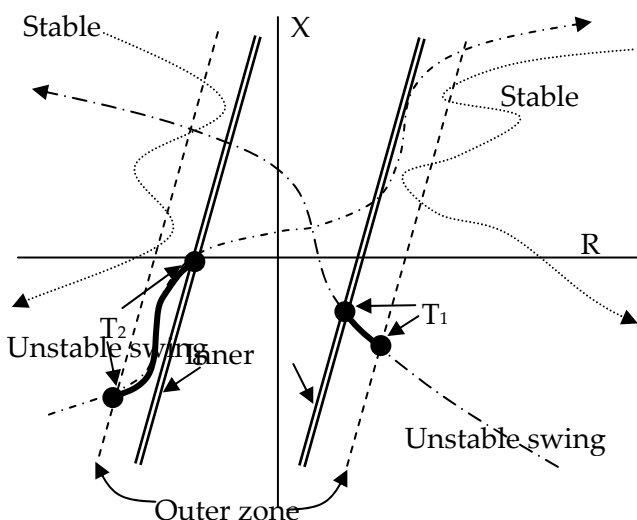
1.5.3 Third Task: Adaptive Out-of-Step Protection on Critical Tie-Lines

It is recognized that a group of generators going out of step with the rest of the power system is often a precursor of a complete system collapse. Whether an electromechanical transient will lead to stable or unstable condition has to be determined reliably before appropriate control action could be taken to bring the power system to a viable steady state. Out-of-step relays are designed to perform this detection and also to take appropriate tripping and blocking decisions.

Traditional out-of-step relays use impedance relay zones to determine whether or not an electromechanical swing will lead to instability. A brief description of these relays and the procedure for determining their settings is provided here.

In order to determine the settings of these relays it is necessary to run a large number of transient stability simulations for various loading conditions and credible contingencies. Using the apparent impedance trajectories observed at locations near the electrical center of the system during these simulation studies, two zones of an impedance relay are set, so that the inner zone

Figure 2: Traditional Out-of-Step Relay Parameters Using Reactance Type Relays and Timers.



Source: VA Tech, 2010

is not penetrated by any stable swing. This is illustrated in the following figure (which uses reactance type of relay characteristics).

The outer zone is shown by a dashed line, and the inner zone is shown by a double line. Note that all the stable swing trajectories (shown by dotted lines) remain outside the inner zone, while all the unstable swing trajectories penetrate the outer as well as the inner zone. Although only two impedance characteristics are shown for stable and unstable cases, in reality a large number of such impedance loci must be examined. The time duration for which the unstable swings dwell between the outer and inner zones are identified as T_1

and T_2 for the two unstable characteristics shown in Figure 1.2. The largest of these dwell times (with an added margin) is chosen as the timer setting for the out-of-step relay. If an actual observed impedance locus penetrates the outer zone, but does not penetrate the inner zone before the timer expires, the swing is declared to be a stable swing. If it penetrates the outer zone and then the inner zone before the timer runs out, it is an unstable swing. Stable swings do not require any control action, whereas unstable swings usually lead to out-of-step blocking and tripping actions at pre-determined locations.

Traditional out-of-step relays are found to be unsatisfactory in highly interconnected power networks. This is because the conditions assumed when the relay characteristics are determined become out-of-date rather quickly, and in reality the electromechanical swings that do occur are quite different from those studied when the relays are set. The result is that traditional out-of-

step relays often misoperate: they fail to determine correctly whether or not an evolving electromechanical swing is stable or unstable. Consequently their control actions also are often erroneous, exacerbating the evolving cascading phenomena and perhaps leading to an even greater catastrophe.

Wide area measurements of positive sequence voltages at networks (and hence swing angles) provide a direct path to determining stability using real-time data instead of using pre-calculated relay settings. This problem is very difficult to solve in a completely general case. However, progress could be made towards an out-of-step relay which adapts itself to changing system conditions. Angular swings could be observed directly, and time-series expansions could be used to predict the outcome of an evolving swing. It is highly desirable to develop this technique initially for known points of separation in the system. This is often known from past experience, and use should be made of this information. In time, as experience with this first version of the adaptive out-of-step relay is gained, more complex system structures with unknown paths of separation could be tackled. It should be noted that a related approach was developed for a field trial at the Florida-Georgia interface. [3]

CHAPTER 2:

Model Validation

2.1 Introduction

The objective of Task 2.1 was to validate the system model to be used in developing an adaptive protection system which balances security and dependability in critical segments of the California power grid as it responds to changing system conditions. The system conditions were determined by real-time phasor measurements thus aiding in consistent power delivery. In order to achieve this goal, a model of the California system needed to be created and tested. Model validation for power systems is normally accomplished by comparing the model's outputs to real measurements of system events. For this research, a model containing only generation facilities physically located in California (the *reduced* model) was derived and then validated against the WECC full system model. Because there were no exact measurements of operating conditions and only a limited number of captured events exist, comparing the outputs of the two models was more useful than comparing the reduced model to inadequate real system data. The WECC and the West Coast Independent System Operators (ISOs) and transmission planners collaborated to create the full WECC model. This model consisted of 15,353 buses and 128.63 GW of load.

2.2 Model Translation

The original proposal for this research required the translation of the California model from the General Electric (GE) Positive Sequence Load Flow (PSLF) software format used by the WECC utilities to the Power Technology Incorporated (PTI) Power System Simulation for Engineering (PSSE) format required by Virginia Tech. Initial testing of the new data revealed that the translated steady-state model produced similar results, but the dynamic data could not be accurately translated from GE-PSLF to PTI-PSSE format.

PG&E provided a system model in the GE-PSLF version 13.0 format. In order to translate the WECC model data to PSSE format, Virginia Tech used the standard commercial program package made by PTI. When the translating package was applied to the steady-state model, it was translated and verified easily. However, the program produced errors claiming there were "unrecognizable dynamic models" when trying to translate the dynamic model. Further review of the translated dynamic model revealed severe inaccuracies.

After Virginia Tech, PG&E and PSSE attempted translating the model unsuccessfully, it was determined that the effort required to produce an accurate model translation was beyond the scope of the project. On the advice of the TAG team, Virginia Tech requested additional funding from the CIEE to acquire the GE-PSLF software and to train three students with the software.

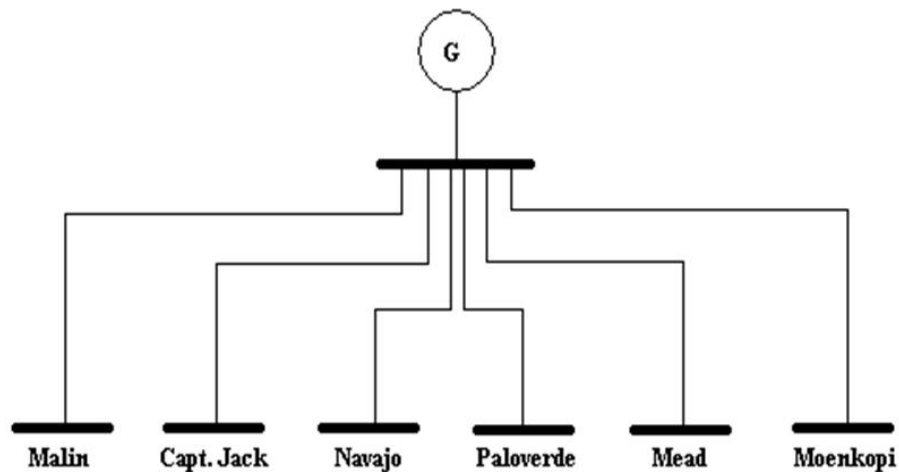
Funding for the acquisition of the software and the student training was approved in the summer of 2008. By the end of fall of 2008, the students were trained and had converted and

validated the California model in the heavy winter case. This report presents the procedures and results of the validation process.

2.3 Initial Reduced Model

The reduced California model was based on the 2007 heavy winter WECC full loop model. The aim of the reduced model was to have the system model inside California identical to the full loop WECC model while the area outside of California was replaced with equivalents. The initial California model tested by Virginia Tech consisted of 2,345 buses and 27.75 GW of load, with most busses less than 115 kV replaced with equivalent loads. These six interties to California, see Figure 2.1, were chosen for the reduced model because they had the lines with the largest power flows in the full model. There were additional lines between California and the rest of the WECC system but they had lower operating voltages and carried significantly less power. These other interconnections were modeled as generators in the load flow and as constant power loads or injections for dynamic simulations.

Figure 3: One Machine Equivalent of WECC System



Source: VA Tech, 2010

The equivalent generator was sized to have its inertia constant, H, equal to the weighted sum of the inertias of all the machines in the WECC outside California equation (2.1.)

$$H_{system} = \frac{J_{system} \omega_0^2}{2 \sum S_{base}} \quad (2.1)$$

$$\text{Where } J_{system} = \frac{2 \sum_{all_i} H_i S_{base_i}}{\omega_0^2} \quad \text{and} \quad S_{system} = \sum_{all_i} S_{base}$$

The values obtained for the model are: H = 3.77 seconds, J = 11,376,000 kg-m², and S = 214,169 megaVoltAmps (MVA).

In the first reduced model, inaccuracies were introduced by the equivalent generators. However, comparisons of steady state results obtained during the validation indicated that the model was sufficiently accurate for use in the development of the adaptive on-line adjustment of the protection system's security-dependability balance. This meant that the steady state calculations verified that reduced model met the specifications of Task 2. Unfortunately, the dynamic validations showed that the voltage the California model experienced higher transient deviations and oscillations. In addition, the system frequency returned to 60 Hz very quickly which is unrealistic for major power outages. These dynamic inconsistencies made the model invalid for the other tasks on this project and led to improvements on the reduced model.

2.4 Validation of Initial Reduced Model

2.4.1 Steady State Analysis

Steady state operation was validated by comparing the load flow results of the reduced model and the full WECC model. The Virginia Tech team expected that the load flow for the reduced model should be accurate since neighboring systems and low voltage buses were carefully replaced with equivalent generators or loads. However, differences arose in the cases where static loads were replaced with generators and vice versa. In addition, load tap changers and static Volt-Amp Reactive (VAR) devices which were automatically adjusted when solving the load flow in the full model may not even exist in the reduced model. Their absence caused a discrepancy because those devices would automatically adjust the power flow in the full model.

As recommended by the TAG team, Path 15 was chosen for system validation for adaptive protection. The tables below compare the voltage and bus angle at Path 15 buses after different disturbances. Malin was used as the swing bus for both models. All of the monitored buses had an operating voltage of 500kV.

Table 2.1: Initial Conditions at Path 15 Buses

	Voltage		Angle	
	CA	WECC	CA	WECC
Round Mountain	1.0774	1.0776	11.20	11.27
Table Mountain	1.0708	1.0710	7.82	7.92
Vaca-Dixon	1.0723	1.0724	1.93	2.07
Tesla	1.0697	1.0698	-0.28	-0.13
Metcalf	1.0663	1.0663	-4.65	-4.50
Moss Landing	1.0719	1.0719	-4.38	-4.23
Los Banos	1.0835	1.0835	-3.61	-3.45
Gates	1.0931	1.0931	-4.39	-4.24
Diablo Canyon	1.0612	1.0612	2.17	2.32
Midway	1.0856	1.0856	-6.02	-5.86
Malin	1.0800	1.0800	15.71	15.71

Source: VA Tech, 2010

Table 2.2: Malin – Round Mountain #2 Line Trip

	Voltage		Angle	
	CA	WECC	CA	WECC
Round Mountain	1.0767	1.0773	7.72	7.93
Table Mountain	1.0709	1.0716	4.6	4.87
Vaca-Dixon	1.0722	1.0728	-0.97	-0.63
Tesla	1.0691	1.0696	-3.04	-2.67
Metcalf	1.0658	1.0662	-7.4	-7.01
Moss Landing	1.0714	1.0718	-7.12	-6.72
Los Banos	1.083	1.0834	-6.33	-5.9
Gates	1.0928	1.0931	-7.12	-6.66
Diablo Canyon	1.061	1.0612	-0.56	-0.08
Midway	1.0853	1.0856	-8.74	-8.26

Source: VA Tech, 2010

Table 2.3: Generation Drop at Diablo (1150 MW)

	Voltage		Angle	
	CA	WECC	CA	WECC
Round Mountain	1.0666	1.0777	9.28	11.36
Table Mountain	1.0547	1.071	4.67	8.05
Vaca-Dixon	1.0547	1.0727	-2.71	2.35
Tesla	1.0522	1.069	-5.66	-0.11
Metcalf	1.0531	1.0659	-10.93	-4.69
Moss Landing	1.0611	1.0718	-11.48	-5.29
Los Banos	1.0736	1.0845	-11.96	-5.96
Gates	1.0903	1.098	-14.71	-8.56
Diablo Canyon	1.0741	1.078	-12.68	-6.49
Midway	1.0853	1.0911	-17.1	-10.84

Source: VA Tech, 2010

Table 2.4: Generation Drop at Sunset G (225 MW)

	Voltage		Angle	
	CA	WECC	CA	WECC
Round Mountain	1.0756	1.0778	10.83	11.29
Table Mountain	1.0681	1.0713	7.21	7.95
Vaca-Dixon	1.0694	1.073	1.05	2.13
Tesla	1.0668	1.0702	-1.3	-0.11
Metcalf	1.0641	1.0668	-5.84	-4.51
Moss Landing	1.0702	1.0723	-5.73	-4.41
Los Banos	1.082	1.0841	-5.19	-3.91
Gates	1.0925	1.0939	-6.32	-5.01
Diablo Canyon	1.0611	1.0616	0.07	1.39
Midway	1.0856	1.0867	-8.2	-6.87

Table 2.5: Tesla – Los Banos 500kV Line Trip

	Voltage		Angle	
	CA	WECC	CA	WECC
Round Mountain	1.0759	1.0763	11.21	11.32
Table Mountain	1.0681	1.0687	7.84	8
Vaca-Dixon	1.068	1.0686	1.95	2.18
Tesla	1.0643	1.0649	-0.24	0.03
Metcalf	1.0624	1.0629	-5.2	-4.91
Moss Landing	1.0693	1.0697	-5.49	-5.16
Los Banos	1.0824	1.0829	-5.63	-5.26
Gates	1.0923	1.0927	-6.34	-5.94
Diablo Canyon	1.0609	1.061	0.22	0.64
Midway	1.0849	1.0854	-7.97	-7.54

Source: VA Tech, 2010

The result of the load flows was fairly close, especially for the line trips. The generation drop at Diablo, see Table 2.3, yielded the greatest disparity between the two models; however, this was the least likely event to occur. In the event of a generation drop of such magnitude, a special protection system (SPS) would be triggered. A SPS was not modeled in this study. The bus angles for the Diablo generation drop contingency were significantly different in the two models, but the same trend can be seen in each set of buses. For example, the bus with the largest change in angle after the drop was the same for both models. This was the bus at Malin.

2.4.2 Dynamic Analysis

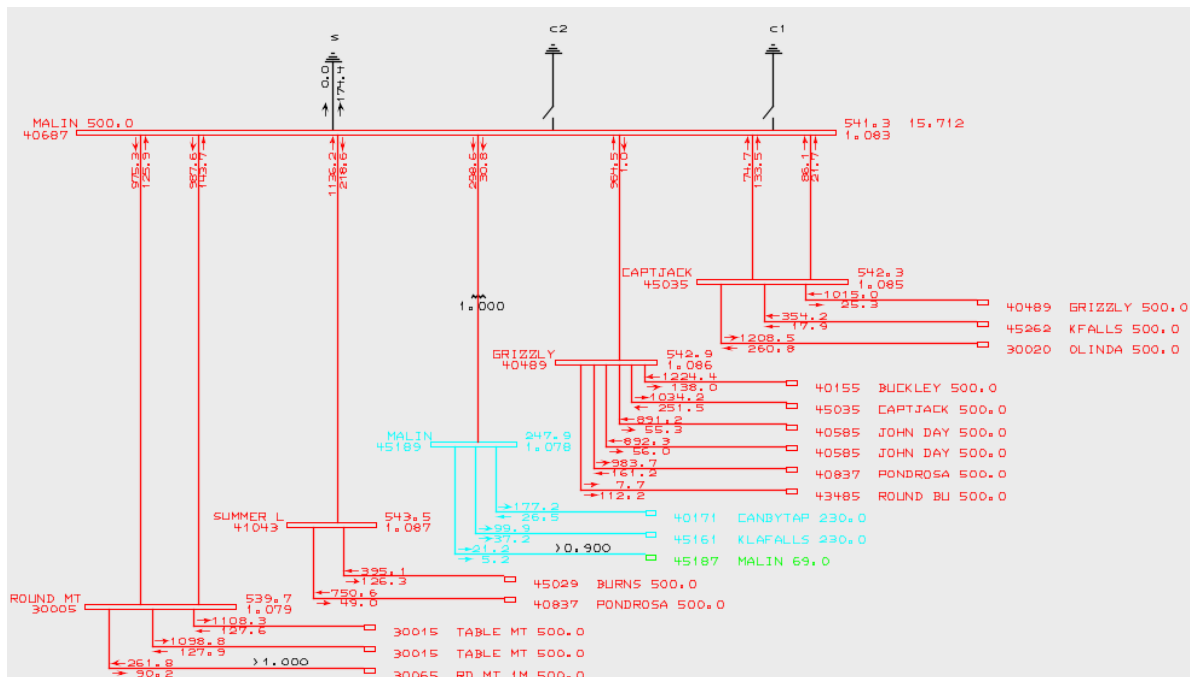
To validate the system dynamic model for the real-time alarms for encroachment of relay trip characteristics, simulations were run for three contingencies in Path 15:

- Malin – Round Mountain 1.2s 3 phase fault
- Diablo generation drop
- Sunset G. generation drop

2.4.2.1 Case 1. Malin – Round Mountain Fault

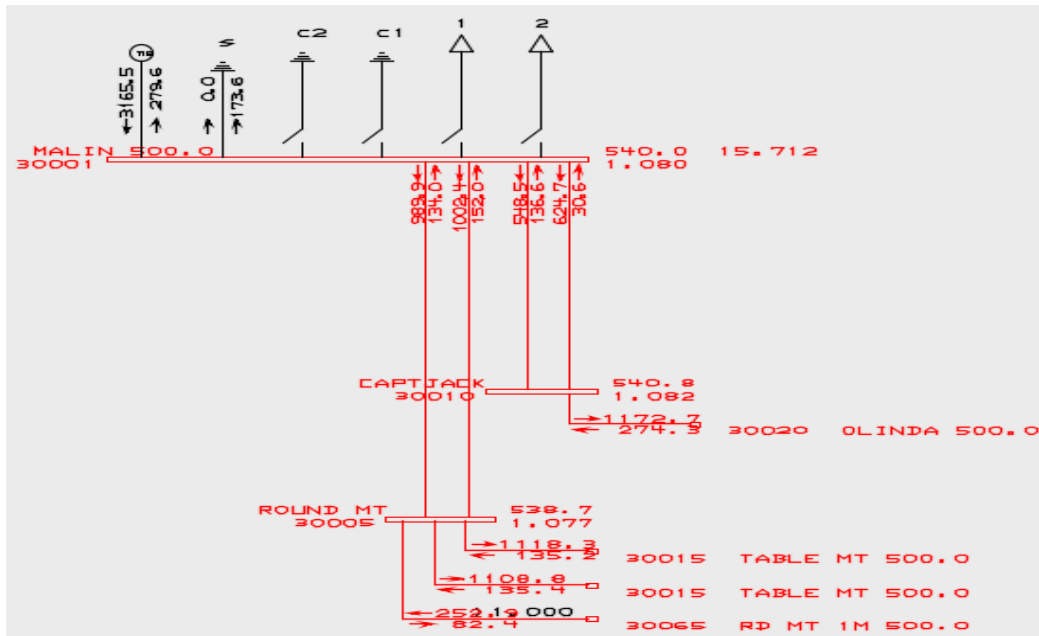
A dynamic simulation was run to simulate a disturbance on the Malin – Round Mountain 500kV line. See Figure 2.2. The disturbance was a 1.2s fault that was cleared simultaneously at both ends of the line. The voltage, frequency, and bus angle are observed at Malin and a distant Path 15 bus, Tesla.

Figure 4: WECC Model – Malin Bus



Source: VA Tech, 2010

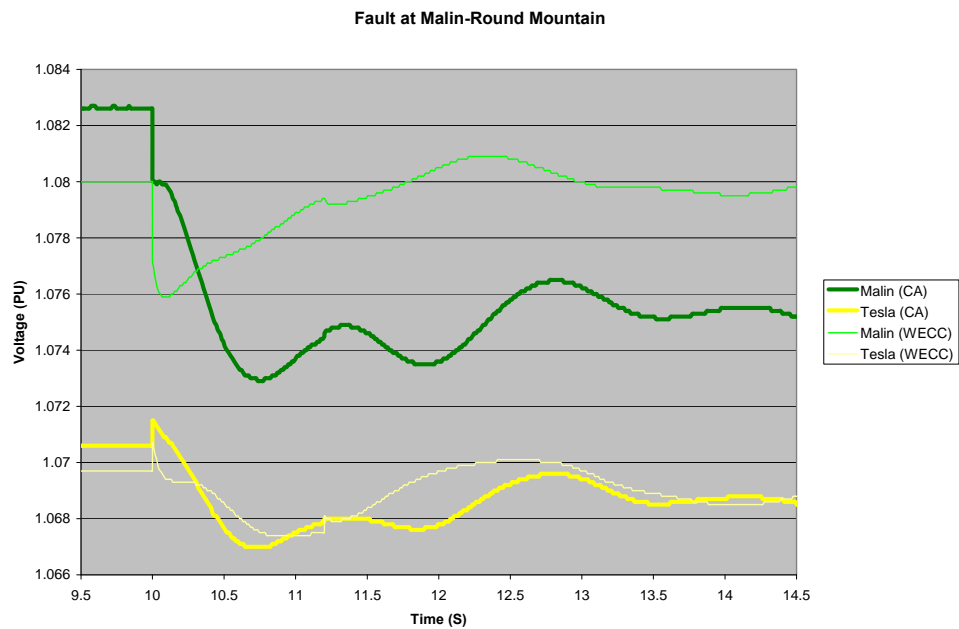
Figure 53: California Model – Malin Bus



Source: VA Tech, 2010

For the reduced California model the Malin bus in the WECC model was modified by replacing three buses and the low voltage buses connected to them with a generator such that the real and reactive power flows remained the same. See Figure 2.3. The system topology at Tesla was unchanged.

Figure 6: Voltage Plot Comparison for Case 1



Source: VA Tech, 2010

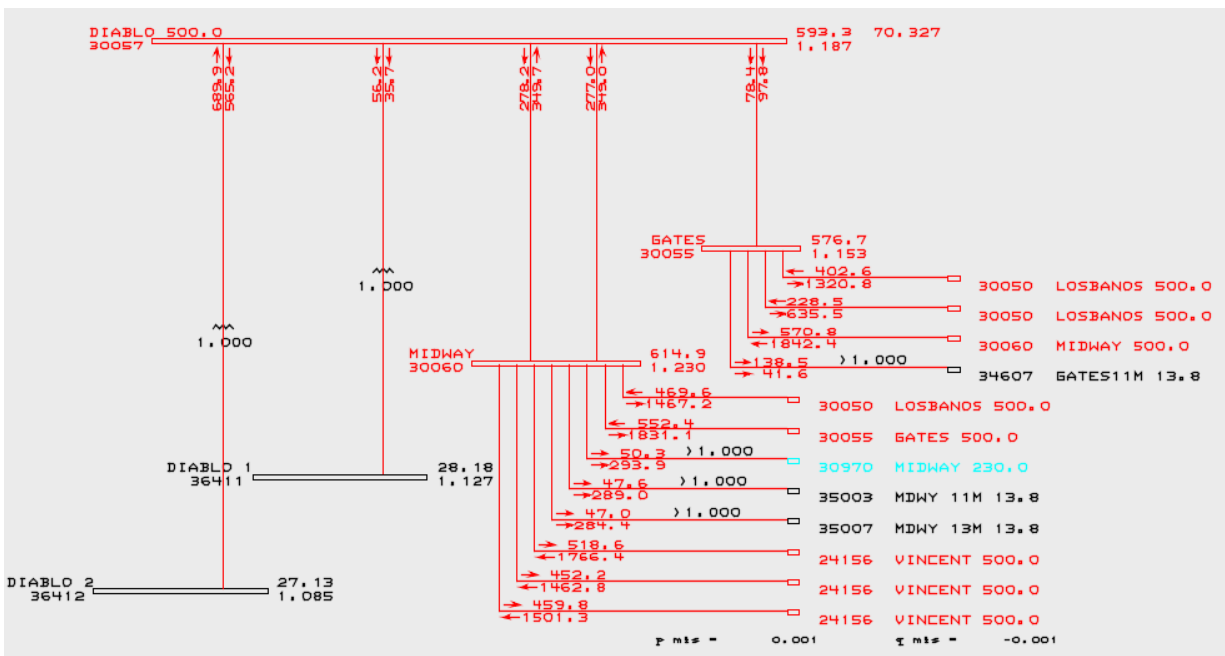
Figure 2.4 shows the voltage magnitude plots for Case 1. These curves showed that the transient voltage response was significantly different in the two models. The oscillations, transient, and steady-state deviations in the voltage were higher for the California model than for the WECC model. This indicated that there was less damping in the California model because of a decrease in system inertia. Reduced damping was most likely caused by modeling many generators and motors as a single machine without properly computing the equivalent inertia.

In the WECC model, the voltage at Malin started rising to its pre-fault value almost immediately; whereas, in the California model, the voltage did show a significant rise. The WECC model included reactive devices that would turn on to compensate for the low voltage. However, in the California model, three of the buses connected to Malin were removed which disconnected several of these devices. The results showed that the dynamics for the two models were somewhat different. It should be noted that the voltage range on this plot is less than 0.02 pu (10kV) so the results were not as drastically different as they appear.

2.4.2.2 Case 2. Diablo Generation Drop

There are nuclear plants at Diablo 1 and Diablo 2 generating 1150 MW each. See Figure 2.5. The generator at Diablo 1 was tripped and voltages and frequencies were observed at Diablo, Tesla, and Moss Landing.

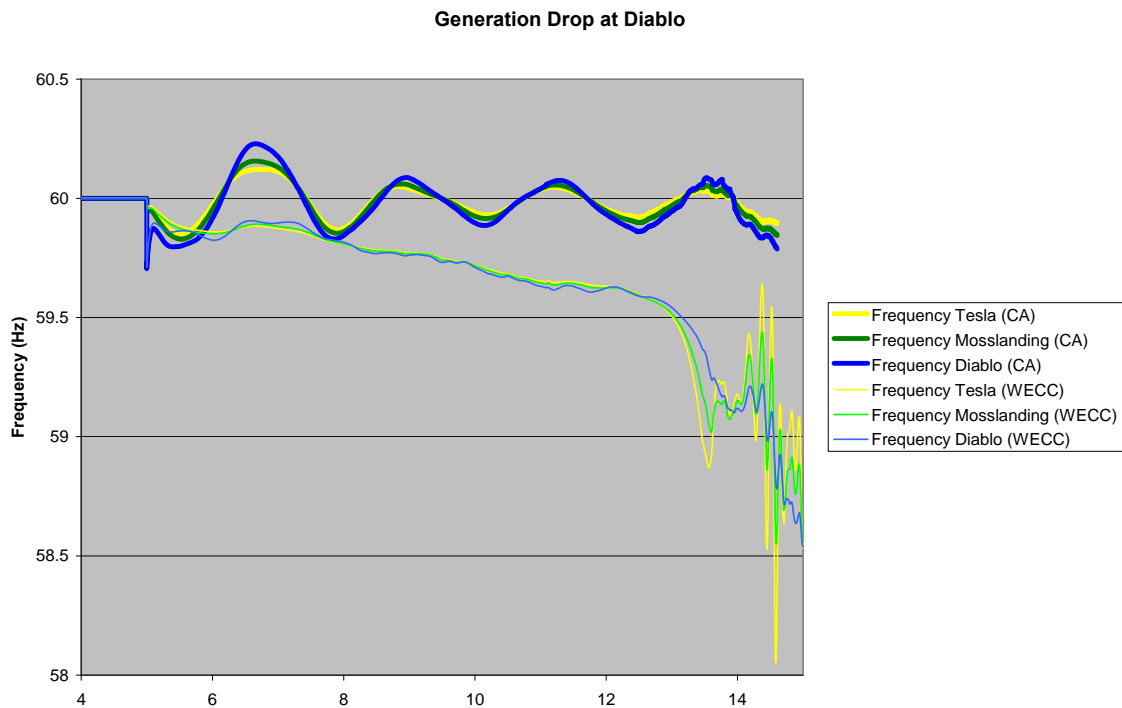
Figure 7: WECC and Californian Model – Diablo



Source: VA Tech, 2010

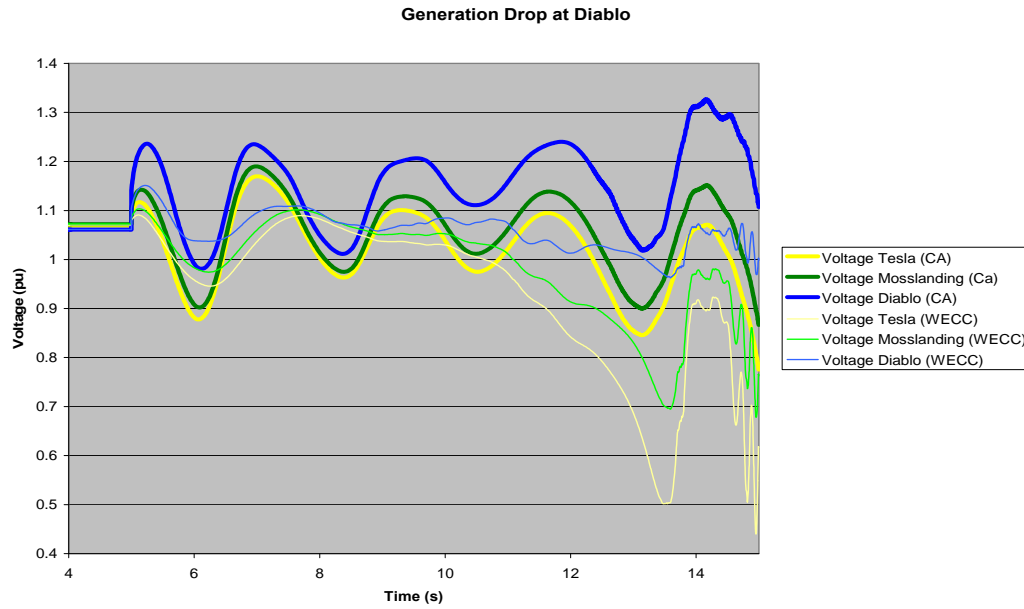
Figures 2.6 and 2.7 showed completely different results for the two models in this test case. The WECC model was clearly heading to instability and there was a large amount of under voltage and under frequency load shedding towards the end of the simulation. There was only a small amount of load shedding between 13s and 15s in the California model. The reduced California model showed that the frequency was constant even though there was a large oscillation and a slight voltage increase. Based on the voltage plot, it was likely that the California model would also become unstable, but over a longer period of time than the WECC model.

Figure 8: Frequency Plots Comparison for Case 2



Source: VA Tech, 2010

Figure 97: Voltage Magnitude Plots Comparison for Case 2



Source: VA Tech, 2010

2.4.2.3 Case 3. Sunset G Generation Drop

There are three generators at Sunset generating 75MW each. All three generators were tripped and voltages and frequencies were observed at Diablo, Tesla, and Moss Landing.

This scenario produced significantly different frequency responses at each bus. See Figure 2.8 The system frequency in the California model returned to 60 Hz very quickly; whereas, the WECC model showed a permanent frequency deviation. The voltage plots were very similar for the two models, but the WECC model showed considerably more damping. See Figure 2.9.

Figure 10: Frequency Plots Comparison for Case 2

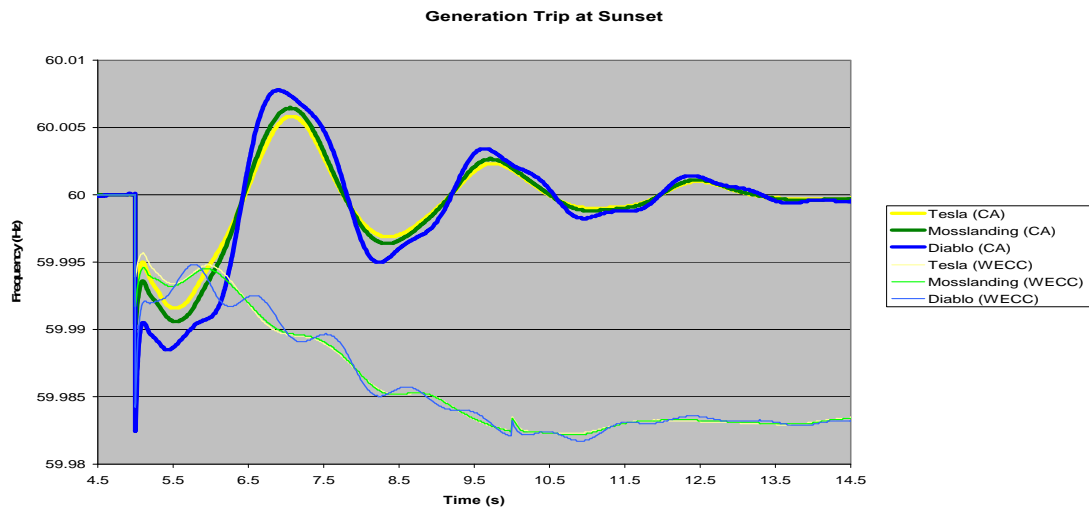
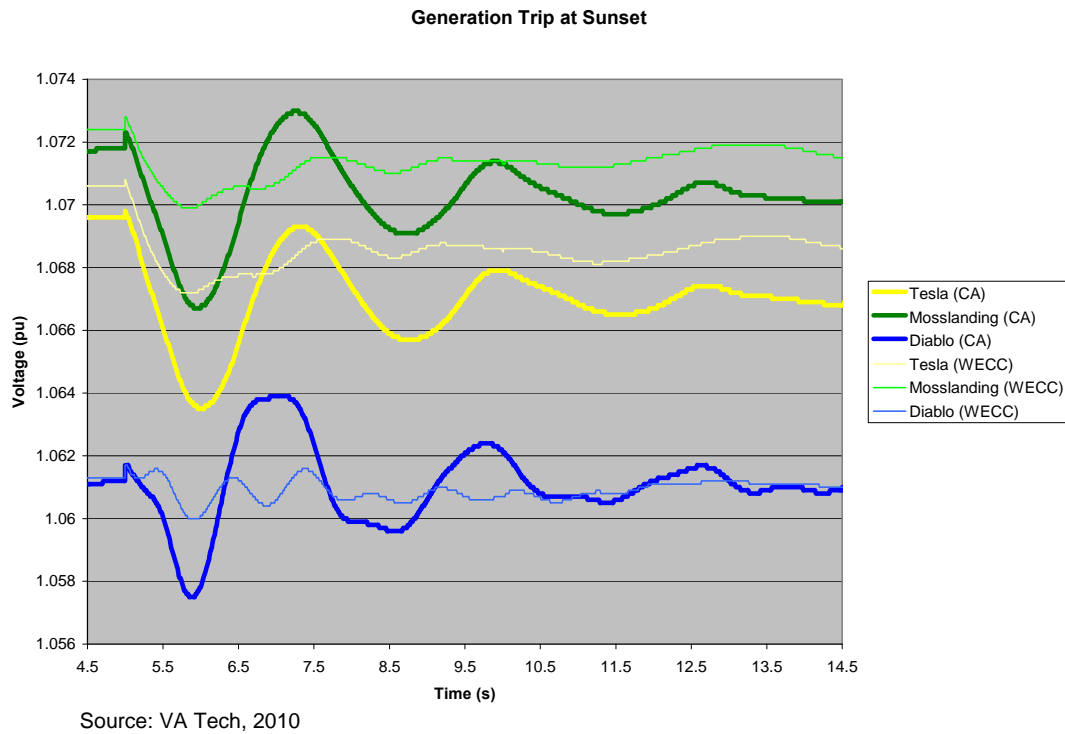


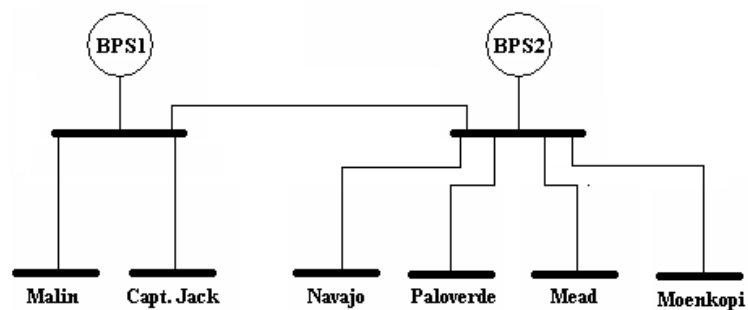
Figure 11: Voltage Magnitude Plots Comparison for Case 2



2.5 Model Improvement

In consultation with the TAG team, PG&E engineers and Virginia Tech researchers derived a new reduced California model. This new reduced California model consisted of two equivalent generators representing the WECC system to the north and east of California. See Figure 2.10. This allowed the dynamics of the two areas to be represented separately. There was a relatively high impedance line between the two equivalent machines, which represented the actual impedance between the two areas.

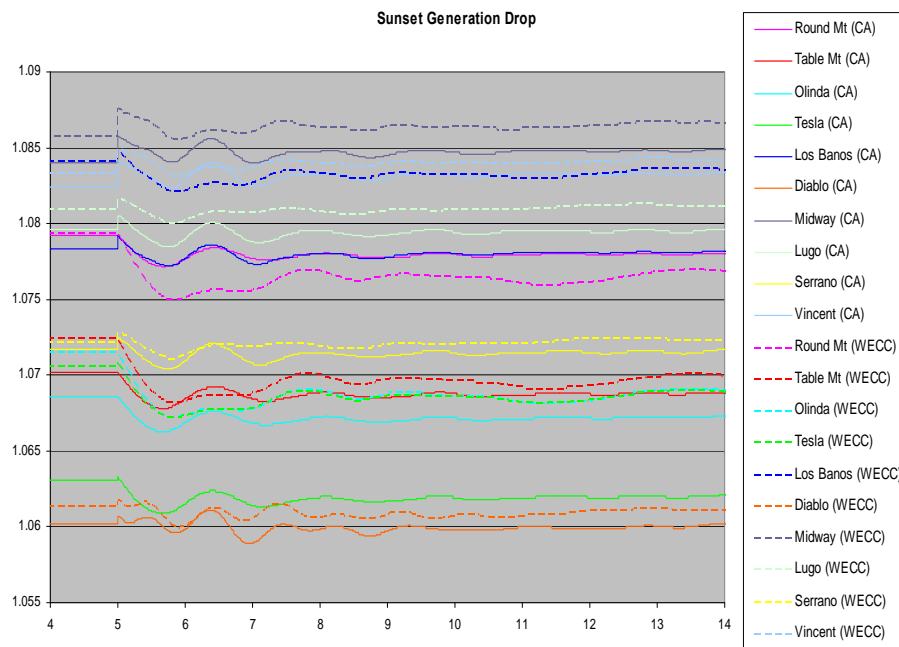
Figure 12: Two Machine Equivalent Non-California WECC System



Source: VA Tech, 2010

The dynamic response of the new improved model was tested with similar cases and was proven to be acceptable for all the tasks of this project. Figure 2.11 and Figure 2.12 show the voltage and frequency response at different locations in California for the Sunset Generation Drop case. Figure 2.13 and Figure 2.14 show similar plots for the Table Mountain – Vaca Dixon Line trip case. When a generation drop and a line trip occurred, the signature and time response of voltage and frequency signals were consistent.

Figure 13: Comparative Voltage Responses for the Sunset Generation Drop Case



Source: VA Tech, 2010

Figure 14: Comparative Frequency Responses for the Sunset Generation Drop Case

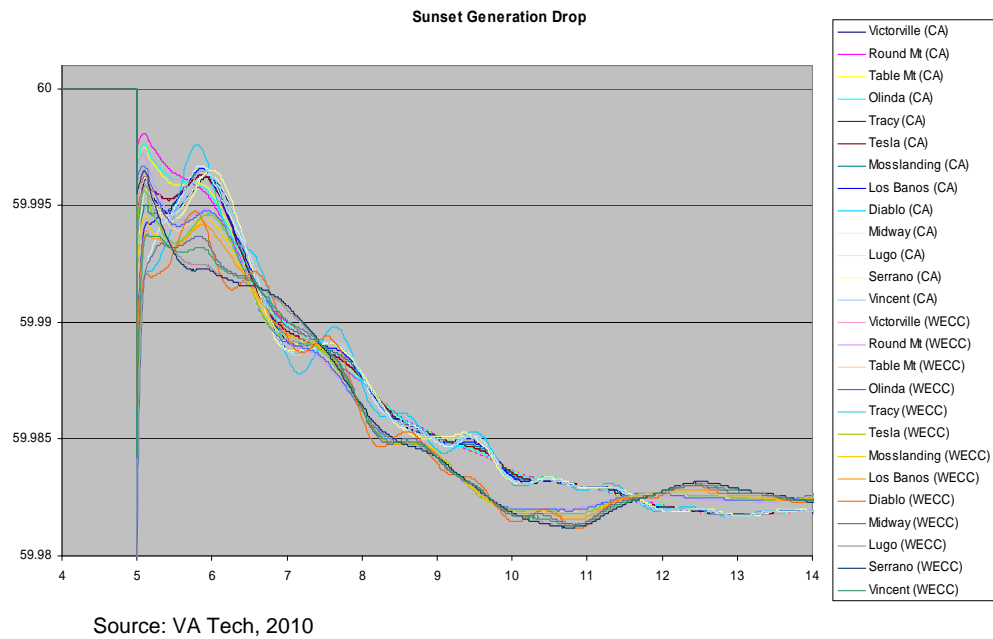


Figure 15: Comparative Voltage Responses for the Table Mt-Vaca Dixon Line Trip

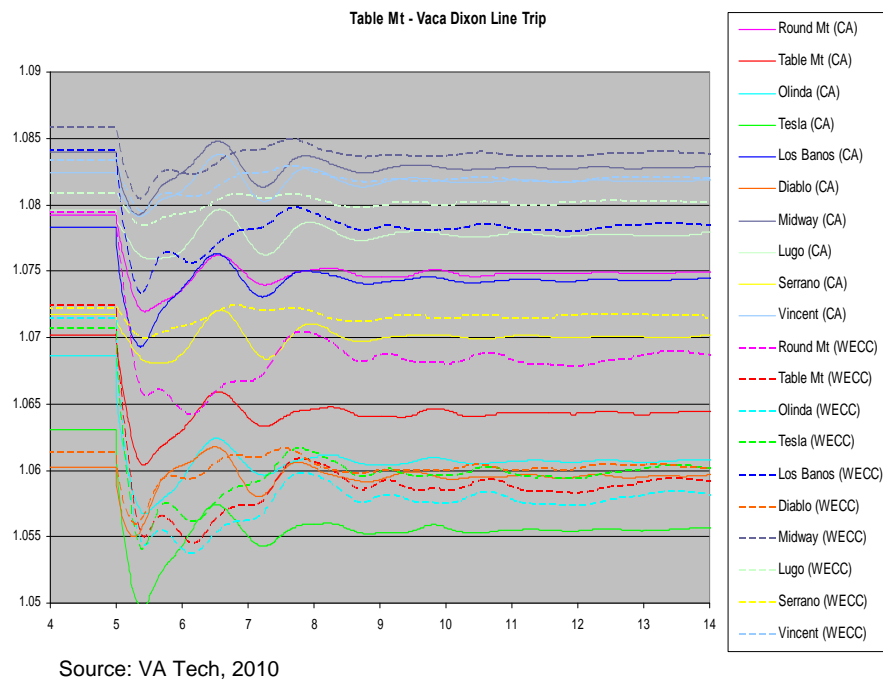
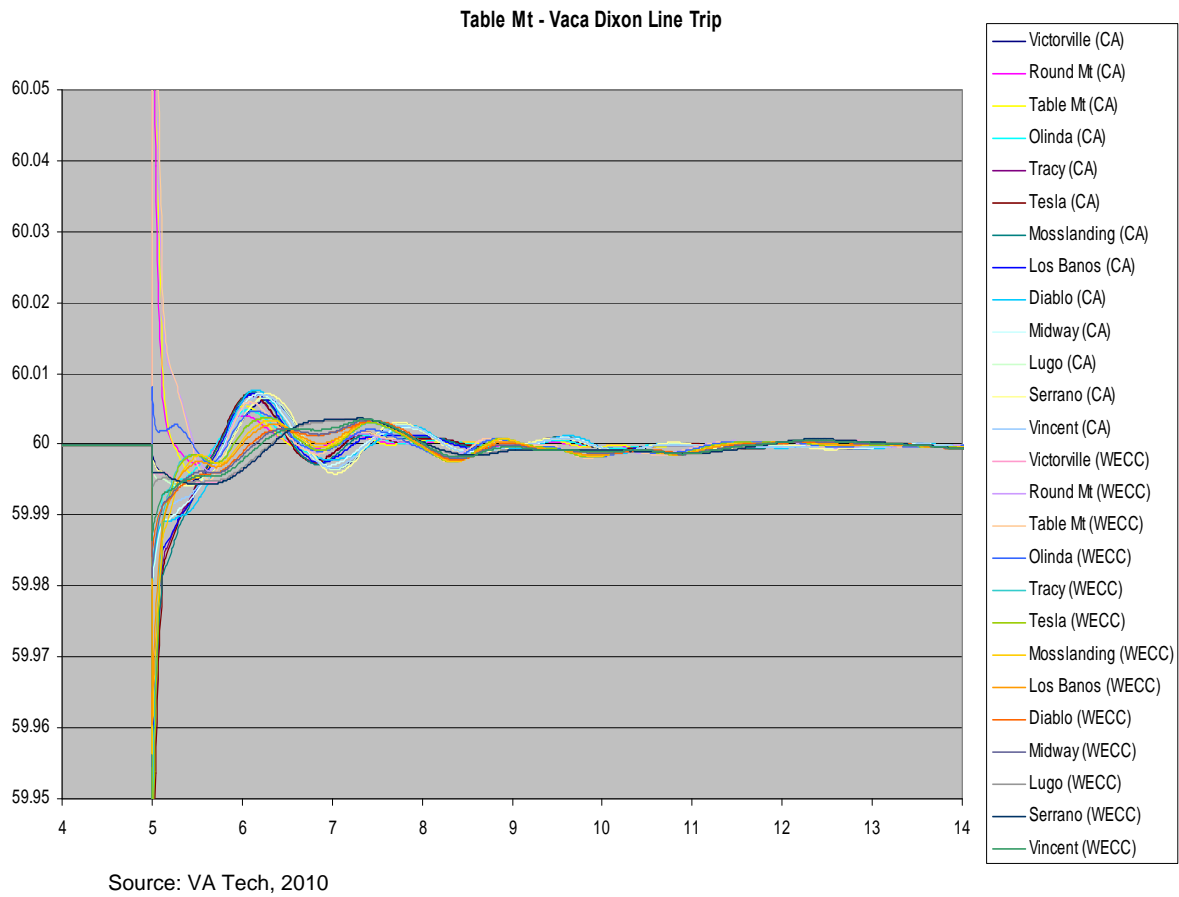


Figure 16: Comparative Frequency Response for the Table Mt-Vaca Dixon Line Trip



CHAPTER 3:

Online Adjustment of the Protection System's Security-Dependability Balance

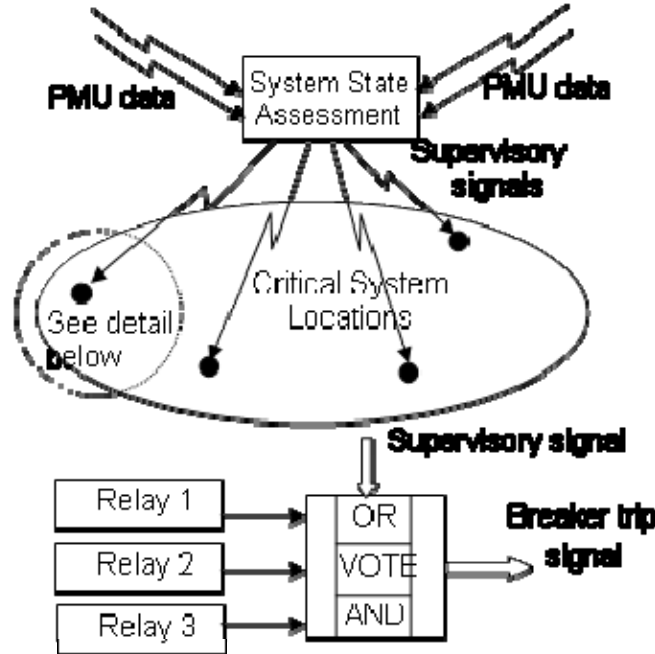
3.1 Introduction

The technical objective of this research was to utilize real-time synchronized phasor measurement data to improve system protection by making it adapt to the current system state. By using real-time wide area measurements (WAMS), it was possible to establish optimum protection policies and settings for critically located relaying systems. In particular, adaptive adjustment of dependability and security, alarming on potential load encroachment, and more intelligent out-of-step relaying tasks were improved with the use of WAMS. Task 2 focused on developing a method for using real-time wide area measurement data and existing protective relays to create a system which adaptively adjusted dependability and security.

The existing protection system was designed to be dependable at the cost of reduced security. A relay has two failure modes. It can trip when it should not trip (a false trip) or it can fail to trip when it should trip. The two types of reliability have been designated as security and dependability by protection engineers. Dependability is defined as the measure of the certainty that the relays operate correctly for all faults for which they are designed to operate. Security is the measure of the certainty that the relays will not operate incorrectly. The existing protection systems have multiple zones of protection making them redundant and biased toward dependability. This means that a fault is always cleared by some relays. There are typically multiple primary protection systems that rely on different principles. In addition, there are usually multiple backup systems that trip if all primary systems fail to trip. Protection systems designed like this yield a system that almost always clears the fault but permits a large numbers of false trips. Increased dependability is desirable when the power system is in a normal "healthy" state. The high speed fault clearing it delivers is highly desirable to avoid instabilities in the network. As a result, occasional false trips occur and are considered an acceptable risk under system normal conditions. However, when the system is highly stressed, false trips exacerbate disturbances and lead to cascading events.

An attractive solution is to adapt the security - dependability balance in response to changing system conditions as determined by real-time phasor measurements. The concept of adaptive relaying recognizes that relays need to change their characteristics to suit the prevailing power system conditions at that time. With three primary digital protection systems, it is possible to implement an adaptive security – dependability scheme by using voting logic. See Figure 3.1. In this configuration, if any of the three relays sees a fault, the breaker trips. To increase security, two of the three relays must see the fault before a trip signal is sent to a breaker. This prevents cascading and creates a more reliable system. The price paid for this increased security under stressed system conditions is that there is reduced dependability, which is acceptable. The advantage of the adaptive voting scheme is that the relays are not physically modified and the tripping logic responds to system conditions.

Figure 17: Adjustment of Dependability-Security Balance Under Stressed System Conditions



Source: VA Tech, 2010

3.2 Relay Critical Locations

The first goal of Task 2 was to determine key locations on the California power system where an insecure relay would be detrimental to the viability of the power system during stressed system conditions. Next, an adaptive protection system which will balance security and dependability in response to changing system conditions as determined by real-time phasor measurements was developed.

This section of the report presents the results of tasks aimed to:

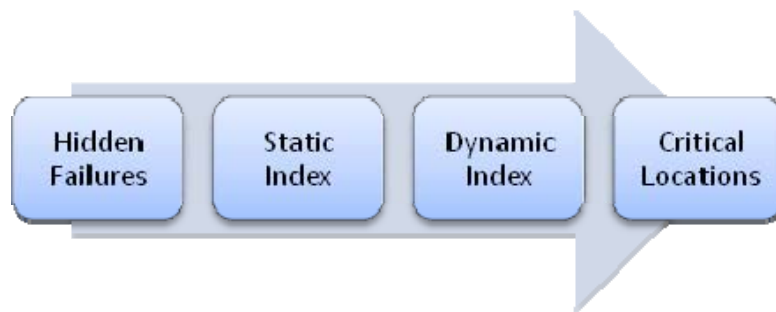
- Determine the critical locations for relays with adaptive adjustment capability,
- Document the developed algorithms and logic to determine if the relay needs to transition from dependable to secure settings, and
- Determine a list of optimal locations for PMUs whose information is required for the relays with adaptive adjustment capability.

3.2.1 Determining the Location of Critical Relays

For Task 2, the critical locations for “on-line adjustment of protection system's security-dependability” were those locations where a false trip caused by a hidden failure was most detrimental to the California transmission system. The critical locations listed in this report were

determined from an analysis of the reduced California model developed for this project and the recommendations of the TAG. For this task, the TAG recommended Virginia Tech focus only on California's Path 15 and Path 26. To determine the critical locations, an exhaustive analysis of the hidden failures on Path 15 and Path 26 was performed using a combination of a static index and a dynamic index. See Figure 3.2.

Figure 18: Methodology to Identify the Critical Locations of the Power System

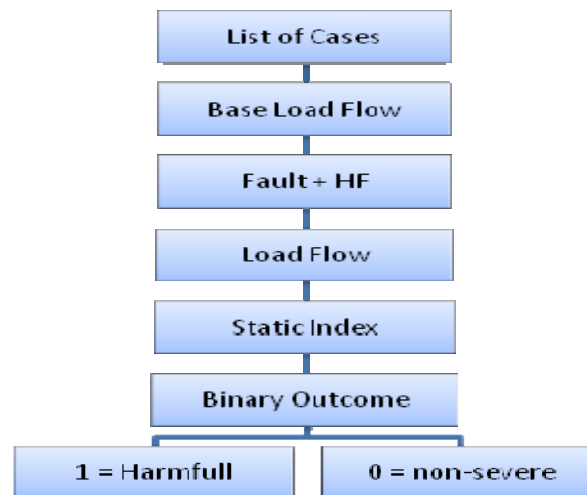


Source: VA Tech, 2010

3.2.1.1 Static Index

The methodology used for finding the static index was fully automated using the industry standard PSLF/GE software and its' programming language (EPCL). Figure 3.3 depicts the flow diagram of the procedure used to compute the static index.

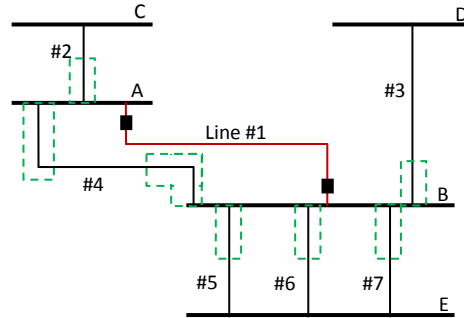
Figure 19: Static Index Flow Diagram



Source: VA Tech, 2010

The first step was to create an exhaustive list of the cases to be studied. For this task and following the recommendation of the TAG, an exhaustive list was derived for Path 15 and Path 26 in the California system. To exemplify the procedure, consider a hidden failure in the relay protecting Line 1 connected between Bus A and Bus B. See Figure 3.4.

Figure 20: Sample Hidden Failure and Regions of Vulnerability



Source: VA Tech, 2010

The structure of pointers embedded in the EPCL software enabled the identification of adjacent lines connected to the line of interest. Without loss of generality, consider the protective device to be an impedance relay with a timer defect for Zone 2. The region of vulnerability was denoted by the dashed rectangles. Any fault lying within any of these regions will cause an unwanted disconnection of Line 1. The list of all possible cases for this sample is given. See Table 3.1.

Table 3.1: List of Cases Derived for Figure 3.4

Case	Type	Line
1	Fault	Line #2
	Hidden Failure	Line #1
2	Fault	Line #3
	Hidden Failure	Line #1
3	Fault	Line #4
	Hidden Failure	Line #1
4	Fault	Line #5
	Hidden Failure	Line #1
5	Fault	Line #6
	Hidden Failure	Line #1
6	Fault	Line #7
	Hidden Failure	Line #1

Source: VA Tech, 2010

To compute the static index, it was assumed that a fault within the region of vulnerability had occurred. Next, two lines were tripped, the faulted line and the line with the hidden failure. Then, the program solved the load flow. The pre-operating conditions and the post-operation conditions were compared. An output equal to zero meant that no dynamic simulation was required since the consequence of the hidden failure was negligible. An output equal to one indicated that the case was potentially harmful, and its severity had to be assessed by the dynamic index.

The following are general parameters that should be accounted for when distinguishing potentially harmful cases from safe ones. Voltage violations are of interest especially if under voltage load shedding (UVLS) protection schemes are implemented. A typical setting for low voltage violation is 0.93 per unit (pu). However, there may be different limits where UVLS are placed. The upper voltage limit depends on the line rated voltage. In general, most 500 kV lines are operated at 1.05 pu. Also, the algorithm accounts for the voltage drop in short transmission lines. The accepted limit is a 5 percent drop. The thermal limit is another parameter that needs to be taken into account. A heavily loaded line may trip an over-current relay. Furthermore, the angle difference across the line may jeopardize the steady-state stability of the system. Table 3.2 shows the limit for the acceptable values of the parameters used to determine potentially harmful cases.

Table 3.2: Static Index Settings

Parameter	Limit
Line Loadability	110%
Bus voltages	0.93 to 1.055
Maximum voltage drop across a line	0.05
Maximum bus voltage change	0.07 pu
Convergence	Yes/No

Source: VA Tech, 2010

It should be noted that some sense of time is included in the analysis. By turning automatic tap changers on or off, phase shifters and inter-area controls allow for the system state at different points in time to be determined. Since the severity of each case was assessed using 10 second dynamic simulations, the settings previously discussed are turned off for the determination of the static index.

3.2.1.2 The Dynamic Index

Once the cases with a significant impact on the system were identified, the dynamic index was used. Figure 3.5 shows the flow diagram of the dynamic index. A 10 second dynamic simulation was run and the integral square generator angle (ISGA) score was computed. Protection relays and load shedding devices were modeled so it was possible for the original contingency and the hidden failure to cause a cascading sequence of events.

Figure 21: Flow Diagram of the Dynamic Index



Source: VA Tech. 2010

The severity of each case was assessed based on the amount of change in the generator angle from the center of angle (COA). A convenient reference for generator angles is the COA. The integral square generator angle (ISGA) [4] index computed a weighted sum of the difference between generator angles and the center of angle. See Equation 3.1.

$$ISGA = \frac{1}{T \cdot S_T} \int_0^T \sum_i^N S_i \cdot (\delta_i(t) - \delta_{COA}(t))^2 dt \quad (3.1)$$

Where M_i is the machine inertia, δ_i is the generator angle and δ_{COA} is the center of angle.

Stable cases had a nonzero number and events with diverging generator angles had the largest scores.

The ISGA is a coherency-based index and it is customized to find the critical location ranking. This score enabled the distinction between stable and unstable cases at a glance. Stable cases had a relatively small number while unstable cases had the largest scores. It should be noted that this index is not a form of kinetic energy for the network. The useful characteristics of this index included:

- The index was proportional to the size of the machine losing synchronism. We assigned weights to rotor angle deviations by the size of the machine. Therefore, larger machines losing synchronism were more greatly penalized by the index.
- The index was inversely proportional to the time when a machine loses synchronism. Since it was being integrated over time, the more quickly the synchronism was lost, the larger the index was.
- The index was proportional to the number of generators that lost synchronism. A larger number of diverging generators implied a larger score. For stable cases, the ISGA index represented the electro-mechanical oscillations sustained by the generators due to the applied disturbance.

The complete list of ISGA scores is shown in Appendix C. As an example, consider a partial list of simulation results for four cases. See **Error! Reference source not found.** The first case in **Error! Reference source not found.**, Case 350, had the largest score and it determined the optimal location to place the adaptive security - dependability protection scheme. Protection relays at any one of the three 500 kV parallel lines connecting Midway-Vincent were the best candidates for an adaptive scheme. The ISGA score was comparatively large compared to other cases in the table. Figure 3.6 depicts a plot of generator's rotor angle excursions in Area 24, SCE. The plot clearly indicated that the system split apart with one group of coherent machines north and another one in the south.

In the second case in the table, Case 237, the applied disturbance caused more than 2000 MW of generation to be removed from the system. Figure 3.7 shows the rotor angles of two large generators drifting away from the system. The rest of the generators in the system remained coherent. The third and fourth cases in the table showed non-severe, stable cases. The ISGA score

for Case 269 was slightly larger than Case 115. The difference between the plots shown in Figure 3.8 and Figure 3.9 **Error! Reference source not found.** is subtle, but it can be seen that in Case 269, the generators undergo larger and longer sustained oscillation. This meant that Case 269 had a larger ISGA score.

To conclude, the Midway-Vincent path was determined to be the system critical location. A schematic of the backbone 500 kV transmission lines in California is shown in **Error! Reference source not found.** Figure 3.10. The figure highlights the optimal placement for the security - dependability adaptive scheme. Based on practical experience, the advisory committee of the VT-CIEE research project confirmed that the critical location suggested by the proposed procedure was accurate.

Table 3.3: ISGA Score of Four Different Cases

CASE	FAULT	Bus From	Bus To	ISGA
350	F	MIDWAY	VINCENT	6721.188
350	HF	MIDWAY	VINCENT	
350	HF	MIDWAY	VINCENT	
237	F	GATES	DIABLO	4316.469
237	HF	DIABLO	MIDWAY	
237	HF	DIABLO	MIDWAY	
269	F	DIABLO	MIDWAY	9.7647
269	HF	MIDWAY	VINCENT	
269	HF	MIDWAY	VINCENT	
115	F	TABLE MT	VACA-DIX	7.7235
115	HF	ROUND MT	TABLE MT	
115	HF	TABLE MT	TESLA	

Source: VA Tech, 2010

Figure 226: Generator Rotor Angles of Study Case 350 – ISGA Score: 6721

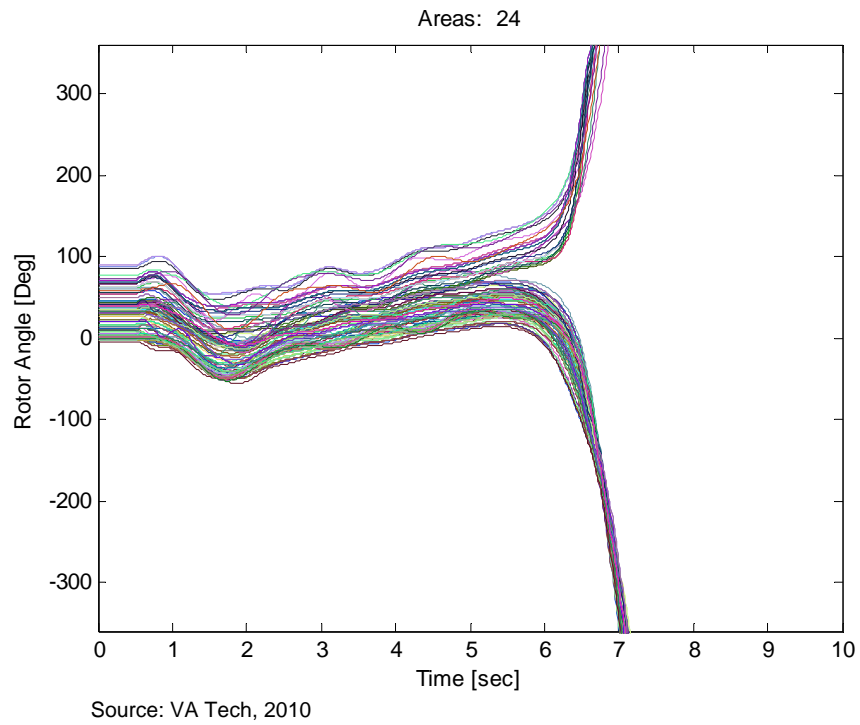


Figure 23: Generator Rotor Angles of Study Case Number 237 – ISGA Score: 4316

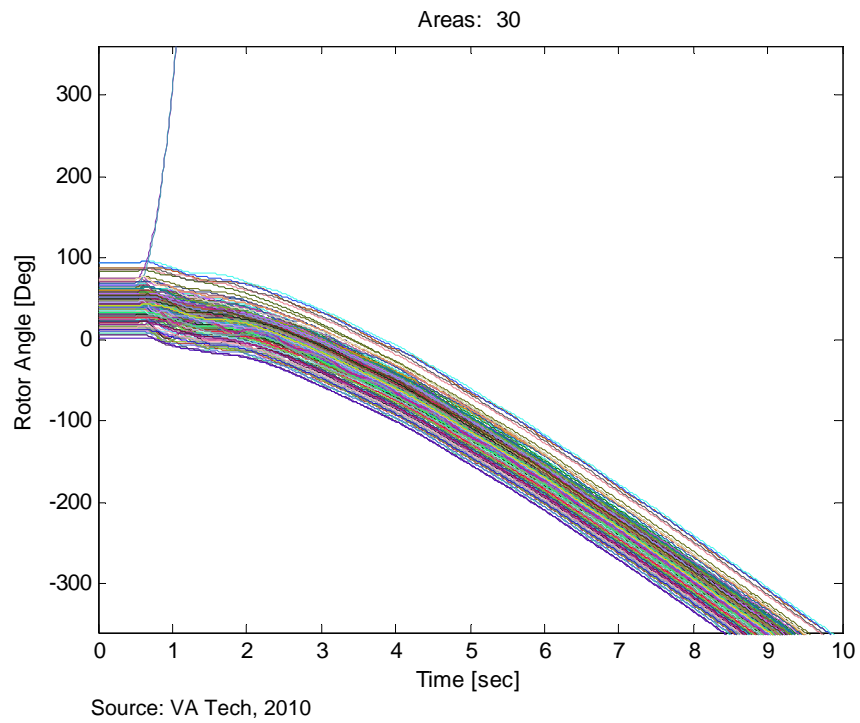


Figure 24: Generator Rotor Angles of Study Case Number 269 – ISGA Score: 9.76

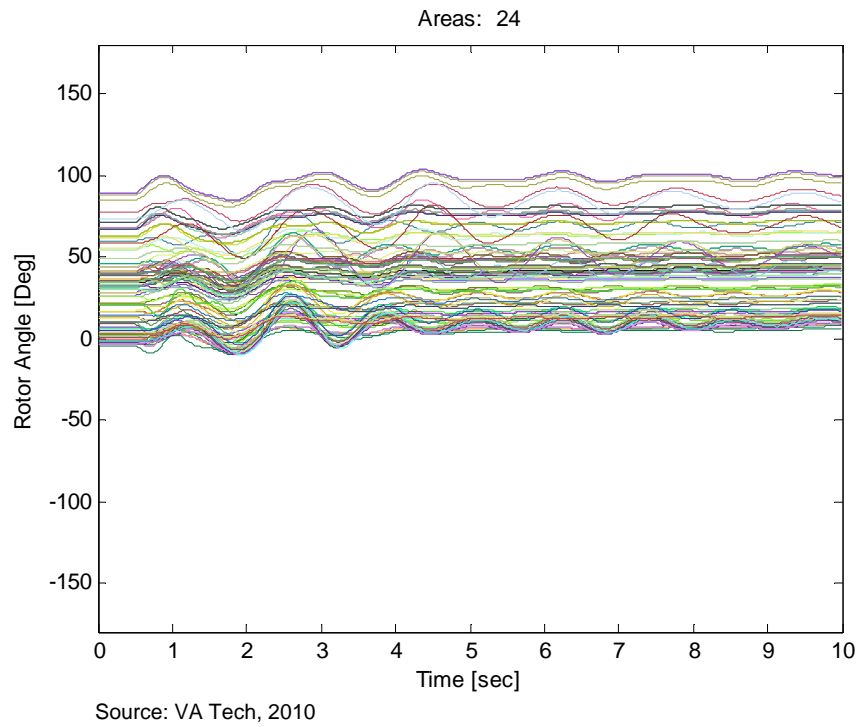


Figure 25: Generator Rotor Angles of Study Case Number 115 – ISGA Score: 7.72

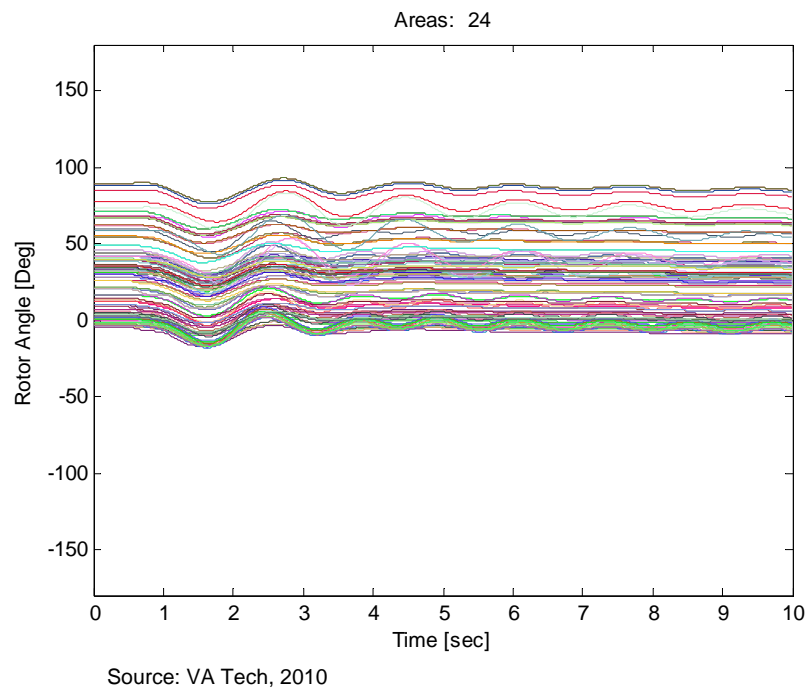
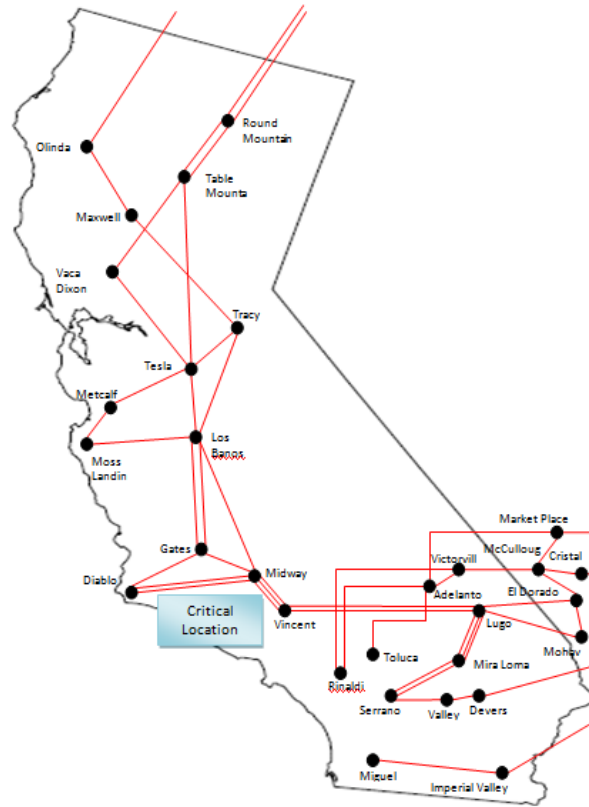


Figure 26: Schematic: 500 Kv Buses and Lines in California



Source: VA Tech, 2010

Midway-Vincent is determined to be the system critical location. It is the location where an adaptive security - dependability scheme is most beneficial.

3.2.1.3 The Critical Locations

A hidden failure is a permanent defect in a relay that does not manifest itself until another system event (usually a fault) occurs nearby. The result is a double contingency. In this research project, all simulation cases consisted of a 3-phase line fault and four cycles later the faulted line was cleared and an adjacent line was also tripped by relay mis-operation due to a hidden failure. The dynamic simulation was run for a total of 10 seconds so that the protective system could be properly observed. Using the model developed for this project, 66 cases were run on Path 15 and Path 26. The cases are shown in Appendix B.

The critical locations were determined using the results from the ISGA function. Appendix C shows the results from simulation cases using ISGA for assessing the severity of the disturbance. Table 3.4 shows the ten most critical cases along Path 15 and Path 26 as calculated using both severity assessment techniques.

Table 3.4: The Critical Locations (Path 15 and Path 26)

Ranking	Case	Type	From	To	Normalized Score
1	58	F	Midway	Vincent	0.99672
		HF	Midway	Diablo	
2	60	F	Midway	Vincent	0.99437
		HF	Midway	Vincent	
3	61	F	Midway	Vincent	0.99126
		HF	Midway	Vincent	
4	65	F	Vincent	Lugo	0.98434
		HF	Vincent	Lugo	
5	64	F	Vincent	Lugo	0.98248
		HF	Vincent	Midway	
6	66	F	Vincent	Midway	0.97897
		HF	Vincent	Midway	
7	56	F	Midway	Los Banos	0.9778
		HF	Midway	Vincent	
8	54	F	Midway	Los Banos	0.97285
		HF	Midway	Gates	
9	14	F	Los Banos	Tracy	0.96949
		HF	Los Banos	Moss Landing	
10	31	F	Gates	Midway	0.96472
		HF	Gates	Diablo	

Source: VA Tech, 2010

These results showed that the most critical location of the selected paths was located on the three parallel lines connecting Midway and Vincent. The adaptive voting scheme was placed to protect the most heavily loaded of these three lines.

3.3 Adaptive Voting Scheme and PMU Locations

The voting scheme consisted of three relays that vote to decide whether to trip or not to trip the line. However, the voting occurred only when the state of the system was such that a hidden failure had compromised its stability. This meant the goal of adapting security and dependability according to the system state was achieved. The following scenarios further clarify how the voting scheme accomplished the objective:

If the system was stressed, the protection system was biased towards security since tripping due to a hidden failure may jeopardize the system. Under this condition the relays voted.

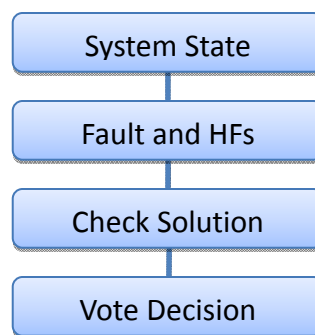
Conversely, if the system was lightly loaded and considered to be safe, the protection was biased towards dependability. No voting occurred and the main protection device (the one currently in use) was responsible for protecting the line.

It was necessary to emphasize that the relay settings were not changed before, during or after the fault. The adaptive security - dependability was achieved by the redundancy of protection devices.

3.3.1 Methodology

Figure 3.11 shows the flow diagram of the methodology proposed to implement the voting scheme.

Figure 27: Methodology to Develop the Voting Scheme



Source: VA Tech, 2010

First, it was necessary to determine a considerable number of stressed and safe conditions to provide adequate system state variation for testing. In order to achieve this, a total of 4,150 load flow simulations were performed; one for each state variation. The system variation was accomplished by load scaling the different areas in California.

Under each of these 4,150 different system states, a fault and two hidden failures were applied at the lines connecting Midway – Vincent. The convergence of the load flow was then analyzed. If the solution diverged, it meant that the removal of the line due to a hidden failure under that

particular system state puts the system at risk. Therefore, when these system states occurred, the protection system was biased towards security. The relay voted and resulted in an output equal to one.

If the solution converged, having a trip due to a hidden failure was not too detrimental for the system. Therefore, these system states required the power system to be biased towards dependability. The relay did not vote and was represented by an output equal to zero.

In each of these cases, voltage magnitudes, voltage angle, real and imaginary currents are measured on every 500 kV bus in the system. The location of these measurements showed possible PMU locations which were determined by the data mining procedure.

3.3.2 Data Mining and PMU Placement

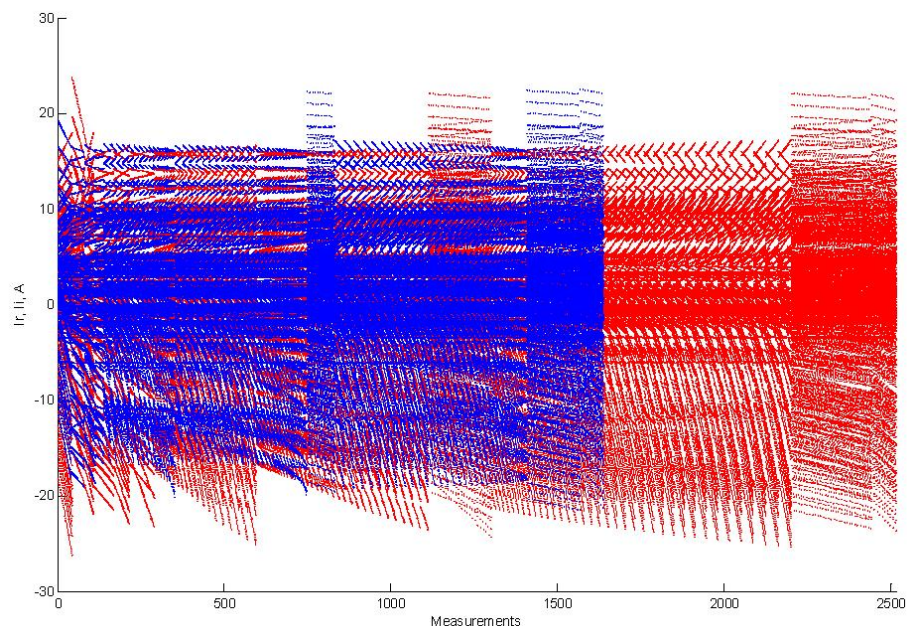
Classification and Regression Trees (CART) is commercially available software that builds decision trees. Two inputs were required to build a decision tree:

Target (dependent variable): The variable to be predicted. For the voting scheme, the target is the solution of the load flow: a zero or a one.

Predictor (independent variables): The variables used to predict the target. For the voting scheme, the predictors were the measurement taken by the theoretical PMUs placed at every 500 kV bus.

In Figure 3.12, the blue and red points represent the 4,150 system states determined from the dynamic index and static index. Blue points represent where the system remains stable after a hidden failure. Red points represent those cases where the system is under stressed conditions. The x-axis lists the case number and the y-axis gives the value of the real current between Tesla and Los Banos for each of the cases.

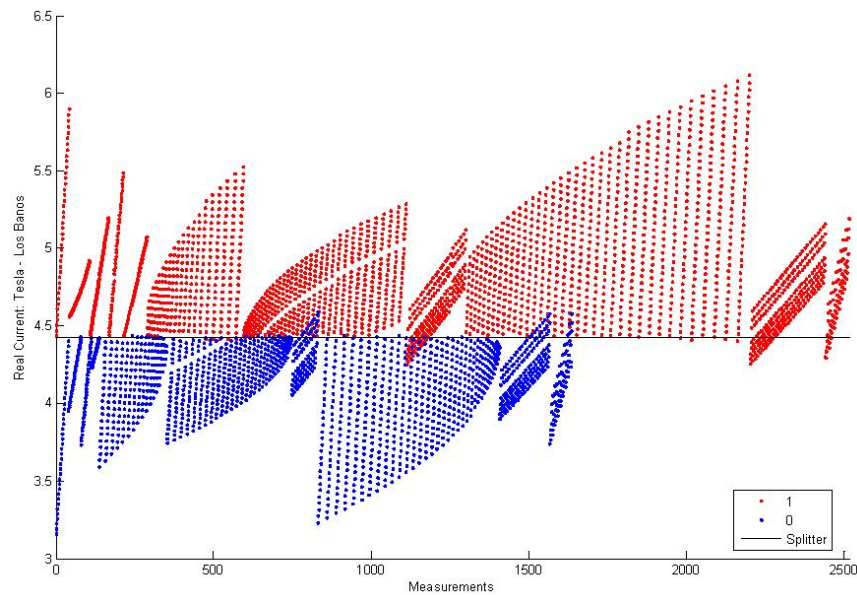
Figure 28: Sample Data Input to CART Data Mining Software



Source: VA Tech, 2010

Figure 3.13 shows the first split of the decision tree grown using CART. This single node in the decision tree can differentiate between a stressful and un-stressful condition for 90 percent of the cases.

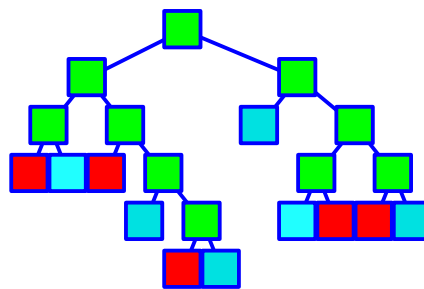
Figure 29: CART First Splitting Node



Source: VA Tech, 2010

An eleven node tree was constructed for Task 2. The accuracy of decision trees is usually represented by the area under the Receiver Operating Characteristic (ROC) curve. The proposed tree had a ROC equal to 0.99, meaning that one out of 100 cases was predicted incorrectly. The tree schematic is presented in Figure 3.14 and the detailed trees with parameters can be found in Appendix A.

Figure 30: Decision Tree Schematic



Source: VA Tech, 2010

More than 130 predictors (independent variables) were given to CART. After building the tree, only some measurements were needed to make a splitting decision at each node in the tree. These measurements determined the placement of the PMUs. Table 3.5 presents these locations.

Table 3.5: PMU Placement for the Adaptive Relay Scheme

BUS NAME
Los Banos
Devers
El Dorado
Pittsburg (reference)

Source: VA Tech, 2010

3.4 Performance Evaluation and Functional Specifications

In order to test the performance of the decision tree with out-of-sample data, further test cases were created by simulating circuit element outages. The objective was to induce additional system operating points to determine how well the tree reacted to topology changes. The out-of-sample data consisted of new system operating conditions obtained by simulating outages in:

- Generators delivering more than 200 MW,
- Loads consuming more than 200 MW, and
- Transmission lines of 230 kV and 500 kV.

3.4.1 Heavy Winter Model

The out-of-sample data for the heavy winter case data consisted of 660 system operating conditions. Each of these outages was simulated under diverse loading conditions. The results of the test are summarized in **Error! Reference source not found.6**, **Error! Reference source not found.7**, **Error! Reference source not found.8**, and Table 3.99. Of the 660 cases, 14 cases were misclassified by the decision tree; an error rate of approximately 2 percent. Of those 14 cases, only 2 stressed states were misclassified as a class zero. This result showed an outstanding performance of the decision tree. If the system undergoes significant departures from the model assumptions, a new decision tree should be built. The proposed out-of-sample test only attempted to assess tree's robustness under small departures.

Table 3.6: Out of Sample Test: Generator Outage

	Classified class 0	Classified class 1
True class: 0	30	5
True class: 1	0	45

Source: VA Tech, 2010

Table 3.7: Out of Sample Test: Load Outage

	Classified class 0	Classified class 1
True class: 0	117	1
True class: 1	0	50

Source: VA Tech, 2010

Table 3.8: Out-of-Sample Test: 230 Kv Lines Outage

	Classified class 0	Classified class 1
True class: 0	132	0
True class: 1	0	132

Source: VA Tech, 2010

Table 3.9: Out-of-Sample Test: 500 Kv Lines

	Classified class 0	Classified class 1
True class: 0	62	6
True class: 1	2	78

Source: VA Tech, 2010

3.4.2 Heavy Summer Model

The out-of-sample data consisted of 1,138 system operating conditions. Each of these outages was simulated under diverse loading conditions. The results of the test are summarized in Table

3.10, Table **Error! Reference source not found.**3.11, Table 3.12, and Table 3.13. Out of the 1,137 cases, 49 cases were misclassified by the decision tree; an error rate of approximately 4.3 percent. The tree performed adequately when subjected to topology changes.

Table 3.10: Heavy Summer Out-of-Sample Test: Generator Outage

	Classified class 0	Classified class 1
True class: 0	107	2
True class: 1	6	112

Source: VA Tech, 2010

Table 3.11: Heavy Summer Out-of-Sample Test: Load Outage

	Classified class 0	Classified class 1
True class: 0	154	0
True class: 1	7	37

Source: VA Tech, 2010

Table 3.12: Heavy Summer Out-of-Sample Test: 230 Kv Lines Outage

	Classified class 0	Classified class 1
True class: 0	278	0
True class: 1	25	284

Source: VA Tech, 2010

Table 3.13: Heavy Summer Out-of-Sample Test: 500 Kv Lines

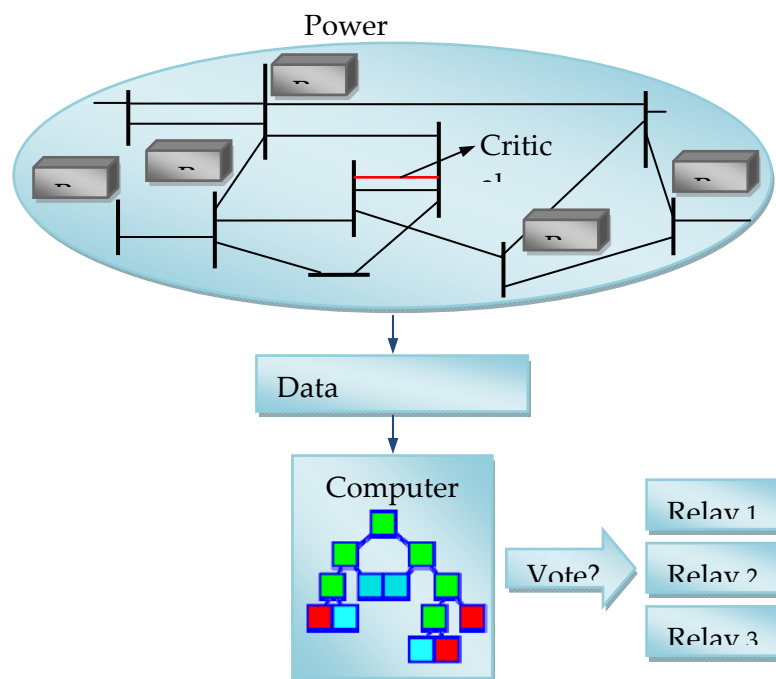
	Classified class 0	Classified class 1
True class: 0	62	6
True class: 1	3	54

Source: VA Tech, 2010

3.4.3 Functional Specification

A functional overview of the security - dependability adaptive voting scheme is given by the schematic shown in Figure 5.1. Wide-area measurements were obtained with the aid of PMUs at the selected buses which provided enough information to determine if a bias towards security was needed. Measurements were collected by a data concentrator at the control center and used by the decision computer to determine the state of the power system which was then classified as either stressed or safe. If the system was stressed, a signal was sent to the digital relays, at the pre-determined critical location. This signal enabled the voting scheme and biased the protection system towards security. If the system was found to be safe, the voting scheme was disabled and only one relay functioned in the protection scheme. Therefore, it was biased towards dependability.

Figure 31: Functional Overview of the Security – Dependability Adaptive Scheme



Source: VA Tech, 2010

3.4.3.1 PMU Minimum Specification

The PMU must comply with the IEEE-C37.118 or latest synchrophasor standard, communicate to the data concentrator at a minimum rate of two measurements per second and send the data in real/imaginary format. Table 3.16 lists the PMU measurements required for the heavy summer case. Table 3.14 lists the measurements required for the surrogate PMU for the heavy summer case. Surrogate measurements are recommended as a back-up decision tree if the primary PMU's data is missing.

Table 3.14: Splitting Attributes of the Heavy Winter Decision Tree

Attribute	PMU measurement
Ir1106	Real Current: Tesla – Los Banos
Ir1104	Real Current: Tracy – Los Banos
Ii3850	Imaginary Current: Palo Verde - Devers

Source: VA Tech, 2010

Table 3.15: List of Surrogates for Heavy Winter Case

Node	Primary Split	Surrogate	Predictive Association
1	$Ir1106 \leq 4.42$	$Ir1104 \leq 4.16$ (Tesla – Los Banos)	0.93
2	$Ir1104 \leq 4.21$	Angle Round MT ≤ 16.88	0.64
3	$Ir1104 \leq 4.07$	$Ii1115 \leq -2.02$ (Gates - Diablo)	0.75
4	$Ir1106 \leq 4.4$	$Ir1104 \leq 4.15$	0.52
9	$Ii3850 \leq 0.13$	$Ir87 \leq 5.04$ (Victorville - McCullough)	0.55

Source: VA Tech, 2010

Table 3.16: Splitting Attributes of the Heavy Summer Decision Tree

Attribute	PMU measurement
Ir19	Real Current: Palo Verde – Devers
Ii735	Imaginary Current: Devers – Valley SC
Ir415	Real Current: El Dorado - McCullough

Source: VA Tech, 2010

Table 3.17: List of Surrogates for the Heavy Summer Case

Node	Primary Split	Surrogate	Predictive Association
1	$Ir19 \leq 16.52$	$Ir472 \leq -4.98$ (Mohave – El Dorado)	0.93
2	$Ii735 \leq -0.47$	$Ii1033 \leq 1.38$ (Diablo - Midway)	0.17
3	$Ii735 \leq -0.44$	$Ii1033 \leq 1.38$ (Diablo - Midway)	0.72
4	$Ir415 \leq -1.05$	$Ii1022 \leq 1.53$ (Moss Landing – Los Banos)	0.79
7	$Ir19 \leq 16.92$	$Ir472 \leq -5.26$ (Mohave – El Dorado)	0.78

Source: VA Tech, 2010

3.4.3.2 Data Concentrator Specifications

The data concentrator collects all PMU data and sends a single time-aligned data string to the decision computer. A data concentrator is recommended but not required for the system specifications. Because there are not many PMUs, the time alignment of PMU data can also be performed by the decision computer.

3.4.3.3 Decision Computer Specifications

A computer at the control center implemented the decision trees for the heavy winter and heavy summer cases. Due to the low operational burden of the decision trees, the decision computer requirements were minimal. Network or serial communication ports were required for communication between the decision computer, the data concentrator, and the computer relay at the critical location. Appendix A shows the decision tree for the heavy winter and heavy summer cases.

CHAPTER 4:

Real-Time Alarms for Encroachment of Relay Trip Characteristics

4.1 Introduction

The technical objective of this research was to use real-time synchronized phasor measurement data to provide improved protection system supervision to make it adaptive to prevailing system state. By using real-time WAMS, it is possible to determine optimum protection policies and settings for critically located relaying systems. In particular, adaptive adjustment of dependability and security, alarming on potential load encroachment, and more intelligent out-of-step relaying tasks can be improved with the use of WAMS. Task 3 focused on developing a method for using real-time wide area measurement data and the existing protection system data base to determine which of the relay characteristics are in danger of being encroached upon during a catastrophic event. Where such a scenario was discovered, appropriate countermeasures were developed.

One of the lessons learned from a study of past blackouts is that many relays have settings which, when originally specified, were appropriate for all assumed system conditions and contingencies but which, because of the changes in power system conditions over the years are no longer viable. Some examples of such settings which depend upon assumed system conditions are back-up zones of distance relays, certain overcurrent relays, out-of-step relays and loss-of-field relays. Consider the loadability of a back-up zone of a distance relay. When it is set, it is checked for adequacy for assumed peak loading conditions, credible contingencies, and certain failure modes of the primary relaying system. As power systems change in time, it is not always possible to revise the relay settings either because of a manpower shortage, or due to oversight on the part of the protection engineer. Some system changes may be a result of unforeseen contingencies which depress system voltages beyond normal expectations. In any case, as system conditions change, a setting once thought to be safe is actually being encroached upon by prevailing loading and voltage conditions. Since these are quasi-steady-state phenomena, if they lead to an encroachment of the relay trip characteristic they would lead to an inappropriate trip of the relay and may well start a cascading process. Indeed, the catastrophic blackout of 1965 in eastern North America was precipitated by exactly such an event. A practical strategy must be implemented to provide advance warnings (alarms) to engineers, that under the prevailing and evolving system conditions certain relays are in danger of tripping falsely on load flows or power swings.

4.1.1 Determination of Critical Protection System Locations

Every power system has buses where it is critical that insecure relay operation would be catastrophic in its effect on an evolving incident. Such locations are often well recognized by operating personnel, and would provide a starting group of locations which belong to the critical category. In addition, it is necessary to simulate various loading and contingency conditions,

and systematically investigate the effect of over-tripping by relays following some system event such as a fault, loss of an important line, or loss of generation. Algorithms will be developed to quickly test power system response to over-tripping by some protection systems. Approximations would be acceptable in such an evaluation, and it is expected that the developed algorithms will use linear approximations for load-flows, and time-series prediction techniques for transient instability detection. The outcome of this research will be a list of buses on the study power system which are critical in the sense of relaying security, and which would be candidates for equipping them with an alarm system indicating that an impending system condition may lead to a false trip.

4.1.2 Relay System Database

It will be assumed that information about relays in service at system facilities is available in some data base. From this data base will be extracted a new data base of back-up protection functions and other slower relay functions such as loss-of-field and out-of-step relays at critical buses identified in the previous step. The data base will contain information about relay zone settings and shapes, relay timers, and whether or not the zone shapes depend upon system conditions such as source impedance ratios. For each of these characteristics, a two-stage alarm level will be defined with the help of system relay engineers. The idea is that as the prevailing loading conditions cross the alarm thresholds, the system engineer will be informed about the potential for relay characteristic encroachment which exists on the system. The last phase of this research will identify countermeasures which can be applied to relieve the alarm condition.

4.1.3 Wide Area Measurement-Based Critical Relay Condition Monitoring

The wide area measurements provided by the PMUs will be used to track in real time system phenomena and their influence on the critical relays in the system. For example, where impedance relays are involved in back-up functions such as step-distance relays, out-of-step relays, or loss-of-field relays, the apparent impedance seen by the relays will be tracked as a dynamic locus in real time. From these loci one would be able to determine when the alarm levels are violated, and appropriate alarms will be generated for relay engineers, and possibly for the control center.

One aspect of this research task is to determine optimum PMU locations so that the relevant relay responses could be monitored accurately. A strategy for placing PMUs will be developed so that one would start with a small number of PMUs to begin the implementation of this system with possible incomplete observability coverage, and then increase the number of PMUs in stages so that complete observability of the parameters of interest could be achieved. The research is of course dependent on the study system chosen, and it is expected that the collaborating utility (PG&E) will assist in selecting the system model and relay system data base.

4.1.4 Countermeasures

Countermeasures for conditions which have led to alarms would be of various types depending upon criticality of the approaching event and available time to activate the relief measures. For example, the countermeasures may include an engineering review of the relay settings in light of the activated alarm. Of course, this would be a process which would require considerable time to implement, and would not be used in real-time. If the alarm is activated when a cascading situation is imminent, the countermeasure would have to involve immediate action: this may include generation re-dispatch, load curtailment, line switching, and so forth. These countermeasures would be prepared as a look-up table ahead of time, and modified in real time based upon prevailing system state.

4.2 Relay-Critical Locations and Characteristics

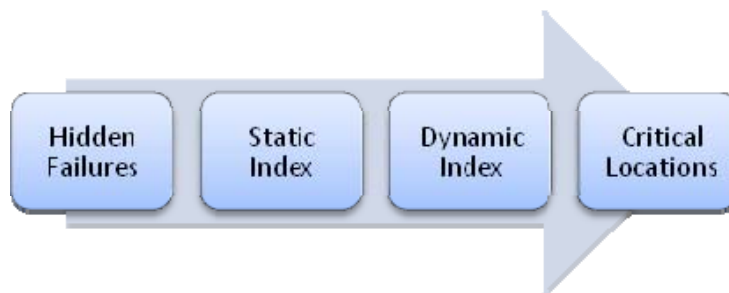
This section of the final report presents the results which determined the critical relay locations from real-time alarms for encroachment of relay trip characteristics. Also, it documents the relay types and characteristics to be included in the relay data bases.

4.2.1 Critical Locations for Real-Time Alarms for Encroachment of Relay Trip Characteristics

The critical locations of a power system are the locations where a relay mis-operation would have the most detrimental effects on the system. The relay characteristic encroachment alarms were implemented on protective devices in these locations.

The critical locations listed in this report were determined based on analysis of the California model and the recommendations of the TAG. For Task 3, the TAG recommended Virginia Tech focus on Path 15 and Path 26. An exhaustive analysis of the hidden failures on Path 15 and Path 26 was performed using a combination of the static index and a dynamic index to determine the critical locations. See Figure 4.1.

Figure 32: Methodology to Identify the Critical Locations of the Power System

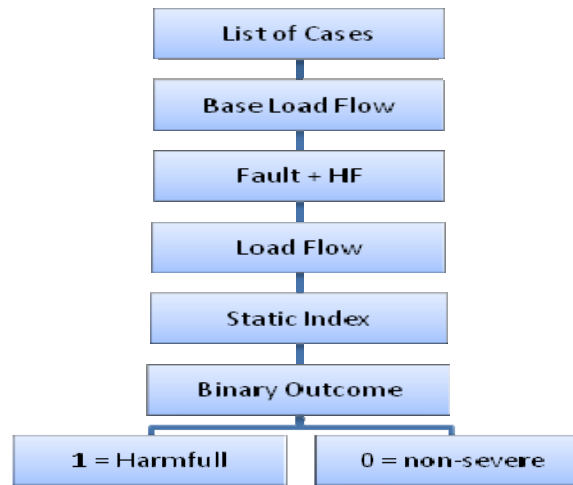


Source: VA Tech, 2010

4.2.1.1 Static Index

The methodology used for the Static index was fully automated using the industry standard PSLF/GE software and its programming language EPCL. Figure 4.2 depicts the flow diagram of the procedure used to compute the static index.

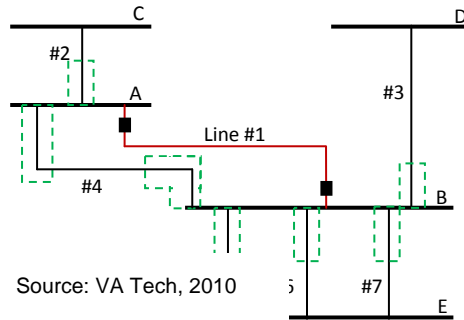
Figure 33: Static Index Flow Diagram



Source: VA Tech, 2010

The first step is to create an exhaustive list of the cases to be studied. A list was derived for Path 15 and Path 26 in the California system. To exemplify the procedure, consider a hidden failure in the relay protecting Line 1 connected between Bus A and Bus B of Figure 4.3.

Figure 34: Sample Hidden Failure and Regions of Vulnerability



The structure of pointers embedded in the EPCL software enables the identification of adjacent lines connected to the line of interest. Without loss of generality, consider the protective device to be an impedance relay with a timer defect for Zone 2. The region of vulnerability is denoted by the dashed rectangles. Any fault lying within any of these regions will cause an unwanted disconnection of Line 1. The list of all possible cases for this sample is given in Table 4.1.

Table 4.1: List of Cases Derived for Figure 4.3

Case	Type	Line
1	Fault	Line #2
	Hidden Failure	Line #1
2	Fault	Line #3
	Hidden Failure	Line #1
3	Fault	Line #4
	Hidden Failure	Line #1
4	Fault	Line #5
	Hidden Failure	Line #1
5	Fault	Line #6
	Hidden Failure	Line #1
6	Fault	Line #7
	Hidden Failure	Line #1

Source: VA Tech, 2010

To compute the static index, it is assumed that a fault within the region of vulnerability has occurred. Then, two lines are tripped, the faulted line and the line with the hidden failure. Next, the program proceeds to solve the load flow. The pre-operating conditions and the post-operation conditions are compared. An output equal to zero means that no dynamic simulation is required since the consequence of the hidden failure is negligible. Having an output equal to one means that the case is potentially harmful and its severity needs to be assessed by the dynamic index.

The general parameters that should be taken into account to distinguish potentially harmful cases from safe ones are presented next. Voltage violations are of interest if UVLS protection schemes are implemented. A typical setting for a low voltage violation is 0.93 pu, but different limits in locations where UVLS are placed may be specified. The upper voltage limit also depends on the line rated voltage. In general, most 500 kV lines are operated at 1.05 pu. The algorithm also cares about voltage drop in short transmission lines. The accepted limit is a 5 percent drop. Thermal limit is another parameter that needs to be taken into account. A heavily loaded line may trip an over-current relay. Furthermore, the angle difference across the line may jeopardize the so called steady-state stability of the system. Table 4.2 summarizes the limits used in our model.

Table 4.2: Static Index Settings

Parameter	Limit
Line Loadability	110%
Bus voltages	0.93 to 1.055
Maximum voltage drop across a line	0.05
Maximum bus voltage change	0.07 pu
Convergence	Yes/No

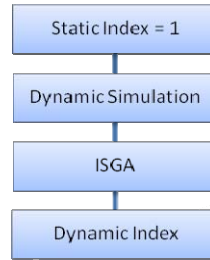
Source: VA Tech, 2010

It should be recognized that some sense of time is included in the analysis. By turning on or off automatic tap changers, phase shifters and inter-area controls the system state at different points in time can be determined. Since the severity of each case will be assessed using 10 second dynamic simulations, the settings previously discussed are turned off for the determination of the static index.

4.2.1.2 The Dynamic Index

Once the cases with a significant impact on the system have been identified, the dynamic index is used. Figure 4.4 shows the flow diagram of the dynamic index. A 10 second dynamic simulation is run and the ISGA score is computed. Protection relays and load shedding devices are modeled so it is possible for the original contingency and hidden failure to result in a cascading sequence of events.

Figure 35: Flow Diagram of the Dynamic Index



Source: VA Tech. 2010

The severity of each case is assessed from the generators point of view. A convenient reference for generator angles is the COA. The ISGA [4] index used in this task computes a weighted sum of the difference between generator angles and the center of angle, Equation 4.1.

$$ISGA = \frac{1}{T \cdot S_T} \int_0^T \sum_i^N S_i \cdot (\delta_i(t) - \delta_{COA}(t))^2 dt \quad (4.1)$$

Where M_i is the machine inertia, δ_i is the generator angle and δ_{COA} is the center of angle.

Stable cases will have a nonzero number while events with diverging generator angles will have the largest scores.

The ISGA is a coherency-based index and it is customized for the critical location ranking. This score enables the distinction between stable and unstable cases at a glance. Stable cases will have a relatively small number, while unstable cases will have the largest scores. It should be noted that this index is not a form of kinetic energy for the network. It is important to stress some useful characteristics of this index:

- The index is proportional to the size of the machine losing synchronism. We are assigning weights to rotor angle deviations by the size of the machine. Therefore, larger machines losing synchronism will be greatly penalized by the index.
- The index is inversely proportional to the time when a machine loses synchronism. Since it is being integrated over time, the sooner synchronism is lost the larger the index will be.
- The index is proportional to the number of generators that lose synchronism. A larger number of diverging generators implies a larger score. For stable cases the ISGA index

represents the electro-mechanical oscillations incurred by the generators due to the applied disturbance.

The complete list of ISGA scores is shown in Appendix C. As an example, consider a partial list with four cases; the simulation results are shown in **Error! Reference source not found.**. The first case in **Error! Reference source not found.**, case 350, has the largest score and it determines the optimal location to place the adaptive security/dependability protection scheme. Protection relays at any one of the three 500 kV parallel lines connecting Midway-Vincent are the best candidates for an adaptive scheme. The ISGA score is large compared to other cases in the table. Figure 4.5 depicts a plot of generator's rotor angle excursions in area 24, Southern California Edison. The plot clearly indicates that the system splits apart with a group of coherent machines north from the path and another one in the south.

In the second case in the table, case 237, due to the applied disturbance more than 2,000 MW of generation are removed from the system. Figure 4.6 shows two large generators drifting away from the system. The rest of the generators in the system remained coherent. The third and fourth cases in the table show non-severe, stable cases. The ISGA score for case number 269 is slightly larger than case 115. The difference between the plots shown in Figure 4.7 and **Error! Reference source not found.**8 is subtle, but after careful inspection, it can be seen that in case 269 the generators undergo larger and longer sustained oscillations, which renders a larger ISGA score.

To conclude, the Midway-Vincent path was determined to be the system critical location. A schematic of the backbone 500 kV transmission lines in California is shown in Figure 4.9. The figure highlights the optimal placement for the security/dependability adaptive scheme. Based on practical experience, the advisory committee of the VT-CIEE research project confirmed that the critical location suggested by the proposed procedure was accurate.

Table 4.3: ISGA Score of Four Different Cases

CASE	FAULT	Bus From	Bus To	ISGA
350	F	MIDWAY	VINCENT	6721.188
350	HF	MIDWAY	VINCENT	
350	HF	MIDWAY	VINCENT	
237	F	GATES	DIABLO	4316.469
237	HF	DIABLO	MIDWAY	
237	HF	DIABLO	MIDWAY	
269	F	DIABLO	MIDWAY	9.7647
269	HF	MIDWAY	VINCENT	
269	HF	MIDWAY	VINCENT	
115	F	TABLE MT	VACA-DIX	7.7235
115	HF	ROUND MT	TABLE MT	
115	HF	TABLE MT	TESLA	

Source: VA Tech, 2010

Figure 36: Generator Rotor Angles of Study Case Number 350. ISGA Score: 6721

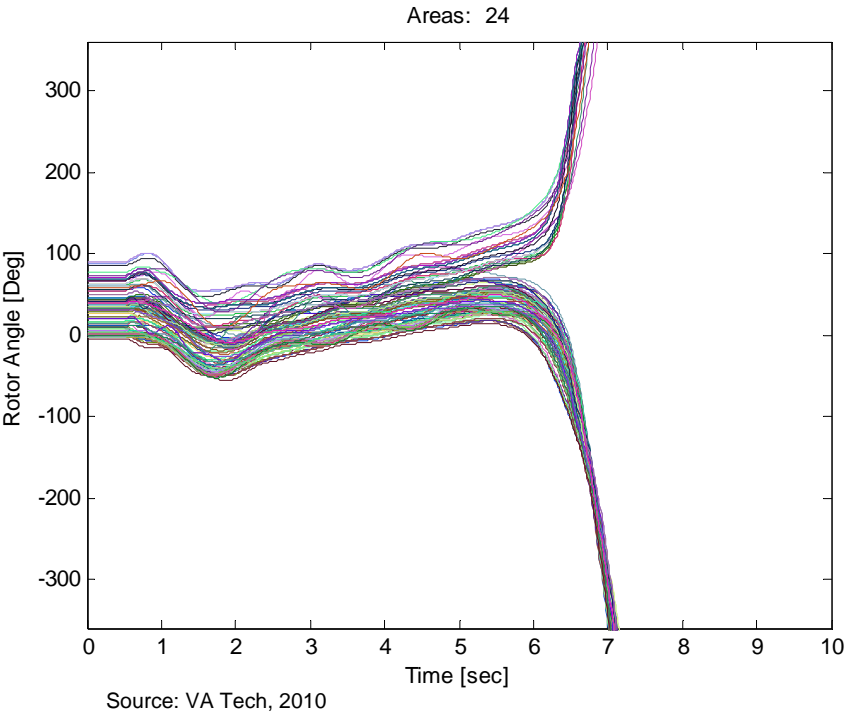


Figure 37: Generator Rotor Angles of Study Case Number 237. ISGA Score: 4316

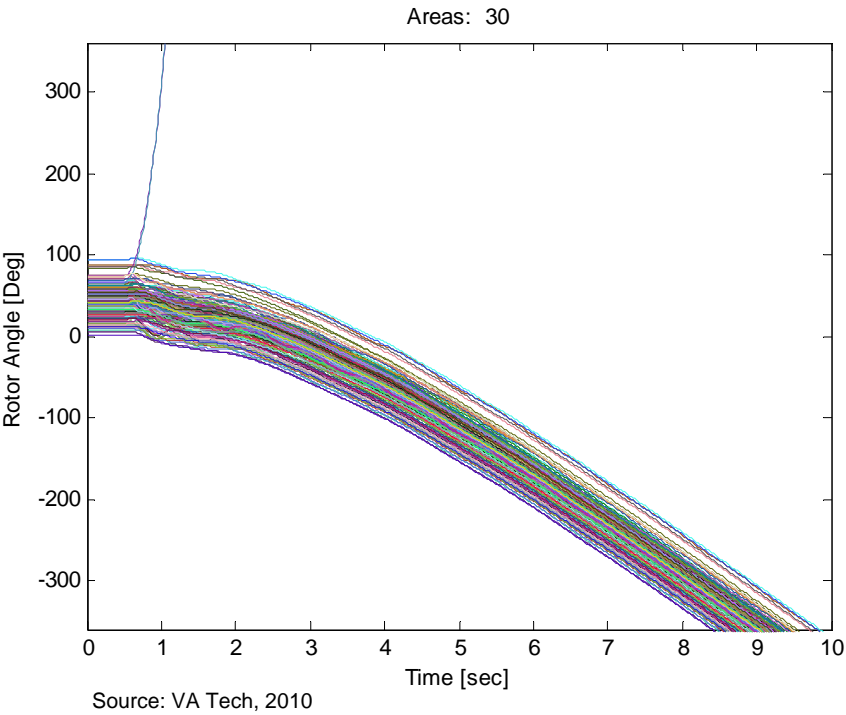


Figure 38: Generator Rotor Angles of Study Case Number 269. ISGA Score: 9.76

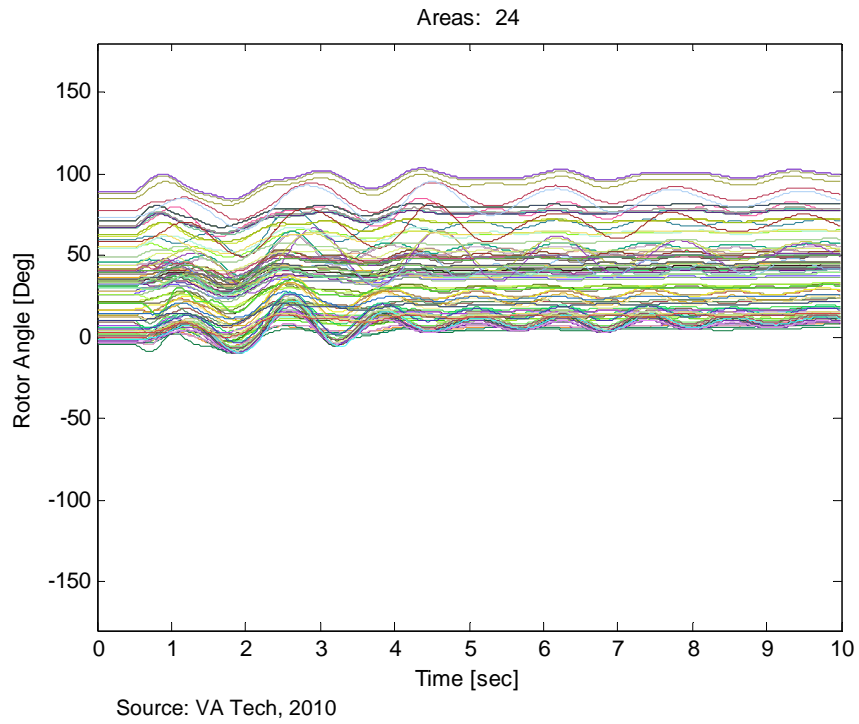


Figure 398: Generator Rotor Angles of Study Case Number 115. ISGA Score: 7.72

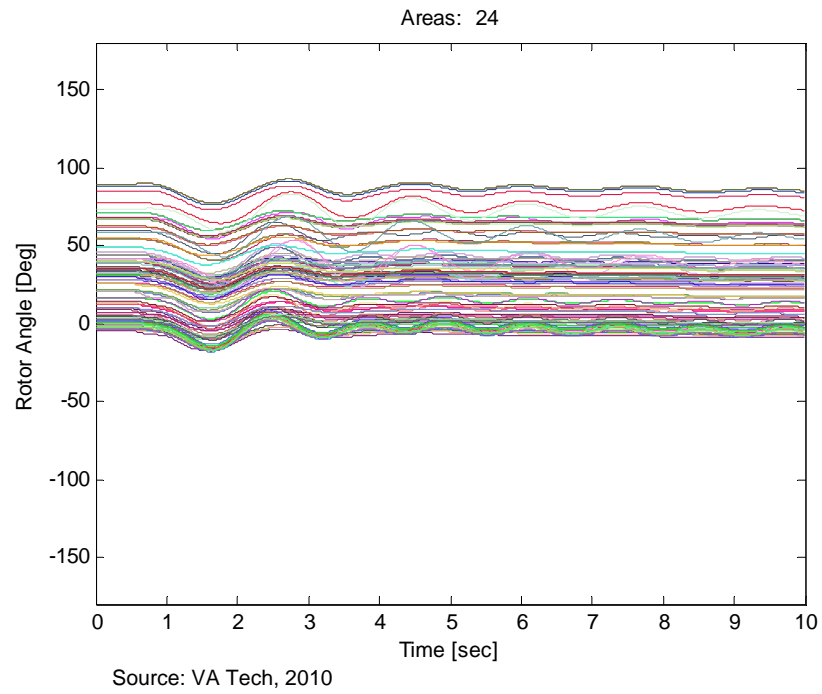
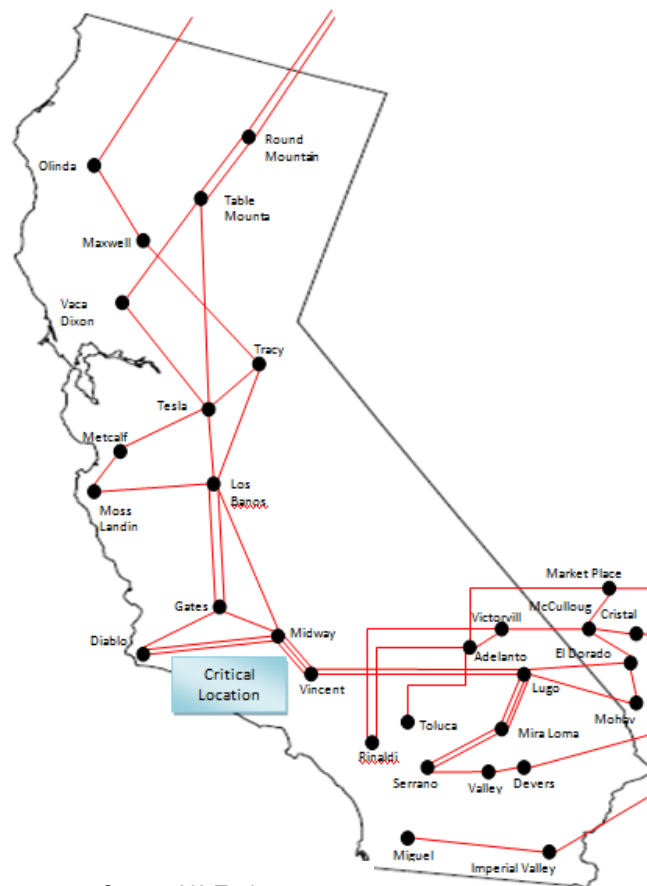


Figure 409: Schematic: 500 kV Buses and Lines in California



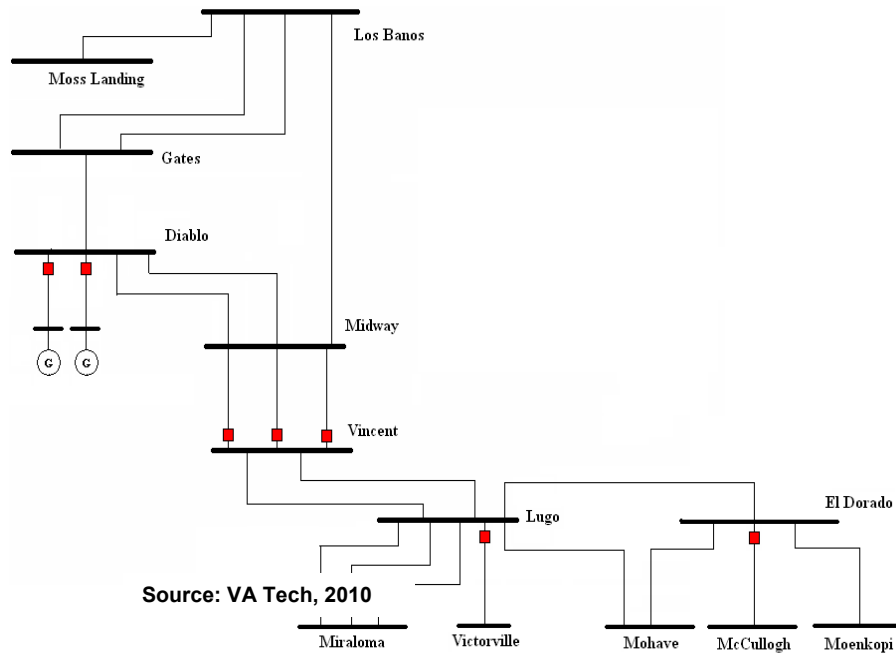
Source: VA Tech, 2010

Midway-Vincent is determined to be the system critical location. It is the location where an adaptive security - dependability scheme is most beneficial.

4.2.1.3 Critical Relay Locations

Figure 4.10 below shows that there were only 7 protective relays modeled on Path 15 and Path 26. Two Out-of-Step relays at Diablo, and five under-frequency line tripping relays. With this model, it is possible to lose two of the three Midway – Vincent lines without the third line tripping due to overloading and depressed voltages. In addition, areas in which the protective devices were properly modeled will exhibit more severe disturbances as the relays remove additional generators and lines.

Figure 41: Diagram of Protective Devices on Path 15 and Path 26



Based on the critical cases of Table 4.3 and the existing relays in Paths 15 and Path 26, an assessment of the distance relays which are most susceptible to encroachment due to power swings or increasing power flow revealed the following relay locations as the most critical. They are listed in the order of decreasing criticality:

- Midway – Vincent ck 3 500kV
- Midway – Vincent ck 2 500kV
- Midway – Vincent ck 1 500kV
- Los Banos – Midway ck 2 500kV
- Diablo – Midway ck 3 500kV
- Diablo – Midway ck 2 500kV
- Vaca-Dixon – Cottonwood 230kV

4.2.1.4 PMU Locations

Based on the analysis of the system model and the selected relay critical locations phasor measurement units at Midway 500kV, Los Banos 500kV, Diablo 500kV, and Vaca-Dixon 230kV were needed to monitor the critical relays.

4.2.2 Documentation of Relay Types and Characteristics to Be Included in Relay Database

The objective of this Task was to identify relays that were most susceptible to false tripping due to encroachment of their trip characteristics by an increase in loading or power swings. Alarms

were created to alert relay engineers and operators of occurrences where the relay was near tripping due to power swings and when encroachment was imminent. The alarm used phasor measurement units to calculate the apparent impedance seen by a relay, and then compared it to the trip characteristics of the relay. Alarms were placed at every relay in the system that was considered critical. Critical relays were those that were most at risk of encroachment as determined by exhaustive contingency analysis.

4.2.2.1 Alarms of Distance Relays

For distance relays, the primary concern was the minimum perpendicular distance of the apparent impedance from the relay's trip zone. When this distance reduces below 50 percent of the impedance of the line, an alarm was issued to warn of the potential for encroachment. A supervisory boundary which is a concentric circle with a radius 50 percent larger than the radius of Zone 2 is used to determine when the impedance had moved too close to the relay's trip characteristics. In PG&E, Zone 2 is the largest zone and covers 120 percent of the line.

A contingency analysis under heavy winter and heavy summer conditions revealed that for no combinations of outages and three phase faults did either the power swing or the post-disturbance load flow cause encroachment of distance relays on critical 230kV and 500kV lines in California. This was largely due to the fact that there is no third zone and the second zone is very short. Despite this, the alarms are an efficiency tool for protection engineers who may not have the time to revisit relay settings periodically. The alarm warns of potential encroachment with time to revisit the settings before encroachment actually does occur.

The alarms for distance relays have been developed and fully tested for relays on all 230kV and 500kV lines in California. The results indicated that none of these relays were susceptible to encroachment under heavy summer and heavy winter conditions.

4.2.2.2 Alarms of Loss-of-Excitation Relays

For distance relays and loss-of-excitation relays, the primary concern was the minimum perpendicular distance of the apparent impedance from the relay's trip zone. When this distance reduces below 50 percent of the impedance of the line, an alarm was issued to warn of the potential for encroachment. A supervisory boundary which is a concentric circle with a radius 50 percent larger than the trip region is used to determine when the impedance has gotten too close to the relay's trip characteristics.

4.2.2.3 Alarms for Out-of-Step Relays

Out-of-step relay settings have been known to become obsolete and mis-operate in the same way that distance and loss-of-field relays do. However, it is far more difficult to measure the proximity to encroachment of a distance relay. Changes in system topology, generation dispatch, and loads affect the size and speed of power swings as well as the center of inertia of the power system.

Alarms for out-of-step relays were based on identifying contingencies that cause significant changes in the location of the swing center and the size and speed of stable swings at the location of the out-of-step relay. When these critical contingencies occur, an alarm is issued indicating that the out-of-step relay is at risk of tripping for stable swings. Phasor and Supervisory Control and Data Acquisition (SCADA) measurements may be used to determine when these contingencies occur.

This process sets the boundaries for the out-of-step relay by identifying the largest stable swings. In the rare occasion that the settings for some swings are mutually exclusive, the alarms send a signal to alter the out-of-step relay settings when the system conditions require it. One of the main advantages of this process is that it automates the settings of out-of-step relays and makes it easy to revisit the settings periodically when the system model is updated.

To test this process a program was written in PSLF to perform the following functions:

- For different system conditions all significant N-1 and N-2 outages (500kV lines and generators above 400MW) and the most severe three phase faults are simulated.
- The size and speed of each stable power swing is quantified.
- Each stable power swing was compared to the out-of-step relay's settings to test for encroachment. If the settings were unavailable, each stable swing was compared to swings in the normal operating case.
- A list was created of the contingencies that caused encroachment of the out-of-step relay's settings. If the settings were unavailable, a list of the contingencies that significantly increased the size of the swing was developed.
- A list of the locations where PMUs would be required to detect each contingency is created.

Steps 1-5 should be repeated for every out-of-step relay in the system.

An algorithm was developed to find the contingencies that make out-of-step relays lose their ability to differentiate between stable swings and unstable swings. The advantage of this system design was that it was fully automated in GE-PSLF so that as the model changed or new out-of-step relays were inserted, the program can be easily re-run. When sufficient phasor measurement units were available, it was possible to automatically detect the N-1 or N-2 conditions for which an out-of-step relay's settings were incorrect and issue an alarm accordingly.

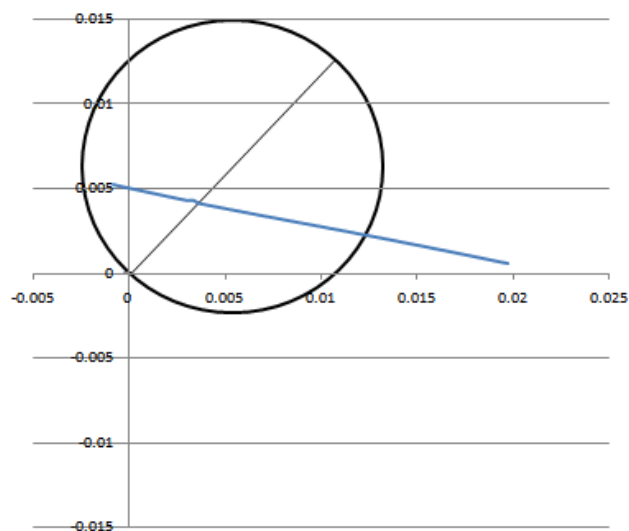
4.3 Relay Encroachment System

4.3.1 Introduction

Distance, loss-of-excitation, and out-of-step tripping relays were all susceptible to over-tripping due to load encroachment, changes in the system topology, and other changes in operating conditions. For distance and loss-of-excitation relays, the alarms were created by defining a

supervisory boundary in the apparent impedance plane. The supervisory boundary was a concentric circle 50 percent larger than the largest zone of the relay. If the apparent impedance crossed the supervisory boundary, an alarm indicated that the risk of false tripping due to encroachment of the relay trip characteristics was imminent. The trip characteristics of out-of-step tripping relays were defined in the impedance plane with timers which meant that it was more difficult to measure encroachment on the relay trip characteristics. To reduce the difficulty, alarms for out-of-step relays were based on identifying conditions and contingencies that caused significant changes in the location of the swing center. This means that the trajectory of the apparent impedance of an unstable swing at the location of the relay may or may not encroach on the inner zone. The swing center is the location in the power system where the voltage magnitudes are small or zero because the areas that are swinging against each other are 180° apart. This location is identifiable through simulation. Figure 4.11 showed the apparent impedance trajectory that was observed by an out-of-step relay at the Captain Jack side of the Captain Jack – Olinda line. For an unstable condition, the apparent impedance moved through the inner zone of a typical out-of-step relay causing the relay tripped correctly.

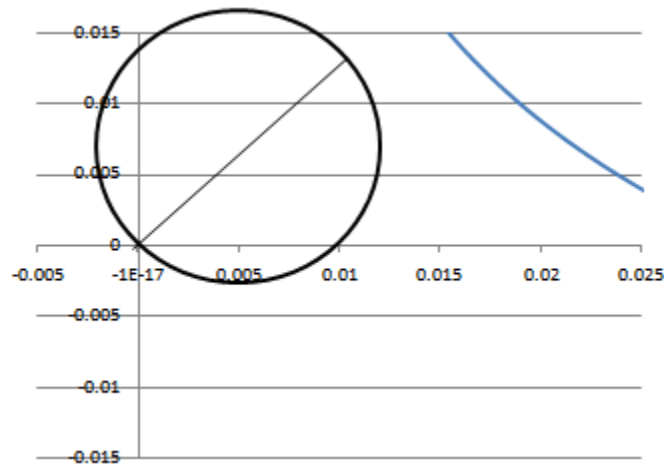
Figure 42: OOS Swing at Captain Jack – Olinda



Source: VA Tech, 2010

Figure 4.12 shows the same contingency, but this time the Maxwell-Tracy line was out-of-service before the contingency occurred. Now, the trajectory has changed so much that a typical out-of-step relay at Captain Jack would not trip even though the power swing was still unstable.

Figure 43: OOS Swing at Captain Jack – Olinda with Maxwell - Tracy Out-of-Service



Source: VA Tech, 2010

The Maxwell-Tracy outage was only one of several outages that caused a typical out-of-step relay at Captain Jack to lose its ability to identify unstable swings. A list of the outages and operating conditions for which this relay did not perform correctly will have to be generated through offline studies. Phasor measurements and SCADA can be used in real-time to detect these conditions and trigger an alarm.

The alarms for distance relays and loss-of-excitation relays required a PMU at the location of each relay and communication channels to send data to the control center in real-time. These alarms were intended for protection engineers (not operators) since the settings of the relays may need to be reviewed in detail. Essentially, it is an efficiency tool for protection engineers who may not have the time to revisit relay settings as often as the system requires.

4.3.2 Identifying Crucial Alarms

Occasionally, alarms due to load encroachment arise when severe contingencies cause the power flow along a line to increase. If it is a low-probability event and the apparent impedance was still encroaching upon the characteristic, this may not be of concern to a protection engineer. The crucial alarms are the ones that occur daily during peak conditions because this indicates a sustained problem.

Alarms generated due to encroachment by power swings were investigated and the initiating event was identified. If the size of the swing was large enough that the apparent impedance came close to the instantaneous trip zones, it indicated a high risk of false tripping for future swings. However, if a fast-moving swing only came close to the zones with time delays, then the risk of false tripping was relatively low. Additionally, if the initiating event was a relatively insignificant event, such as short fault on a medium voltage line, then the alarm was considered crucial since it was likely that a larger event would cause a false trip.

Ideally, out-of-step tripping relays should function properly for all reasonable system conditions. However, in some cases, it may be difficult to set the relays so that they perform securely and dependably for a wide range of cases. In such situations, an alarm is created by identifying the conditions for which the relay will fail to trip. If an alarm frequently occurs for the same condition, this scenario should be identified as a frequent operating state and countermeasures should be taken to ensure that there is adequate system protection in this state.

4.3.3 Determining Countermeasures for Alarms

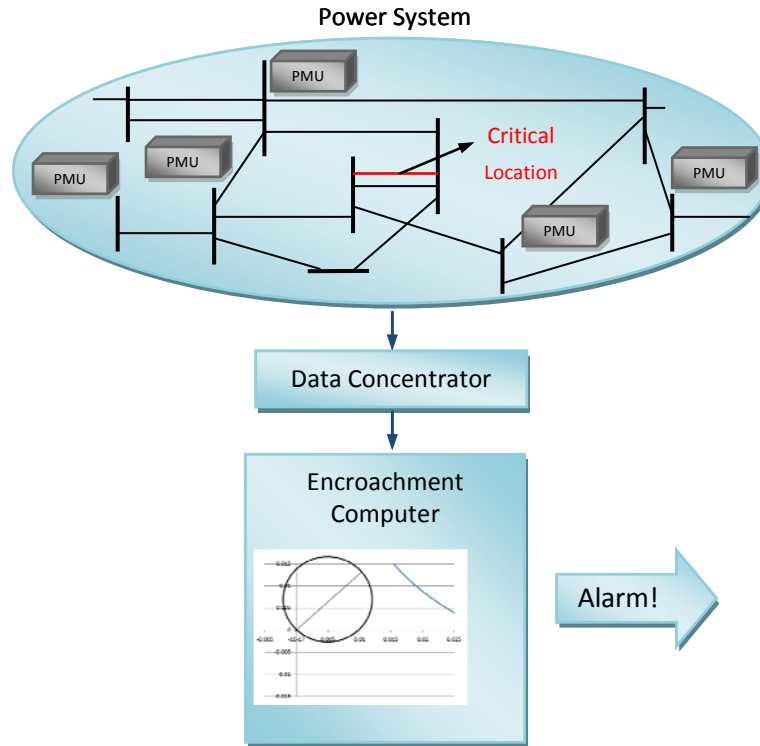
With digital relays, it is possible to take automatic actions when an alarm is generated. The trip region of distance relays and loss-of-excitation relays could be shrunk or reshaped to prevent load encroachment without impacting security. Many digital relays already use a load encroachment function that reshapes the trip region for all conditions. This idea is improved upon by only reshaping the trip region when the situation requires it. Additionally, power swing blocking is used to prevent false tripping when the speed of the apparent impedance trajectory indicates that it is not a fault. Out-of-step relays can automatically switch to alternative settings when it is recognized that the existing settings are inappropriate for the prevailing system conditions. Automatic actions depend heavily on the proper functioning of phasor measurement units, digital relays, and communication channels. Defects in any of these elements can result in false tripping or a failure to trip.

The alarms described here call the protection engineer's attention to a potential problem, provides information on the problem, and in some cases, gives recommendations. For alarms relating to the encroachment of distance relays and loss-of-excitation relays, the trajectory of the apparent impedance before and after the encroachment is shown along with all the power system variables measured at the relay's terminals. This information and the line parameters allow an engineer to decide how to adjust the settings. Alarms for out-of-step relays indicate which system condition triggered the outage, the location of the new swing center of the system, and how the settings on the out-of-step relay should be changed to ensure protection during this condition. The apparent impedance trajectory at the relay's location is observed through simulation and the recommended settings are developed accordingly.

4.3.4 Functional Operation

A functional overview of the adaptive out-of-step scheme is given by the schematic shown in Figure 4.13. Wide-area measurements are obtained with the aid of PMUs at the selected buses which provide enough information to determine encroachment conditions at the selected relay locations. Measurements are collected by a data concentrator at the control center and used by the encroachment computer to determine if load is encroaching into the protection zones of the selected relay. If an encroachment is detected, an alarm is sent to the protection engineer to review the settings of the encroached relay.

Figure 44: Functional Overview of the Real-Time Alarms for Encroachment Scheme



Source: VA Tech, 2010

4.3.4.1 PMU Minimum Specification

The PMU must comply with the IEEE-C37.118 or latest Synchrophasor standard, and send voltage angle information to the data concentrator at a minimum rate of 15 measurements per second. A 30 measurement per second rate is preferred. PMUs should be located at the following locations:

- Midway 500kV,
- Los Baños 500kV,
- Diablo 500kV, and
- Vaca-Dixon 230kV.

4.3.4.2 Data Concentrator Specifications

The function of the data concentrator is to collect data from the 10 PMUs and send a single “time-aligned” data string to the out-of-step computer. The data concentrator should be able to handle the 30 samples per second rate of 10 PMUs and provide the time-aligned angles to the out-of-step computer with the minimum delay.

4.3.4.3 Encroachment Alarm Computer Specifications

A computer at the control center will use the PMU data to monitor the load and swing excursions at the selected location. The computer compares the load path and swing centers to the stored values to determine encroachment or swing center variations large enough to trigger an alarm. If the alarm is activated, a protection engineer will investigate the case by evaluating the data file that is saved each time an alarm is triggered.

Serial or network communication channels are required to communicate to the data concentrator and control center computer. The distance relays most susceptible to encroachment due to power swings or increasing power flow are the following relays. They are listed in the order of decreasing criticality:

- Midway – Vincent ck 3 500kV
- Midway – Vincent ck 2 500kV
- Midway – Vincent ck 1 500kV
- Los Banos – Midway ck 2 500kV
- Diablo – Midway ck 3 500kV
- Diablo – Midway ck 2 500kV

Information on the protection settings of the selected relays must be stored and updated periodically in the encroachment alarm computer.

CHAPTER 5:

Adaptive Out-of-Step Protection on Critical Tie-Lines

5.1 Introduction

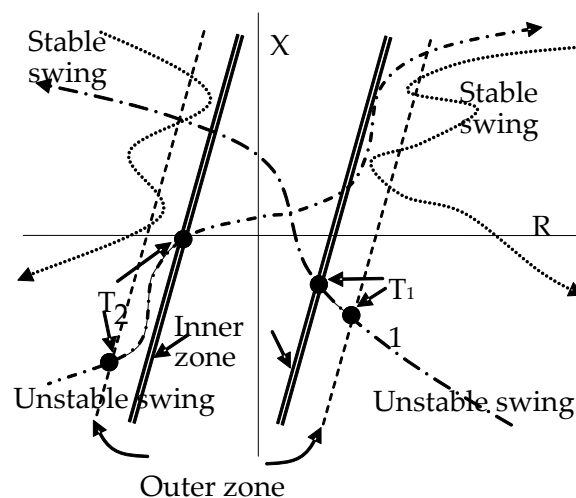
The technical objective of this research was to use real-time synchronized phasor measurement data to provide improved protection system supervision to make it adaptive to prevailing system state. By using real-time WAMS, it is possible to determine optimum protection policies and settings for critically located relaying systems. In particular, adaptive adjustment on of dependability and security, alarming on potential load encroachment, and more intelligent out-of-step relaying tasks can be improved with the use of WAMS. Task 4 focused on developing a method for using real-time wide area data to for real-time out-of-step determination for the developed system model.

5.1.1 Traditional Out-of-Step Relays

It is recognized that a group of generators going out of step with the rest of the power system is often a precursor of a complete system collapse. Whether an electromechanical transient will lead to a stable or an unstable condition has to be determined reliably before appropriate control action could be taken to bring the power system to a viable steady state. Out-of-step relays are designed to perform this detection and also to take appropriate tripping and blocking decisions.

Traditional out-of-step relays use impedance relay zones to determine whether or not an electromechanical swing will lead to instability. A brief description of these relays and the procedure for determining their settings is provided here.

Figure 45: Traditional Out-of-Step Relay



Source: VA Tech, 2010

In order to determine the settings of these relays it is necessary to run a large number of transient stability simulations for various loading conditions and credible contingencies. Using the apparent impedance trajectories observed at locations near the electrical center of the system during these simulation studies, two zones of an impedance relay are set, so that the inner zone is not penetrated by any stable swing. This is illustrated in Figure 5.1.

The outer zone is shown by a dashed line, and the inner zone is shown by a double line. Note that all the stable swing trajectories remain outside the inner zone, while all the unstable swing trajectories penetrate the outer as well as the inner zone. Although only two impedance characteristics are shown for stable and unstable cases, in reality a large number of such impedance loci must be examined. The time duration for which the unstable swings dwell between the outer and inner zones are identified as T_1 and T_2 for the two unstable characteristics shown in the figure. The largest of these dwell times (with some margin) is chosen as the timer setting for the out-of-step relay. If an actual observed impedance locus penetrates the outer zone, but does not penetrate the inner zone before the timer expires, the swing is declared to be a stable swing. If it penetrates the outer zone and then the inner zone before the timer runs out, it is an unstable swing. Stable swings do not require any control action, whereas unstable swings usually lead to out-of-step blocking and tripping actions at pre-determined locations.

5.1.2 Problems With Traditional Out-of-Step Relays

Traditional out-of-step relays are found to be unsatisfactory in highly interconnected power networks. This is because the conditions assumed when the relay characteristics are determined become out-of-date rather quickly, and in reality the electromechanical swings that do occur are quite different from those studied when the relays are set. The result is that traditional out-of-step relays often mis-operate: they fail to determine correctly whether or not an evolving electromechanical swing is stable or unstable. Consequently their control actions also are often erroneous, exacerbating the evolving cascading phenomena and perhaps leading to an even greater catastrophe.

WAMS of positive sequence voltages at networks provide a direct path to determining stability using real-time data instead of using pre-calculated relay settings. This problem is very difficult to solve in a completely general case. However, progress could be made towards an out-of-step relay which adapts itself to changing system conditions. Angular swings could be observed directly, and time-series expansions could be used to predict the outcome of an evolving swing. It is highly desirable to develop this technique initially for known points of separation in the system. This is often known from past experience, and use should be made of this information. In time, as experience with this first version of the adaptive out-of-step relay is gained, more complex system structures with unknown paths of separation could be tackled.

5.1.3 Selection of Study System Base Case

The study was performed using computer simulations of three base cases provided by PG&E who assisted in developing the reduced system model used for this task. A number of studies

simulating stable and unstable swings were performed based on the reduced models, and optimum PMU locations were determined for observing the movement of machine rotors in real time.

5.1.4 Determination of Coherent Groups of Machine

An algorithm was developed for determining the principal coherent groups of machines as the electromechanical swings begin to evolve. Criteria for judging coherency between machines and groups of machines was developed and the centers of angles for each coherent group were used in determining out-of-step condition.

5.1.5 Predicting the Out-of-Step Condition From Real-Time Data

It is of course possible to determine whether or not a swing is unstable by waiting long enough and observing the actual swing. However, to take appropriate control action it is essential to develop a reliable prediction algorithm that provides the stable-unstable classification of an evolving swing in a reasonable time. Assuming that the normal periods of power system swings on a large interconnected power system are of the order of a few seconds, a 250 millisecond target is reasonable. With the observed swing evolution, a time-series approximation to the swings is made to provide the predicted regions of the swings.

5.2 Adaptive Out-of-Step Protection

5.2.1 Introduction

The objective of Task 4 is to develop out-of-step relays that adapt (either blocking or tripping) to changing system conditions based on wide-area measurements taken in key parts of the California system. This section of the report presents the:

- List of PMU locations for observing rotor swings,
- Proposed techniques for determining machine coherency with PMU data, and
- Proposed techniques for determining swing prediction algorithms with PMU data.

5.2.2 List of PMU Location for Observing Rotor Angle Swings

Using the California models developed for this task, a total of 501 cases in each of the three models of the California System (Heavy Winter, Heavy Summer and Light Summer) were simulated. Even though the total number of simulations completed is relatively large (1503), only 9 critical cases were found in which the system breaks apart and the identification of coherent groups can be achieved. More than 9 unstable cases were found, but on the other non-critical cases machines close to the disturbance go out of step and the rest of the system remains stable.

5.2.2.1 Simulations

Two different types of realistic fault scenarios were applied to different locations of the available system models:

Breaker Failure Fault: A line fault followed by the failure to trip of the primary relay causes the set of breaker-failure relays to operate and clear the fault at 10 cycles. This type of fault leads to the isolation of one bus. In order to simulate this fault in the California System, a 10-cycle bus fault was applied at one specific bus followed by the removal of all the lines connected to that bus. This type of fault was applied at each of the 500kV and 230 kV buses in the system.

Two Hidden Failures: As found in Task 2, a 4 cycles line fault between Midway 500kV and Vincent 500kV, the proper removal of the faulted line, and the improper removal of the 2 adjacent lines due to two hidden failures will cause the system to break apart.

5.2.2.2 Critical Cases

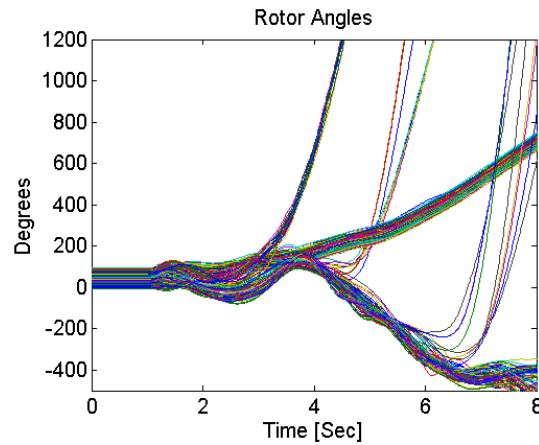
The following critical cases with coherent swings were identified on the available system models:

Heavy Winter Model	
Lugo 500 kV	Breaker Failure
Vincent 500 kV	Breaker Failure
Midway 500kV-Vincent 500 kV	2 Hidden Failures
Heavy Summer Model	
Midway 500 kV	Breaker Failure
Lugo 500 kV	Breaker Failure
Vincent 500 kV	Breaker Failure
Market Place 500 kV	Breaker Failure
Midway 500kV-Vincent 500 kV	2 Hidden Failures
Light Summer Model	
Lugo 500 kV	Breaker Failure

5.2.2.3 Critical Cases Discussions

Figure 5.2, shows the rotor angle response of the system when a breaker failure fault is applied at Vincent 500 kV. A breaker failure fault in Vincent isolates the bus from the grid. This means that the 3 lines from Vincent 500kV to Midway 500kV are removed from the system as well which leads to the separation of the system into 2 subsystems.

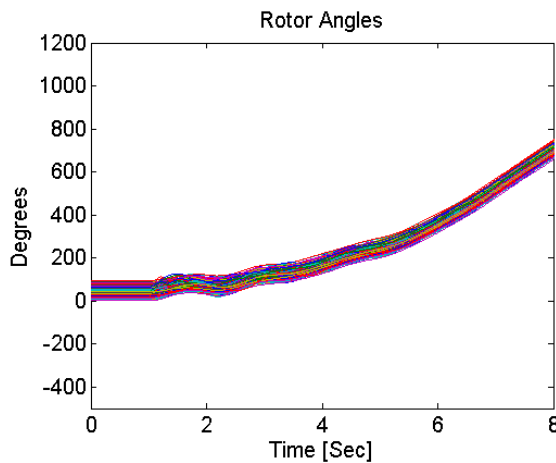
Figure 46: Rotor Angles for Breaker Failure at Vincent 500kv



Source: VA Tech, 2010

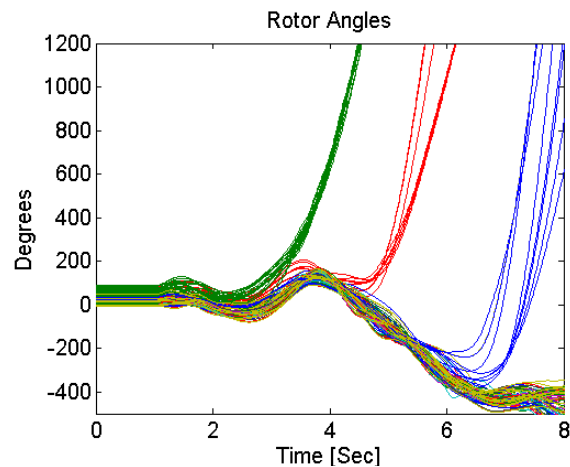
Figure 5.3 shows the classification of these groups. Figure 5.3.a shows area 30 and Figure 5.3.b areas 21, 22, 24 and 26.

Figure 47: a) Rotor Angles for Area 30



Source: VA Tech, 2010

b) Rotor Angles for Southern California



Source: VA Tech, 2010

As seen in Figure 5.3, Area 30 does not present oscillations within its system and none of its generators go out-of-step. On the other hand, Southern California (Areas 21, 22, 24 and 26) is the part of the system where out-of-step conditions are present. Four groups of machines can be identified by inspection of this Figure 5.3.

Three groups of coherent generators go out-of-step in Southern California:

Green	Red	Blue
MC GEN	DPWR#3	MNTV-CT1
LUZ8 G	UNIT5L	MNTV-CT2

A similar behavior was found in all critical cases. In all cases, the system always breaks apart into two subsystems, Northern California (Area 30) and Southern California. Northern California does not have major problems in its system. In Southern California there are several groups of machines that go out-of-step.

5.2.3 PMU Location List

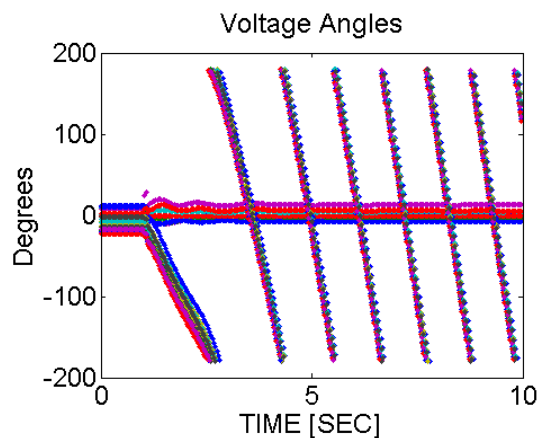
After the nine critical unstable cases were analyzed and the geographical locations of the coherent groups of machines were found, PMUs are recommended at the following 10 locations to detect and monitor coherent groups in the California system.

LOSBANOS	500 kV	KRAMER	230 kV
MORROBAY	230 kV	MNT. VIEW	230 kV
DIABLO	500 kV	HAYNES	230 kV
IMP. VALLEY	230 kV	VULCAN 1	92 kV
MAGUNDEN	230 kV	LITEHIPE	230 kV

5.2.4 Additional PMU Angle Issues

In this task, voltage angle measurements are used to identify out-of-step conditions in the California system. These measurements should be taken on previously selected buses where this kind of behavior is expected to happen.

Figure 48: Wrapped Voltage Angle Due to Frequency Deviation



Source: VA Tech, 2010

One of the challenges of using voltage angle measurements is that the angle data provided by phasor units is constrained only to values between -180 and 180 degrees. This means that a voltage change of +2 degrees from a value of 179° will appear as -179° in the next sample point instead of 181°. This issue makes it difficult to detect constantly increasing or decreasing voltage angles. Figure 5.4 shows this condition.

5.2.4.1 Voltage Angle “UNWRAPPING”

In order to overcome this situation the next algorithm is proposed:

$$\text{Unwrapped (UW) ANGLE}_n = \text{Angle}_n + C_n * 360 \quad (5.1)$$

C = Unwrapping Constant

$$C_0 = 0$$

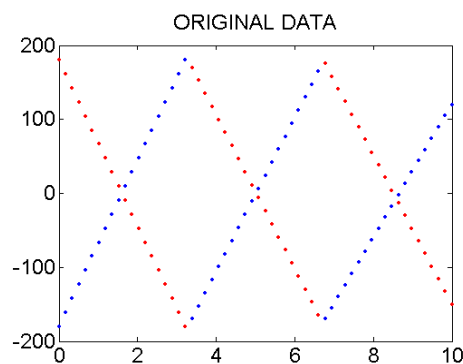
If $\text{Angle}_n - \text{Angle}_{n-1} > 180$, $C_n = C_{n-1} - 1$;

If $\text{Angle}_n - \text{Angle}_{n-1} < -180$, $C_n = C_{n-1} + 1$;

The voltage angle measured by the PMU is replaced by a UW angle” that depends on the “unwrapping” constant C . The initial value of such constant is zero and at every time step the constant is recalculated depending on the variation of the voltage angle.

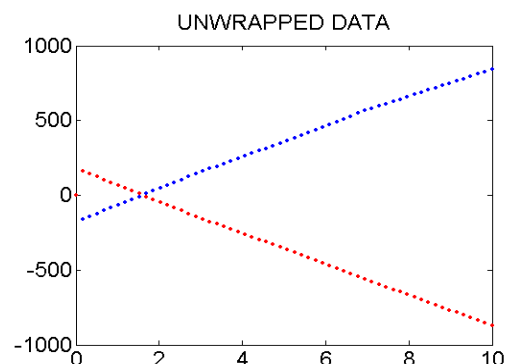
If the change in voltage angle in one time step is greater than 180 degrees, the constant decreases one unit and the algorithm declares that the magnitude of the voltage angle is decreasing; whereas, if the change in voltage angle is smaller than 180 degrees the constant increases one unit and the algorithm declares that the magnitude of the voltage angle is increasing. Figure 5.5a and b show how this algorithm works.

Figure 49: a) Sample Wrapped Angle Plot



Source: VA Tech, 2010

b) Sample Unwrapped Angle Plot



5.2.4.2 Rotor Angles and PMU Voltage Angle

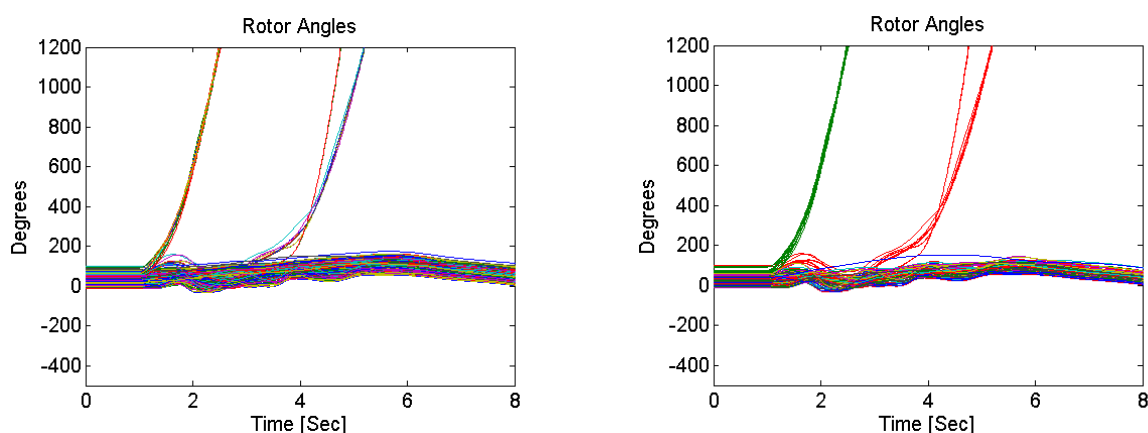
One of the objectives of this task is to develop an algorithm to infer rotor angles from voltage angles. In this section, it will be shown that the PMU voltage angles of selected buses can be used to infer rotor angles; therefore they can be used to detect out-of-step conditions in the system.

In order to demonstrate that PMU voltage angles can be used to infer rotor angles, one of the nine critical cases listed in the previous report will be analyzed.

5.2.4.2.1 Lugo 500 kV (Breaker Failure) – Light Summer

Figure 5.6.a shows the rotor angle response of the system when a breaker failure fault is applied at Lugo 500 kV. Figure 5.6.b shows the color coded classification of the machines into coherent groups (machines in area 30 are not shown).

Figure 50: a) Rotor Angles, Lugo Breaker Failure b) Color-Coded Coherent Groups for Same Failure



Source: VA Tech, 2010

The 6 groups of machines that go out-of-step in Southern California (areas 21,22,24,26) are the following:

Green	Red
HIDEDST1	DPWR#3
MOGEN G	SIGC

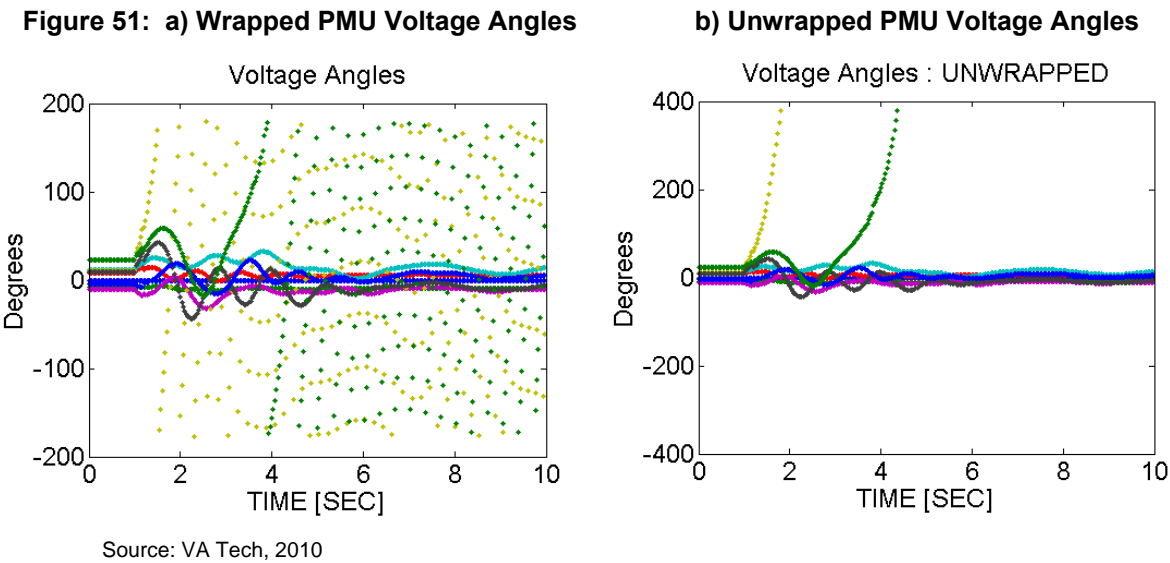
Note: Not all unstable machines are listed

Once the coherent groups are identified, the following step consist of selecting one bus for each coherent group that is close enough to the machines in which the voltage angle is going to be measured.

For this particular case these are the buses where PMU’s are to be placed:

Green	Red
Kramer	Vulcan 1
230 kV	92 kV

Figure 5.7 shows the voltage angles at the buses listed above and some other buses that are needed for other cases. Figure 5.7.b shows how the “unwrapped” voltage angles correctly depict the rotor angles of the coherent groups for this case. A sampling rate of two cycles was used. Similar results were obtained for the other eight critical cases.



5.2.4.2.2 Reference Angle

Los Banos 500 kV is proposed to be the reference for the voltage angle measurements. This bus was selected since it is located in northern California, an area with no important oscillations inside the region. Any 500 kV buses in this area could have been selected for this purpose, except for Diablo 500 kV and Midway 500 kV.

5.2.5 Proposed Techniques for Determining Machine Coherency

There are three ways to do coherency identification: linearization, frequency domain, and time domain. The linearization method is based on the small signal stability analysis, so the coherency is almost fixed and independent of the fault location and loading conditions. Frequency domain method analyzes the oscillation frequency with the coherency identification.

For this task, a time domain method is proposed to identify the coherent groups of generators. The basic idea is:

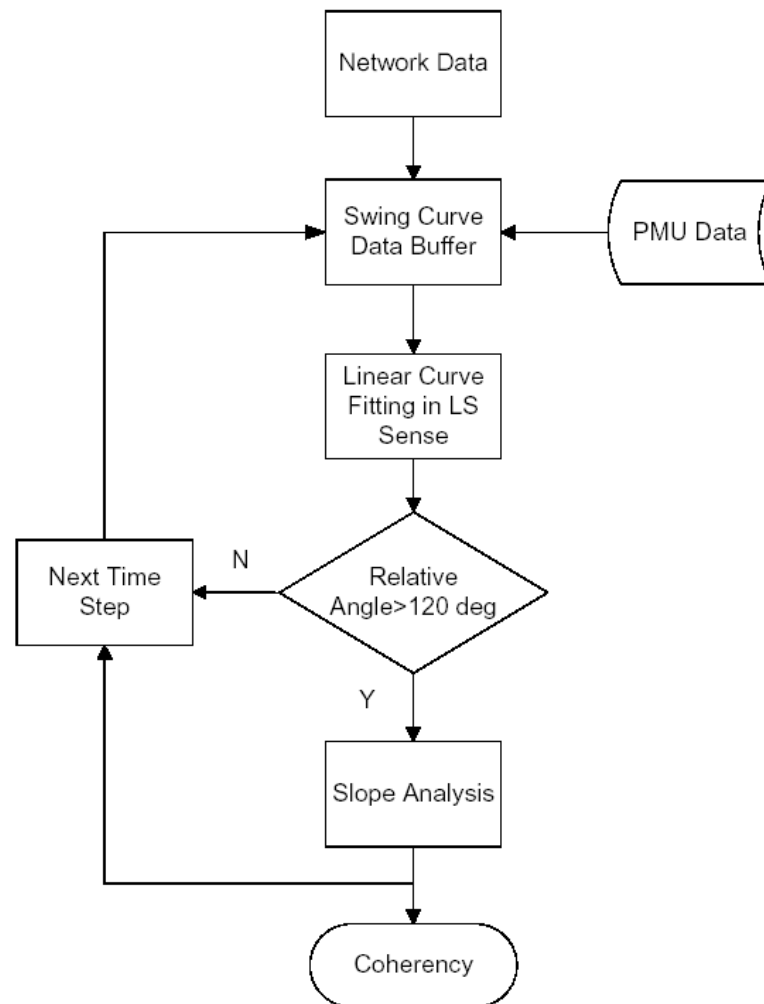
- Measure all generator angles,
- Curve fitting in the Least Square sense,
- Linear model $y=a+bx$,
- Growing window or sliding window, and
- Use the slope b to identify coherency when any angle is bigger than a threshold value (120 degrees).
- The flow chart of the proposed algorithm is shown in Figure 5.8.

This method was first applied to the reduced WECC test system with two variations of the algorithm:

- Moving Window: Once triggered this version of the algorithm uses a fixed side window of data that moves in time as the data is received from the phasor measurement units, Figure 5.9.
- Growing Window: This version of the algorithm starts a data window at the triggering point and the window continues as data is received from the phasor measurement units, Figure 5.10.
- Test Scenarios included stable cases, first-swing unstable cases, and multi-swing unstable cases. Some conclusions are explained as following different angle references like initial values and John Day values were compared and it was concluded as expected that the reference angle does not play a very important role in the method.

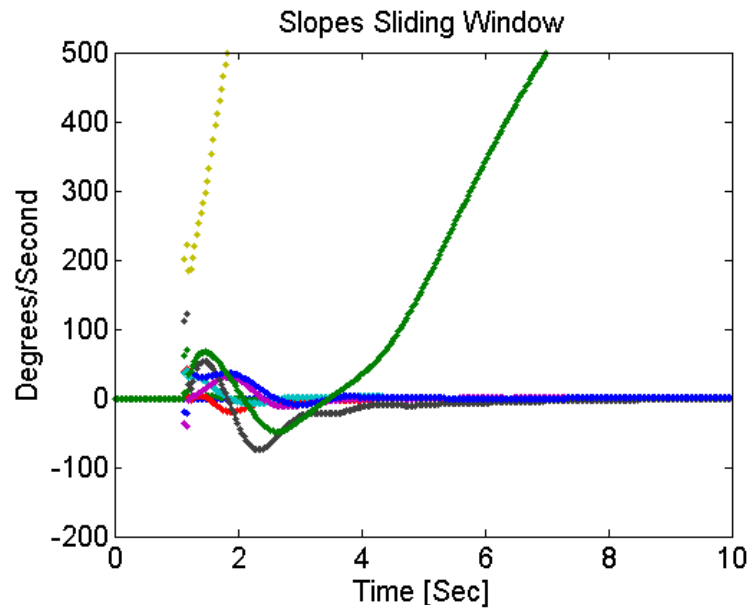
The growing window is very effective in identifying the first-swing unstable cases. However, using sliding window will cause a delay. The bigger the window size, the longer the delay. Using the sliding window is reliable to identify the multi-swing unstable cases because it can stay away from the initial oscillation and give much bigger slope values. The size of sliding window was also studied. In the simulations, a one-second window and a two-second window were used for comparison. The one-second window is faster, but two-second window is more reliable for the identification.

Figure 528: Flow Chart of Proposed Coherency Identification Algorithm



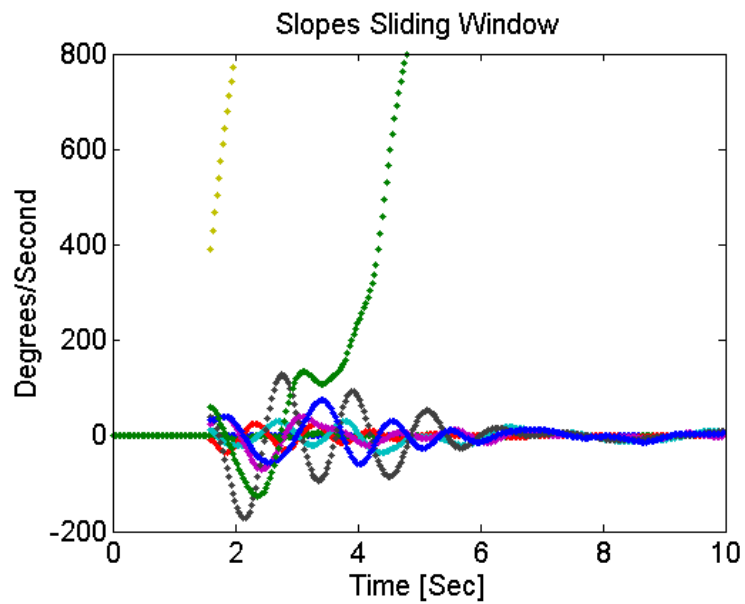
Source: VA Tech, 2010

Figure 53: Growing Window Sample



Source: VA Tech, 2010

Figure 54: Sliding Window Sample. Window size 0.5 Seconds



Source: VA Tech, 2010

5.2.6 Techniques for Performing Swing Prediction Algorithms With PMU Data

Time series analysis is a statistical tool used for analyzing and modeling a sequence of ordered data. This tool can also be used to forecast future data points based on previously recorded observations. In this report an autoregressive model (AR) will be used to predict future voltage angles.

The expression for an autoregressive model order 1 AR(1) is the following:

$$\theta_t = \varphi \theta_{t-1} + \varepsilon \quad (5.2)$$

In this model the forecasted value is related to the immediately previous data point. The parameter (φ) of this model is calculated minimizing the sum of the squared errors (Least Squares Estimation).

$$\min J(\varphi) = \sum_{t=1}^T (\theta_t - \varphi \theta_{t-1})^2 \quad (5.3)$$

Taking the first derivative of $J(\varphi)$ with respect to φ and setting it equal to zero, the following expression for φ is obtained.

$$\varphi = \frac{\sum_{t=1}^T (\theta_t * \theta_{t-1})}{\sum_{t=1}^T (\theta_{t-1})^2} \quad (5.4)$$

5.2.6.1 Autoregressive Model Order 3 – AR(3)

It was found that an AR(3) provided a good estimation for the voltage angle data. An AR(1) and AR(2) model were also studied but the predicted values considerably differed from those obtained in the simulations.

An AR(3) has the following expression:

$$\theta_t = \varphi_1 \theta_{t-1} + \varphi_2 \theta_{t-2} + \varphi_3 \theta_{t-3} + \varepsilon \quad (5.5)$$

The parameters (φ_1, φ_2 and φ_3) are also found minimizing the sum of the squared errors.

$$\varphi_1 = \frac{\sum_{t=1}^T (\theta_t * \theta_{t-1})}{\sum_{t=1}^T (\theta_{t-1})^2} - \varphi_2 \frac{\sum_{t=1}^T (\theta_{t-2} * \theta_{t-1})}{\sum_{t=1}^T (\theta_{t-1})^2} - \varphi_3 \frac{\sum_{t=1}^T (\theta_{t-3} * \theta_{t-1})}{\sum_{t=1}^T (\theta_{t-1})^2} \quad (5.6)$$

$$\varphi_2 = \frac{\sum_{t=1}^T (\theta_t * \theta_{t-2})}{\sum_{t=1}^T (\theta_{t-2})^2} - \varphi_1 \frac{\sum_{t=1}^T (\theta_{t-1} * \theta_{t-2})}{\sum_{t=1}^T (\theta_{t-2})^2} - \varphi_3 \frac{\sum_{t=1}^T (\theta_{t-3} * \theta_{t-2})}{\sum_{t=1}^T (\theta_{t-2})^2} \quad (5.7)$$

$$\varphi_3 = \frac{\sum_{t=1}^T (\theta_t * \theta_{t-3})}{\sum_{t=1}^T (\theta_{t-3})^2} - \varphi_1 \frac{\sum_{t=1}^T (\theta_{t-1} * \theta_{t-3})}{\sum_{t=1}^T (\theta_{t-3})^2} - \varphi_2 \frac{\sum_{t=1}^T (\theta_{t-2} * \theta_{t-3})}{\sum_{t=1}^T (\theta_{t-3})^2} \quad (5.8)$$

$$\begin{bmatrix} \varphi_1 \\ \varphi_2 \\ \varphi_3 \end{bmatrix} = \begin{bmatrix} 1 & \frac{\sum_{t=3}^T (\theta_{t-2} * \theta_{t-1})}{\sum_{t=3}^T (\theta_{t-1})^2} & \frac{\sum_{t=3}^T (\theta_{t-3} * \theta_{t-1})}{\sum_{t=3}^T (\theta_{t-1})^2} \\ \frac{\sum_{t=3}^T (\theta_{t-1} * \theta_{t-2})}{\sum_{t=3}^T (\theta_{t-2})^2} & 1 & \frac{\sum_{t=3}^T (\theta_{t-3} * \theta_{t-2})}{\sum_{t=3}^T (\theta_{t-2})^2} \\ \frac{\sum_{t=3}^T (\theta_{t-1} * \theta_{t-3})}{\sum_{t=3}^T (\theta_{t-3})^2} & \frac{\sum_{t=3}^T (\theta_{t-2} * \theta_{t-3})}{\sum_{t=3}^T (\theta_{t-3})^2} & 1 \end{bmatrix}^{-1} \begin{bmatrix} \frac{\sum_{t=3}^T (\theta_t * \theta_{t-1})}{\sum_{t=3}^T (\theta_{t-1})^2} \\ \frac{\sum_{t=3}^T (\theta_t * \theta_{t-2})}{\sum_{t=3}^T (\theta_{t-2})^2} \\ \frac{\sum_{t=3}^T (\theta_t * \theta_{t-3})}{\sum_{t=3}^T (\theta_{t-3})^2} \end{bmatrix}$$

In this model the future values are calculated using the three previous data points.

5.2.6.2 Considerations

In order to apply this time series analysis to an out-of-step protection scheme the following considerations should be taken into account:

- No relay action would take place in the first 20 cycles after the fault has been cleared. In this period of time the coefficients (φ) will be calculated.
- A rate of 30 messages per second for each PMU will be assumed. It should be mentioned that a higher message rate could improve the performance of this protection scheme.
- 10 points (1/3 seconds) will be forecasted using the autoregressive model described before.
- If the 10th forecasted point falls outside a threshold value in two consecutive predictions, an unstable swing would be declared and protection action should be initiated. Two consecutive predictions are used instead of one to verify the accuracy of the estimated values.
- The starting window size used to calculate the parameters would be 10 points, after the first prediction has been made, the scheme will wait for the next two measurements to arrive and it will delete the first point of the previous sequence of data to forecast the following points.
- Voltage Angles referenced to initial values are used.

5.2.7 Tripping Decisions

A center of angles will be calculated for northern (PG&E) and southern California in every prediction using the 10th forecasted value.

$$\theta_{COA} = \frac{\sum_{i=1}^n S_i \theta_i(t+1)}{\sum_{i=1}^n S_i} \quad (5.9)$$

S_i = MVA rating of the coherent group i

θ_i = Voltage Angle for the group i

Each voltage angle, θ_i , is then compared against its corresponding COA. If there exists a difference of 150 degrees between a given voltage angle and the COA in two consecutive predictions the algorithm declares an unstable swing and the group should be disconnected from the system. The disconnected group is disregarded in the following COA calculation.

5.2.7.1 PG&E-SCE Tripping Decision

If the absolute value of the COA for Southern California is greater than 150 degrees in two consecutive predictions, separation between SCE and PG&E should take place (Midway 500kV- Vincent 500kV). Note that since the reference bus is located in PG&E, the value of 150 in Southern California is actually a value with respect to PG&E.

5.3 Performance Evaluation and Functional Specifications

5.3.1 Performance Evaluation

In this section an evaluation of the swing protection algorithm is presented. The tests were carried out using the simulation outcomes of nine unstable and four stable cases. Each time the swing protection algorithm declared a voltage swing as unstable; the machines associated to that group were disconnected from the system.

Unstable Cases	Stable Cases
1-Breaker F. Lugo 500kV (HW)	10- Breaker F. Imp. Valley 500kV (HW)
2-Breaker F. Vincent 500 kV (HW)	11- Breaker F. Miraloma 500kV (HW)
3-1 Fault & 2 H. Failures Midway -Vincent (HW)	12- 8 cycles fault C. Valley 230 kV(HS)
4- Breaker F. Lugo 500kV (LS)	13- 7 cycles fault Mountain View 230 kV (HS)
5- Breaker F. Midway 500kV (HS)	
6- Breaker F. Lugo 500kV (HS)	
7- Breaker F. Vincent 500 kV (HS)	
8- Breaker F. Market Place 500kV (HS)	
9- 1 Fault & 2 H. Failures Midway –Vincent	

(HS)

5.3.1.1 Unstable Cases

The protection scheme is evaluated based on the time it takes to assert a tripping signal and the accuracy of the signal. The following tables show the times of: start of separation, swing detection, and the time between separation and detection. System separation is assumed when an unstable voltage swing was 50 degrees away from the rest of the system.

Case 1			
Split	Separation	Detection	Difference (ms)
Kramer	1.367	1.633	266
Haynes	2.567	2.767	200
PG&E-SCE	4.267	4.566	299
Magunden	4.633	4.767	134
Vulcan 1	4.733	4.833	100

Case 2			
Split	Separation	Detection	Difference (ms)
Kramer	3.233	3.433	200
Vulcan 1	4.430	4.560	130
Mnt. View	6.800	6.900	100
Haynes	7.933	8.100	167

Case 3			
Split	Separation	Detection	Difference (ms)
Kramer	7.200	7.300	100
Vulcan 1	7.200	7.367	167

Case 4			
Split	Separation	Detection	Difference (ms)
Kramer	1.267	1.567	300
Vulcan 1	3.530	3.767	237

Case 5			
Split	Separation	Detection	Difference (ms)
Diablo	1.367	1.567	200
Morrobay	1.433	1.633	200

Case 6			
Split	Separation	Detection	Difference (ms)
Kramer	1.300	1.567	267
Mnt. View	3.300	3.567	267
Vulcan 1	3.333	3.633	300
Haynes	5.333	5.760	427

Case 7			
Split	Separation	Detection	Difference (ms)
Kramer	3.267	3.467	200
Mnt. View	4.833	5.067	234
Magunden	5.167	5.467	300
Vulcan 1	5.500	5.730	230
Haynes	5.767	6.000	233

Case 8			
Split	Separation	Detection	Difference (ms)
Kramer	1.567	1.667	100
Mnt. View	2.000	2.200	200
Vulcan 1	2.033	2.333	300

Case 9			
Split	Separation	Detection	Difference (ms)
No action needed			

Table 5.1 summarizes the performance of the swing protection algorithm (ms): 217 ms is the average time the algorithm takes to detect an unstable swing. It should be mentioned that no stable swing was tagged as unstable, this implies an accuracy of 100 percent.

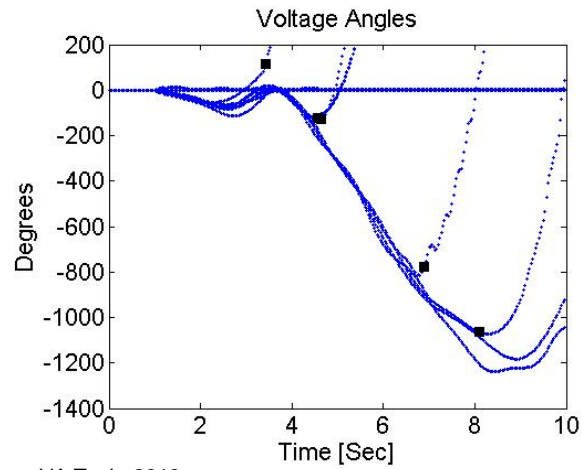
Table 5.1: Summary of Performance Evaluation

Evaluation	
Min	100 ms
Max	427 ms
Median	200 ms
Avg.	217 ms
Std. Dev.	79

Source: VA Tech, 2010

Figure 5.11 depicts the instants of time (black squares) when the algorithm declared an evolving swing as unstable for case 2.

Figure 55: Swing Determination Points

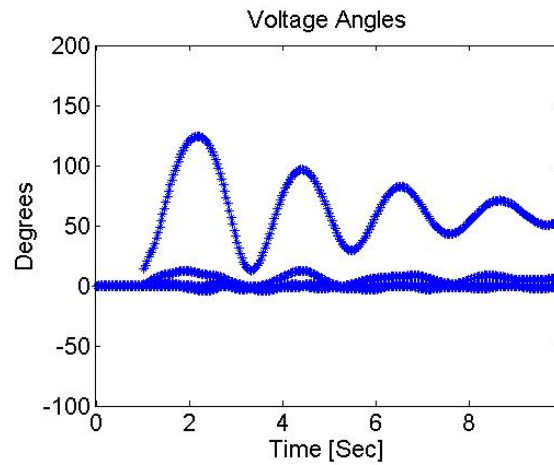


Source: VA Tech, 2010

5.3.1.2 Stable Cases

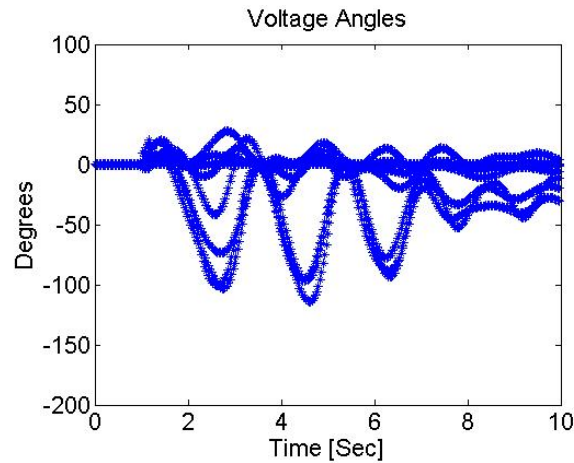
Figures 5.12 and 5.13 show the outcome of the swing protection algorithm applied to two stable cases. As it can be seen, the algorithm did not tag any swing as unstable. An identical result was obtained in the 2 other stable cases.

Figure 56: Swing Detection Algorithm for Stable Case 10



Source: VA Tech, 2010

Figure 57: Swing Detection Algorithm for Stable Case 11

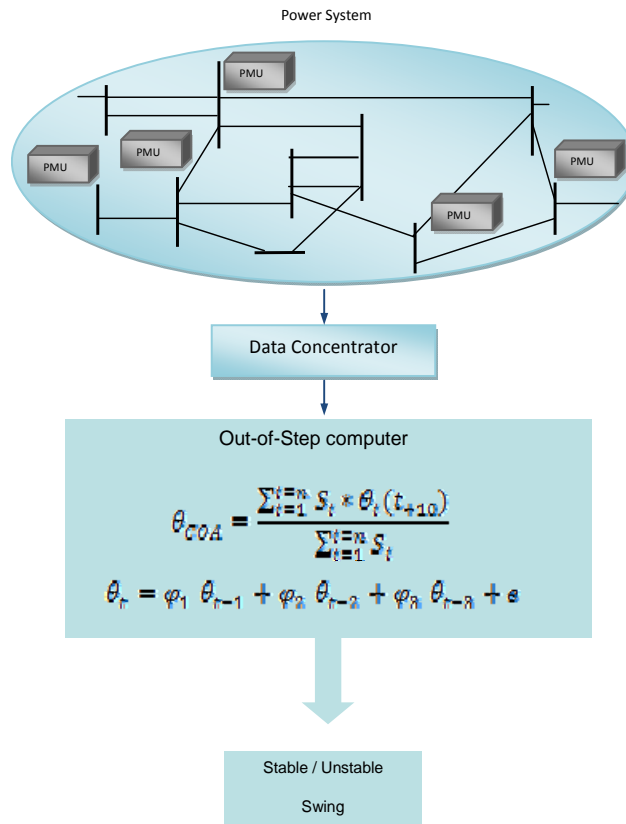


Source: VA Tech, 2010

5.3.2 Functional Specifications

A functional overview of the adaptive out-of-step scheme is given by the schematic shown in Figure 5.15. WAM obtained with the aid of PMUs at the selected buses provide enough information to discriminate between stable and unstable swings. Measurements are collected by a data concentrator at the control center and used by the out-of-step computer to determine the coherent groups and the stable and unstable conditions of detected swings. If a swing is determined to be unstable a signal is sent to the digital out-of-step relay to confirm the out-of-step trip. On the other hand, if the swing is found to be stable, a blocking signal is sent to existing out-of-step relays to avoid tripping on a stable swing.

Figure 58: Functional Overview of the Adaptive Out-of-Step Scheme



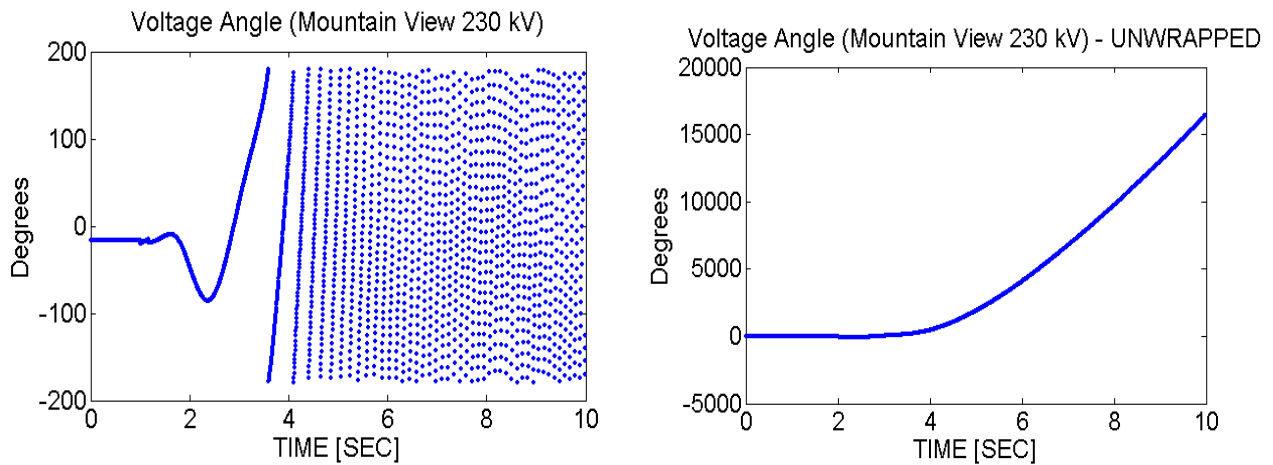
Source: VA Tech, 2010

5.3.2.1 PMU Minimum Specification

The PMU must comply with the IEEE-C37.118 or latest Synchrophasor standard, and send voltage angle information to the data concentrator. The sampling rate of the PMU must allow the developed algorithms to detect the system swings. As stated in section 5.2.4.1 to perform the voltage angle “unwrapping”, a change in the voltage angle of ± 180 degrees has to be detected. In cases where the rate of change of the voltage angle is high and the sampling rate is low, the algorithm may fail to detect such “jumps” and it will be impossible to establish if a voltage angle is increasing or decreasing in magnitude.

The preferred method to solve this problem is to set the PMU sampling rate as high as possible. In the next figures it can be seen that with a sampling rate of 5 cycles the “unwrapped” voltage angle does not describe the actual behavior of the voltage angle, while with a sampling rate of 2 cycles this is achieved. The data was obtained from a simulation.

Figure 59: a) Wrapped Angle at 240 Samples/Sec b) Unwrapped Angle at 240 Samples/Sec



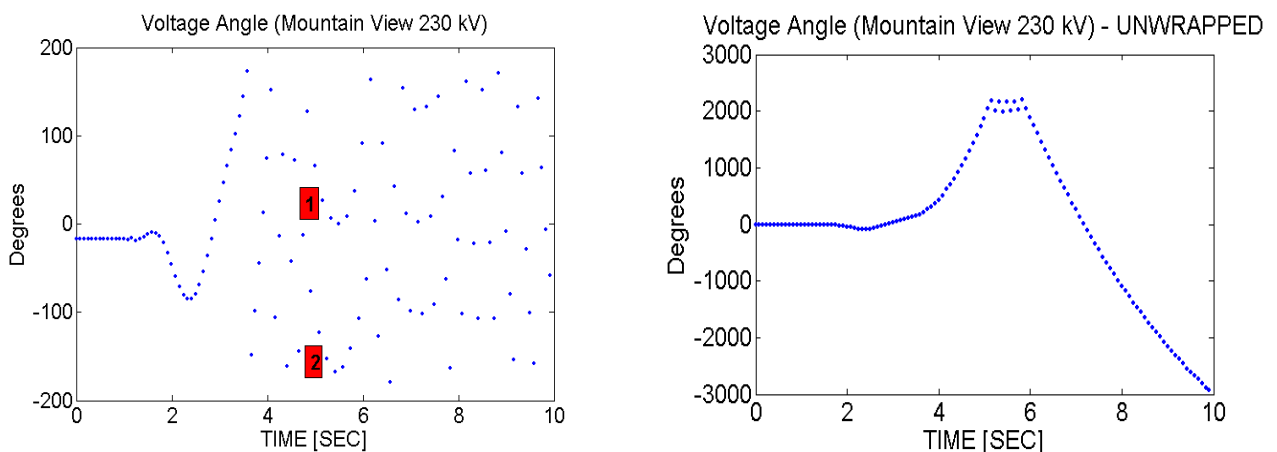
Source: VA Tech, 2010

Figures 5.15 shows how the voltage angle and “unwrapped” voltage angle would look for a sampling rate of 240 samples/second (4 samples per cycle).

Figures 5.16.a shows what the voltage angle for a sampling rate of 12 samples/second (every 5 cycles). Figure 5.16.b shows how the “unwrapping” algorithm fails to describe the behavior of the voltage angle at this sampling rate. The voltage angle difference between points 1 and 2 in Figure 4.6.a is 178 degrees; here is where the algorithm begins to fail.

Figure 60: A) Wrapped Angle at 12 Samples/Sec.

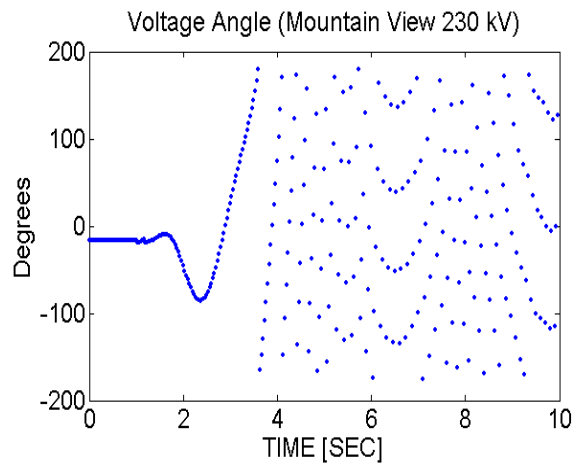
B) Unwrapped Angle at 12 Samples/Sec



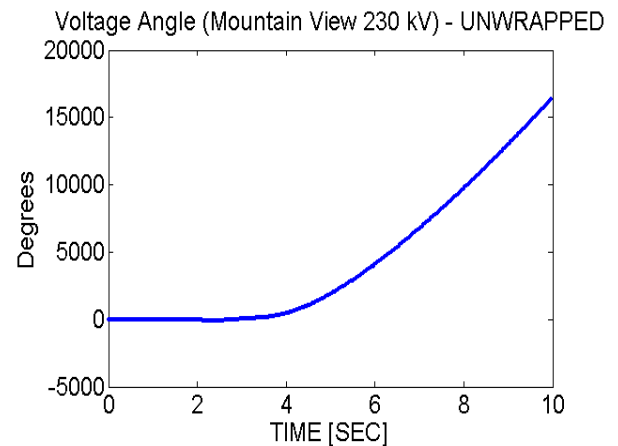
Source: VA Tech, 2010

Figure 5.17 shows the voltage angle for a sampling rate of 30 samples/second (every 2 cycles). Figure 5.17.b shows how the “unwrapping” algorithm perfectly describes the behavior of the voltage angle.

Figure 61: A) Wrapped Angle at 30 Samples/Sec.



B) Unwrapped Angle at 30 Samples/Sec



Source: VA Tech, 2010

A minimum rate of 15 samples per second is required for all PMUS but a 30 samples/second rate is preferred.

5.3.2.2 Data Concentrator Specifications

The function of the data concentrator is to collect data from the 10 PMUs and send a single “time-aligned” data string to the out-of-step computer. The data concentrator should be able to handle the 30 samples per second rate of 10 PMUs and provide the time-aligned angles to the out-of-step computer with the minimum delay.

5.3.2.3 Out-of-Step Computer Specifications

A computer at the control center will implement the following algorithms:

- Angle unwrapping for 10 angles
- Coherence detection algorithm
- Angle prediction algorithms
- Stability Detection Algorithm

To perform these algorithms at the preferred rate of 30 samples per second with minimum delay, a real-time operating system is required to avoid additional delays to the decision process. Fast serial or network communication channels are required to communicate to the data concentrator and field relay units.

CHAPTER 6: Conclusions

The main technical objective of this project was to demonstrate the use of real-time synchronized phasor measurement data to improve the protection system supervision by making it adaptive to prevailing system conditions. To achieve this objective the project focused on four tasks: 1) development of a California system model, 2) development of an adaptive adjustment of dependability and security tool, 3) developing of an alarm on potential load encroachment, and 4) developing of a more intelligent out-of-step relaying tool.

To fulfill the objectives the project team:

- Developed equivalents for the electric system outside California and validated the operation of the California only model with respect to the full West Coast Electric system model.
- Determined, with support of the TAG, the key locations on the California electric power system model where an insecure relaying operation during stressed system conditions would be detrimental to the viability of the power system. Developed a decision tree that uses WAMs to determine when the system is in stressed conditions and a voting scheme should be implemented at the key system location.
- Developed a method for using real-time WAM data and the existing protection system data base to determine which of the relay characteristics are in danger of being encroached upon during a catastrophic event.
- Determined the coherent generator groups in the California System model and use them to implement a technique that uses WAMs to provide a more appropriate out-of-step decision.

Sections 6.1 to 6.4 give the specific conclusions for each of the tasks performed in this project.

6.1 Model Validation

A reduced West Coast power system was developed based on the California model provided and the WECC system information provided by PG&E. The model consists of 3,996 buses, 1,124 generators (647 with dynamic models), 1,913 loads, and a single generator representing the WECC external to California. The validation process performed at Virginia Tech show that this model reflects the behavior of the full WECC model for the major disturbances considered for this project:

- The voltage magnitude response of the reduced California model is similar and consistent with the full WECC California model for the large disturbances, generation drop and line loss, considered for this project.

- The frequency response of the reduced California model is also similar and consistent with the full WECC California model for the large disturbances, generation drop and line loss, considered for this project.
- For the major disturbances considered for this project the derived California model is considered valid.

6.2 Online Adjustment of the Protection System's Security-Dependability Balance

The technical objective of this task focused on developing an adaptive protection system that “adapts” the security - dependability balance in response to changing system conditions as determined by real-time phasor measurements. WAMs provide a real-time assessment of the state of the power system, whether it is in a ‘normal’ or ‘stressed’ state. Based upon this determination made with the phasor measurements, the protection system logic at critical locations is altered to become more ‘secure’ during ‘stressed’ system states, and revert to more ‘dependable’ state when the system returns to ‘normal’ state. To achieve the proposed objectives for this task:

- A reduced west coast power system was developed based on the California model provided and the WECC system information provided by PG&E. The model consists of 3,996 buses, 1,124 generators (647 with dynamic models), 1,913 loads, and a single generator representing the WECC external to California. The validation process performed at Virginia Tech show that this model reflects the behavior of the full WECC model for the major disturbances considered for this task.
- The optimal location for the adaptive protection scheme was derived using a systematic procedure to identify and rank critical location in power systems. The critical location was confirmed, based on practical experience, by the Technical Advisory Group. The Midway-Vincent path was determined to be the system critical location.
- Decision trees were generated for the Heavy Winter and Heavy Summer Models with misclassification rates of 1 percent. For the Heavy Winter model the first split in the tree, real part of the current flowing through the 500 kV line 1106 in the model (Tesla los Banos line) has a misclassification rate of only 4 percent.
- Based on the decision tree derived for the system models PMU locations and the signals to be monitored were determined. Based on the decision trees for the heavy winter and heavy summer cases, PMUs are required at: Los Banos, Devers, El Dorado, and Pittsburg.
- Surrogate (alternative) locations for PMU with similar performance have been determined. Surrogates at: Mohave, Diablo, Moss Landing, Victorville and Angle Round MT can be used to attempt to mimic the partition achieved by the primary split and are good backups for cases where the information of the primary split is missing.
- Performance evaluation of the algorithm with new test cases created by simulating circuit element outages was performed to assess the robustness of the trees to topology changes. The misclassification rate for topology changes was 2 percent for the Heavy Winter case

and 4.3 percent for the Heavy summer case. This misclassification rates are excellent if we consider that when the system undergoes significant departures from the model assumptions, a new decision tree should be obtained. The advocated adaptive protection scheme is susceptible to two types of errors:

- 1) Type I: Fail to vote when a bias towards security would be desirable. This circumstance characterizes the current protection practice, that is, a single protective relay typically biased towards dependability. Therefore, this error, though potentially extremely harmful, is in agreement with existing practice, for example, the status quo.
- 2) Type II: Vote when a bias towards dependability would be preferred. A customary practice to increase security is to implement a voting scheme in which three relays continuously vote, regardless of prevailing conditions. Therefore, under this type of error, the scheme again reduces to current practices.

Examination of the trees indicate that the process produces almost equal numbers of each type of error for the training data.

A functional analysis of the proposed system determined that the system can be implemented with available commercial PMUs, computers and data concentrators if the communication links are available at the selected PMU locations.

6.3 Real-Time Alarms for Encroachment of Relay Trip Characteristics

The technical objective of this task focused on developing a method for using real-time wide area measurement data and the existing protection system data base to determine which of the relay characteristics are in danger of being encroached upon during a catastrophic event. To achieve the proposed objectives for this task:

A reduced west coast power system model was developed based on the California model provided and the WECC system information provided by PG&E. The model consists of 3996 buses, 1124 generators (647 with dynamic models), 1913 loads, and two generators representing the WECC external to California. The validation process performed at Virginia Tech showed that this model reflected the behavior of the full WECC model for the major disturbances considered for this task.

Critical locations for the proposed encroachment alarm system were determined. For this task, the TAG recommended Virginia Tech to focus on California's Path 15 and Path 26. Based on the

TAG recommendation and the analysis of the California Model developed for this task, the following critical locations were determined at the following transmission lines:

- Midway – Vincent ck 3 500kV
- Midway – Vincent ck 2 500kV
- Midway – Vincent ck 1 500kV
- Los Banos – Midway ck 2 500kV
- Diablo – Midway ck 3 500kV
- Diablo – Midway ck 2 500kV
- Vaca-Dixon – Cottonwood 230kV

Based on the analysis of the system model, the selected critical locations where PMUs need to be placed are: Midway 500kV, Los Banos 500kV, Diablo 500kV, and Vaca-Dixon 230kV.

Based on an exhaustive contingency analysis, critical relays were determined as those that are most at risk of encroachment as determined: Distance relays, loss-of-excitation relays and out-of-step relays.

A supervisory boundary, a concentric circle with a radius 50 percent larger than the radius of Zone 2 (in PG&E zone 2 is the largest zone and it covers 120 percent of the line), was used to determine when the impedance had come too close to the relay's trip characteristics for distance relays and loss-of-excitation relays. Contingency analysis of the heavy winter and heavy summer models revealed that no combinations of outages and three phase faults resulted in the power swing or the post-disturbance load flow causing encroachment of the distance relays on critical 230kV and 500kV lines in California.

Alarms for out-of-step relays were based on identifying contingencies that cause significant changes in the location of the swing center and the size and speed of stable swings at the location of the out-of-step relay. An algorithm was developed to determine the contingencies that make out-of-step relays lose their ability to differentiate stable swings from unstable swings. The advantage of this system is that it is fully automated in GE-PSLF so that as the model changes or new out-of-step relays are inserted it can be easily re-run. If sufficient phasor measurement units are available, it may be possible to automatically detect the N-1 or N-2 conditions for which an out-of-step relay's settings are incorrect and issue an alarm accordingly.

The following countermeasures were identified for the selected relay types:

Shrinking or reshaping of the trip region of distance relays and loss-of-excitation relays to prevent load encroachment without impacting their security. Many digital relays already use a load encroachment function that reshapes the trip region for all conditions. This could be improved upon by only reshaping the trip region when the situation requires it.

Power swing blocking for out-of-step relays can prevent false tripping when the speed of the apparent impedance trajectory indicates that it is not a fault. Out-of-step relays could

automatically switch to alternative settings when it recognizes that the existing settings are inappropriate for the prevailing system conditions.

Automatic actions depend heavily on the proper functioning of phasor measurement units, digital relays, and communication channels. Defects in any of these elements could result in false tripping or a failure to trip.

The alarms developed in this task call the protection engineer's attention to a potential problem. For encroachment of distance relays and loss-of-excitation relays, the trajectory of the apparent impedance before and after the encroachment should be stored by the proposed system along with all the power system variables measured at the relay's terminals. Alarms for out-of-step relays, should indicate which system conditions trigger the outage, and the location of the new swing center of the system.

A functional analysis of the proposed system determined that the system can be implemented with available commercial PMUs, computers, and data concentrators if the communication links are available at the selected PMU locations.

6.4 Adaptive Out-of-Step Protection on Critical Tie-Lines

The technical objective of this task focused on developing an adaptive out-of-step algorithm that uses real-time wide area measurement to predict stable or unstable swings in less than 250 milliseconds. To achieve the proposed objectives for this task:

- A reduced west coast power system was developed based on the California model provided and the WECC system information provided by PG&E. The model consists of 3996 buses, 1124 generators (647 with dynamic models), 1913 loads, and a single generator representing the WECC external to California. The validation process performed at Virginia Tech show that this model reflects the behavior of the full WECC model for the major disturbances considered for this task.
- A moving window and a growing window coherence detection algorithm were developed to detect coherence groups and based on the analysis of the California Model the following 10 PMU locations are proposed to detect and monitor coherent groups in the California system.
 - LOSBANOS 500 kV
 - MORRO BAY 230 kV
 - DIABLO 500 kV
 - IMP. VALLEY 230 kV
 - MAGUNDEN 230 kV
 - KRAMER 230 kV
 - MNT. VIEW 230 kV
 - HAYNES 230 kV
 - VULCAN 1 92 kV
 - LITEHIPE 230 kV

An autoregressive model order 3 – AR(3) algorithm was developed to predict angle swings and a COA angle difference of 150 degrees for two consecutive samples was shown to be an effective trigger for detecting unstable swings.

The performance of the proposed adaptive out-of-step algorithms was evaluated. The average time between system separation and its detection is 217 ms. None of the stable swings were tagged as unstable and all unstable swings were properly identified as such.

Operation of the proposed system depends heavily on the proper functioning of PMU, data concentrator, out-of-step computer and communication channels. Defects in any of these elements could result in mis-operation of the proposed system.

A functional analysis of the proposed system determined that the system can be implemented with available commercial PMUs, computers and data concentrators if the communication links are available at the selected PMU locations. A preferred sampling rate of 30 samples/second is recommended for PMUS and a real time operating system is recommended for the out-of-step computer.

GLOSSARY

California	
ISO	California Independent System Operator
CART	Classification and Regression Trees
EPCL	PSLF programming language
GE	General Electric Company
ISO	Independent System Operator
PG&E	Pacific Gas and Electric Company
PSLF	Positive Sequence Load Flow Software
PSSE	Power System Simulation for Engineering
PTI	Power Technology Inc.
pu	per unit
ROC	Receiver Operating Characteristic
SCADA	Supervisory Control and Data Acquisition.
SCE	Southern California Edison
TP	transmission planner
VAR	Volt-Amp Reactive
WAM	wide area measurement
WECC	Western Electricity Coordinating Council

REFERENCES

- [1] Rockefeller, G.D.; Wagner, C.L.; Linders, J.R.; Hicks, K.L.; and Rizy, D.T., "Adaptive Transmission Relaying Concepts for Improved Performance", IEEE Transactions on Power Delivery, v 3, n 4, Oct, 1988, pp 1446-1458
- [2] Horowitz, S.H.; Phadke, A.G.; and Thorp, J.S., "Adaptive Transmission System Relaying", IEEE Transactions on Power Delivery, v 3, n 4, Oct, 1988, pp 1436-1445
- [3] V. Centeno, N. Castro, J. Benton, A. Edris, G. Michel, R. J. Murphy, A. G. Phadke, "Adaptive Out-of-Step Relaying Implementation and Field Tests", Proceedings of the FACTS Conference, October 5-7, 1994, Baltimore, MD.
- [4] Rovnyak, S., et al., Decision trees for real-time transient stability prediction. Power Systems, IEEE Transactions on, 1994. 9(3): p. 1417-1426.

APPENDIX A: Detailed Decision Trees for the Heavy Winter and Heavy Summer Cases

Figure 62: Selected Decision Tree for Heavy Winter Model. Misclassification Rate = 0.99%

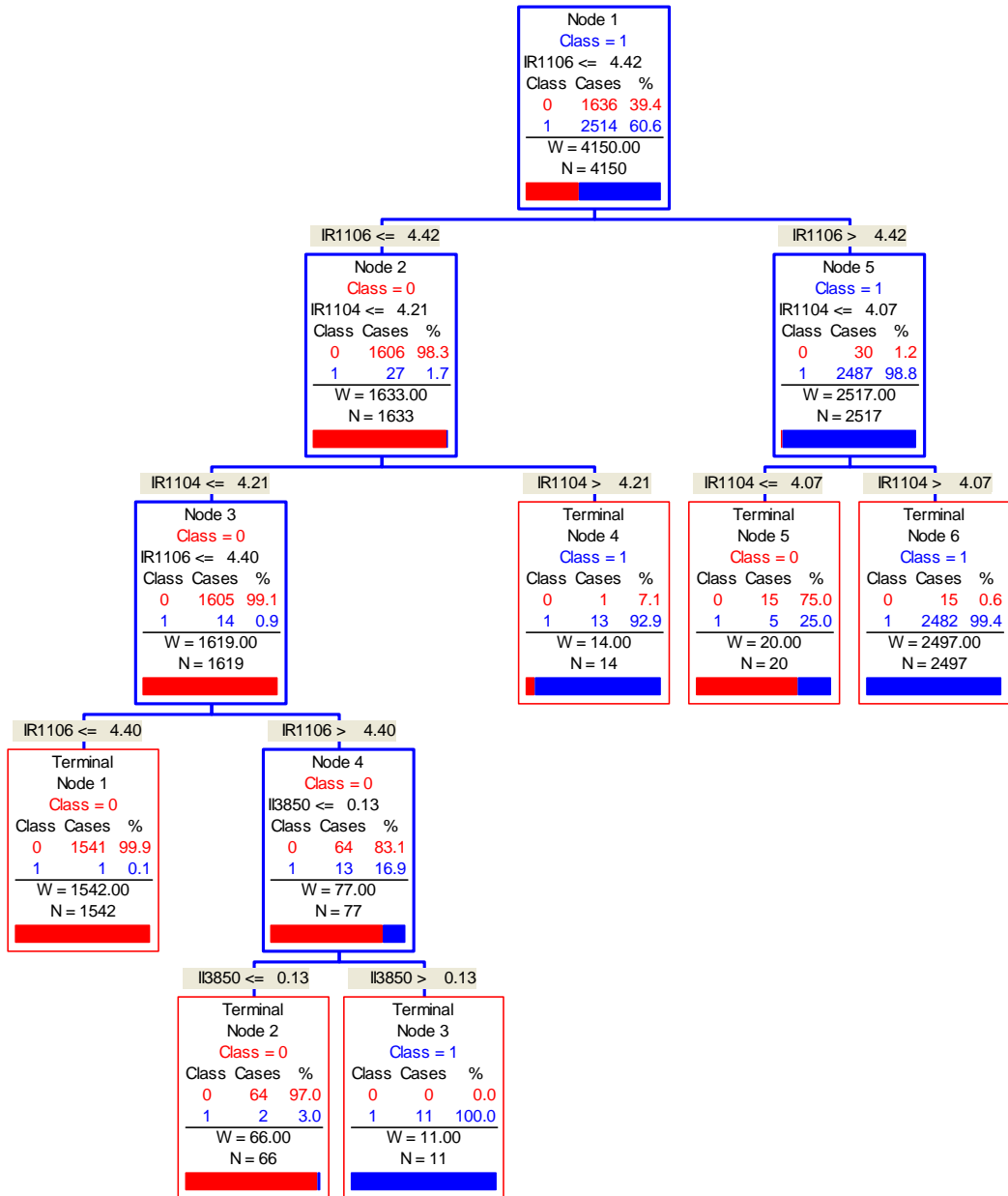
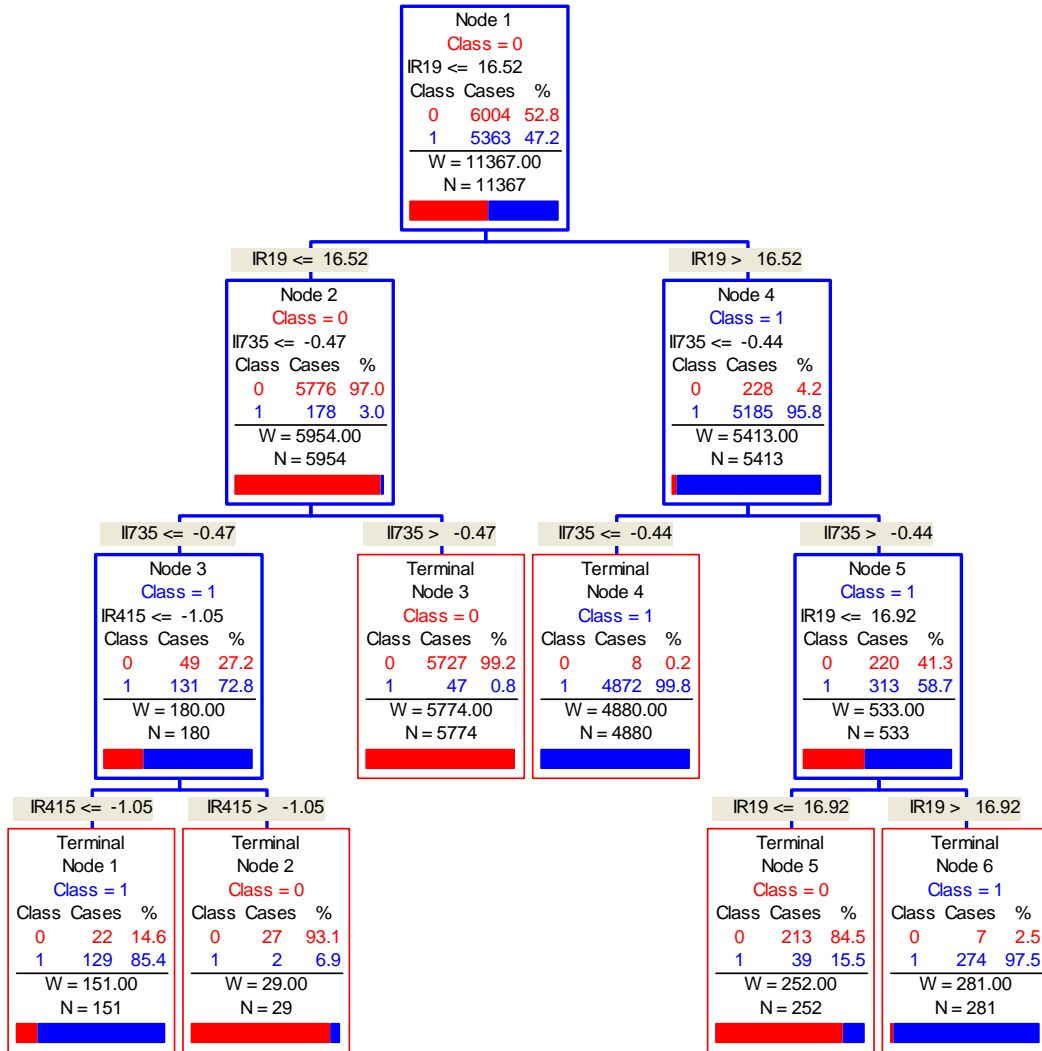


Figure 63: Decision Tree for Heavy Summer Model



APPENDIX B: Simulation Cases

Table B.1: Simulation Cases on Paths 15 and 26

Case	Type	From Bus	To Bus	From Bus	To Bus	Ck
1	Fault	Los Banos	Gates	30050	30055	1
	HF	Los Banos	Gates	30050	30055	3
2	Fault	Los Banos	Gates	30050	30055	1
	HF	Los Banos	Midway	30050	30060	1
3	Fault	Los Banos	Gates	30050	30055	1
	HF	Los Banos	Moss Landing	30050	30045	1
4	Fault	Los Banos	Gates	30050	30055	1
	HF	Los Banos	Tracy	30050	30035	1
5	Fault	Los Banos	Gates	30050	30055	1
	HF	Los Banos	Tesla	30050	30040	1
6	Fault	Los Banos	Gates	30050	30055	3
	HF	Los Banos	Gates	30050	30055	1
7	Fault	Los Banos	Gates	30050	30055	3
	HF	Los Banos	Midway	30050	30060	1
8	Fault	Los Banos	Gates	30050	30055	3
	HF	Los Banos	Moss Landing	30050	30045	1
9	Fault	Los Banos	Gates	30050	30055	3
	HF	Los Banos	Tracy	30050	30035	1
10	Fault	Los Banos	Gates	30050	30055	3
	HF	Los Banos	Tesla	30050	30040	1
11	Fault	Los Banos	Tracy	30050	30035	1
	HF	Los Banos	Gates	30050	30055	1

Case	Type	From Bus	To Bus	From Bus	To Bus	Ck
12	Fault	Los Banos	Tracy	30050	30035	1
	HF	Los Banos	Gates	30050	30055	3
13	Fault	Los Banos	Tracy	30050	30035	1
	HF	Los Banos	Midway	30050	30060	1
14	Fault	Los Banos	Tracy	30050	30035	1
	HF	Los Banos	Moss Landing	30050	30045	1
15	Fault	Los Banos	Tracy	30050	30035	1
	HF	Los Banos	Tesla	30050	30040	1
16	Fault	Los Banos	Midway	30050	30060	1
	HF	Los Banos	Gates	30050	30055	1
17	Fault	Los Banos	Midway	30050	30060	1
	HF	Los Banos	Gates	30050	30055	3
18	Fault	Los Banos	Midway	30050	30060	1
	HF	Los Banos	Tracy	30050	30035	1
19	Fault	Los Banos	Midway	30050	30060	1
	HF	Los Banos	Moss Landing	30050	30045	1
20	Fault	Los Banos	Midway	30050	30060	1
	HF	Los Banos	Tesla	30050	30040	1
21	Fault	Los Banos	Moss Landing	30050	30045	1
	HF	Los Banos	Gates	30050	30055	1
22	Fault	Los Banos	Moss Landing	30050	30045	1
	HF	Los Banos	Gates	30050	30055	3
23	Fault	Los Banos	Moss Landing	30050	30045	1
	HF	Los Banos	Tracy	30050	30035	1

Case	Type	From Bus	To Bus	From Bus	To Bus	Ck
24	Fault	Los Banos	Moss Landing	30050	30045	1
	HF	Los Banos	Midway	30050	30060	1
25	Fault	Los Banos	Moss Landing	30050	30045	1
	HF	Los Banos	Tesla	30050	30040	1
26	Fault	Los Banos	Tesla	30050	30040	1
	HF	Los Banos	Gates	30050	30055	1
27	Fault	Los Banos	Tesla	30050	30040	1
	HF	Los Banos	Gates	30050	30055	3
28	Fault	Los Banos	Tesla	30050	30040	1
	HF	Los Banos	Tracy	30050	30035	1
29	Fault	Los Banos	Tesla	30050	30040	1
	HF	Los Banos	Midway	30050	30060	1
30	Fault	Los Banos	Tesla	30050	30040	1
	HF	Los Banos	Moss Landing	30050	30045	1
31	Fault	Gates	Midway	30055	30060	1
	HF	Gates	Diablo	30055	30057	1
32	Fault	Gates	Midway	30055	30060	1
	HF	Gates	Los Banos	30055	30050	1
33	Fault	Gates	Midway	30055	30060	1
	HF	Gates	Los Banos	30055	30050	3
34	Fault	Gates	Diablo	30055	30057	1
	HF	Gates	Midway	30055	30060	1
35	Fault	Gates	Diablo	30055	30057	1
	HF	Gates	Los Banos	30055	30050	1
36	Fault	Gates	Diablo	30055	30057	1

Case	Type	From Bus	To Bus	From Bus	To Bus	Ck
	HF	Gates	Los Banos	30055	30050	3
37	Fault	Gates	Los Banos	30055	30050	1
	HF	Gates	Midway	30055	30060	1
38	Fault	Gates	Los Banos	30055	30050	1
	HF	Gates	Los Banos	30055	30050	1
39	Fault	Gates	Los Banos	30055	30050	1
	HF	Gates	Diablo	30055	30057	1
40	Fault	Gates	Los Banos	30055	30050	3
	HF	Gates	Midway	30055	30060	1
41	Fault	Gates	Los Banos	30055	30050	3
	HF	Gates	Los Banos	30055	30050	1
42	Fault	Gates	Los Banos	30055	30050	3
	HF	Gates	Diablo	30055	30057	1
43	Fault	Midway	Diablo	30060	30057	2
	HF	Midway	Gates	30060	30055	1
44	Fault	Midway	Diablo	30060	30057	2
	HF	Midway	Los Banos	30060	30050	1
45	Fault	Midway	Diablo	30060	30057	2
	HF	Midway	Vincent	30060	24156	1
46	Fault	Midway	Diablo	30060	30057	2
	HF	Midway	Vincent	30060	24156	2
47	Fault	Midway	Diablo	30060	30057	2
	HF	Midway	Vincent	30060	24156	3
48	Fault	Midway	Gates	30060	30055	1
	HF	Midway	Diablo	30060	30057	2
49	Fault	Midway	Gates	30060	30055	1
	HF	Midway	Los Banos	30060	30050	1

Case	Type	From Bus	To Bus	From Bus	To Bus	Ck
50	Fault	Midway	Gates	30060	30055	1
	HF	Midway	Vincent	30060	24156	1
51	Fault	Midway	Gates	30060	30055	1
	HF	Midway	Vincent	30060	24156	2
52	Fault	Midway	Gates	30060	30055	1
	HF	Midway	Vincent	30060	24156	3
53	Fault	Midway	Los Banos	30060	30050	1
	HF	Midway	Diablo	30060	30057	2
54	Fault	Midway	Los Banos	30060	30050	1
	HF	Midway	Gates	30060	30055	1
55	Fault	Midway	Los Banos	30060	30050	1
	HF	Midway	Vincent	30060	24156	1
56	Fault	Midway	Los Banos	30060	30050	1
	HF	Midway	Vincent	30060	24156	2
57	Fault	Midway	Los Banos	30060	30050	1
	HF	Midway	Vincent	30060	24156	3
58	Fault	Midway	Vincent	30060	24156	3
	HF	Midway	Diablo	30060	30057	2
59	Fault	Midway	Vincent	30060	24156	3
	HF	Midway	Los Banos	30060	30050	1
60	Fault	Midway	Vincent	30060	24156	3
	HF	Midway	Vincent	30060	24156	1
61	Fault	Midway	Vincent	30060	24156	3
	HF	Midway	Vincent	30060	24156	2
62	Fault	Midway	Vincent	30060	24156	3
	HF	Midway	Gates	30060	30055	1
63	Fault	Vincent	Midway	24156	30060	3

Case	Type	From Bus	To Bus	From Bus	To Bus	Ck
	HF	Vincent	Lugo	24156	24086	1
64	Fault	Vincent	Lugo	24156	24086	1
	HF	Vincent	Midway	24156	30060	3
65	Fault	Vincent	Lugo	24156	24086	1
	HF	Vincent	Lugo	24156	24086	2
66	Fault	Vincent	Midway	24156	30060	3
	HF	Vincent	Midway	24156	30060	2

APPENDIX C:

Rankings Using ISGA

Table C.1: Set of Cases Studied With the Dynamic Index

Case	Type	Name	Name	ck	Sec	Line	Dist	ISGA
107	F	ROUND MT	TABLE MT	1	2	1084	0.99	7.7347
107	HF	TABLE MT	VACA-DIX	1	0	1090		
107	HF	TABLE MT	TESLA	1	0	1093		
113	F	ROUND MT	TABLE MT	2	2	1087	0.99	7.7348
113	HF	TABLE MT	VACA-DIX	1	0	1090		
113	HF	TABLE MT	TESLA	1	0	1093		
115	F	TABLE MT	VACA-DIX	1	2	1090	0.01	7.7235
115	HF	ROUND MT	TABLE MT	1	0	1084		
115	HF	TABLE MT	TESLA	1	0	1093		
116	F	TABLE MT	VACA-DIX	1	2	1090	0.01	7.7237
116	HF	ROUND MT	TABLE MT	2	0	1087		
116	HF	TABLE MT	TESLA	1	0	1093		
118	F	TABLE MT	TESLA	1	2	1093	0.01	7.7246
118	HF	ROUND MT	TABLE MT	1	0	1084		
118	HF	TABLE MT	VACA-DIX	1	0	1090		
119	F	TABLE MT	TESLA	1	2	1093	0.01	7.7248
119	HF	ROUND MT	TABLE MT	2	0	1087		
119	HF	TABLE MT	VACA-DIX	1	0	1090		
120	F	TABLE MT	TESLA	1	2	1093	0.99	8.0942
120	HF	VACA-DIX	TESLA	1	0	1101		
120	HF	TRACY	TESLA	1	0	1103		
121	F	TABLE MT	TESLA	1	2	1093	0.99	8.1836
121	HF	VACA-DIX	TESLA	1	0	1101		
121	HF	TESLA	METCALF	1	0	1105		

122	F	TABLE MT	TESLA	1	2	1093	0.99	8.2523
122	HF	VACA-DIX	TESLA	1	0	1101		
122	HF	TESLA	LOSBANOS	1	0	1106		
123	F	TABLE MT	TESLA	1	2	1093	0.99	8.8318
123	HF	TRACY	TESLA	1	0	1103		
123	HF	TESLA	METCALF	1	0	1105		
124	F	TABLE MT	TESLA	1	2	1093	0.99	8.9646
124	HF	TRACY	TESLA	1	0	1103		
124	HF	TESLA	LOSBANOS	1	0	1106		
127	F	VACA-DIX	TESLA	1	2	1101	0.99	8.1008
127	HF	TABLE MT	TESLA	1	0	1093		
127	HF	TRACY	TESLA	1	0	1103		
128	F	VACA-DIX	TESLA	1	2	1101	0.99	8.1892
128	HF	TABLE MT	TESLA	1	0	1093		
128	HF	TESLA	METCALF	1	0	1105		
129	F	VACA-DIX	TESLA	1	2	1101	0.99	8.2585
129	HF	TABLE MT	TESLA	1	0	1093		
129	HF	TESLA	LOSBANOS	1	0	1106		
134	F	TRACY	TESLA	1	1	1103	0.99	8.1073
134	HF	TABLE MT	TESLA	1	0	1093		
134	HF	VACA-DIX	TESLA	1	0	1101		
135	F	TRACY	TESLA	1	1	1103	0.99	8.8394
135	HF	TABLE MT	TESLA	1	0	1093		
135	HF	TESLA	METCALF	1	0	1105		
136	F	TRACY	TESLA	1	1	1103	0.99	8.9719
136	HF	TABLE MT	TESLA	1	0	1093		
136	HF	TESLA	LOSBANOS	1	0	1106		
151	F	TESLA	METCALF	1	1	1105	0.01	8.194

151	HF	TABLE MT	TESLA	1	0	1093		
151	HF	VACA-DIX	TESLA	1	0	1101		
152	F	TESLA	METCALF	1	1	1105	0.01	8.8384
152	HF	TABLE MT	TESLA	1	0	1093		
152	HF	TRACY	TESLA	1	0	1103		
157	F	TESLA	LOSBANOS	1	1	1106	0.01	8.2605
157	HF	TABLE MT	TESLA	1	0	1093		
157	HF	VACA-DIX	TESLA	1	0	1101		
158	F	TESLA	LOSBANOS	1	1	1106	0.01	8.9703
158	HF	TABLE MT	TESLA	1	0	1093		
158	HF	TRACY	TESLA	1	0	1103		
237	F	GATES	DIABLO	1	1	1115	0.99	4316.469
237	HF	DIABLO	MIDWAY	2	0	1118		
237	HF	DIABLO	MIDWAY	3	0	1119		
256	F	DIABLO	MIDWAY	2	1	1118	0.01	4315.375
256	HF	GATES	DIABLO	1	0	1115		
256	HF	DIABLO	MIDWAY	3	0	1119		
269	F	DIABLO	MIDWAY	2	1	1118	0.99	9.7647
269	HF	MIDWAY	VINCENT	1	0	3857		
269	HF	MIDWAY	VINCENT	2	0	3860		
272	F	DIABLO	MIDWAY	3	1	1119	0.01	4315.688
272	HF	GATES	DIABLO	1	0	1115		
272	HF	DIABLO	MIDWAY	2	0	1118		
285	F	DIABLO	MIDWAY	3	1	1119	0.99	9.7257
285	HF	MIDWAY	VINCENT	1	0	3857		
285	HF	MIDWAY	VINCENT	2	0	3860		
298	F	MIDWAY	VINCENT	1	2	3857	0.01	9.7549
298	HF	DIABLO	MIDWAY	2	0	1118		

298	HF	MIDWAY	VINCENT	2	0	3860		
300	F	MIDWAY	VINCENT	1	2	3857	0.01	9.7142
300	HF	DIABLO	MIDWAY	3	0	1119		
300	HF	MIDWAY	VINCENT	2	0	3860		
302	F	MIDWAY	VINCENT	1	2	3857	0.01	2858.255
302	HF	MIDWAY	VINCENT	2	0	3860		
302	HF	MIDWAY	VINCENT	3	0	3863		
304	F	MIDWAY	VINCENT	1	2	3857	0.99	9.6782
304	HF	LUGO	VINCENT	1	0	3442		
304	HF	MIDWAY	VINCENT	2	0	3860		
306	F	MIDWAY	VINCENT	1	2	3857	0.99	9.6782
306	HF	LUGO	VINCENT	2	0	3443		
306	HF	MIDWAY	VINCENT	2	0	3860		
308	F	MIDWAY	VINCENT	1	2	3857	0.99	6389.492
308	HF	MIDWAY	VINCENT	2	0	3860		
308	HF	MIDWAY	VINCENT	3	0	3863		
319	F	MIDWAY	VINCENT	2	2	3860	0.01	9.7545
319	HF	DIABLO	MIDWAY	2	0	1118		
319	HF	MIDWAY	VINCENT	1	0	3857		
321	F	MIDWAY	VINCENT	2	2	3860	0.01	9.7139
321	HF	DIABLO	MIDWAY	3	0	1119		
321	HF	MIDWAY	VINCENT	1	0	3857		
323	F	MIDWAY	VINCENT	2	2	3860	0.01	2773.469
323	HF	MIDWAY	VINCENT	1	0	3857		
323	HF	MIDWAY	VINCENT	3	0	3863		
325	F	MIDWAY	VINCENT	2	2	3860	0.99	9.678
325	HF	LUGO	VINCENT	1	0	3442		
325	HF	MIDWAY	VINCENT	1	0	3857		

327	F	MIDWAY	VINCENT	2	2	3860	0.99	9.6781
327	HF	LUGO	VINCENT	2	0	3443		
327	HF	MIDWAY	VINCENT	1	0	3857		
329	F	MIDWAY	VINCENT	2	2	3860	0.99	6407.404
329	HF	MIDWAY	VINCENT	1	0	3857		
329	HF	MIDWAY	VINCENT	3	0	3863		
344	F	MIDWAY	VINCENT	3	3	3863	0.01	734.7981
344	HF	MIDWAY	VINCENT	1	0	3857		
344	HF	MIDWAY	VINCENT	2	0	3860		
350	F	MIDWAY	VINCENT	3	3	3863	0.99	6721.188
350	HF	MIDWAY	VINCENT	1	0	3857		
350	HF	MIDWAY	VINCENT	2	0	3860		
456	F	LUGO	VINCENT	1	1	3442	0.99	9.6902
456	HF	MIDWAY	VINCENT	1	0	3857		
456	HF	MIDWAY	VINCENT	2	0	3860		
483	F	LUGO	VINCENT	2	1	3443	0.99	9.6902
483	HF	MIDWAY	VINCENT	1	0	3857		
483	HF	MIDWAY	VINCENT	2	0	3860		

Table C.2: Ranking of Cases Along Path 15 and 26 Using the ISGA

Rank	CASE	ISGA
1	58	9.9814
2	61	9.936
3	60	9.9047
4	62	9.8014
5	59	9.7693
6	65	9.6828
7	47	9.6516
8	46	9.6382
9	45	9.6378
10	64	9.635
11	31	9.6101
12	66	9.6015
13	42	9.595
14	36	9.5943
15	34	9.5759
16	43	9.5627
17	35	9.5626
18	44	9.5585
19	57	9.5532
20	63	9.5439
21	56	9.5427
22	22	9.5204

Rank	CASE	ISGA
23	8	9.5194
24	3	9.5002
25	21	9.4984
26	19	9.4798
27	24	9.4787
28	32	9.4742
29	33	9.4674
30	54	9.453
31	40	9.4425
32	1	9.4153
33	25	9.4142
34	30	9.4134
35	6	9.4123
36	41	9.4113
37	17	9.4103
38	23	9.4095
39	7	9.4067
40	14	9.4055
41	27	9.3788
42	10	9.3776
43	5	9.37
44	26	9.3696

Rank	CASE	ISGA
45	9	9.3693
46	12	9.3691
47	4	9.3619
48	11	9.3591
49	20	9.3589
50	29	9.3581
51	18	9.3501
52	13	9.3469
53	2	9.3458
54	16	9.3438
55	28	9.1057
56	15	9.102
57	53	7.9771
58	55	2.1495

APPENDIX D:

Buses of Base System Model for Adaptive Protection

Table D.1: List of Buses of Base System Model for Adaptive Protection

Bus	Name	Bus	Name	Bus	Name	Bus	Name
1	PALOVRDE	1000	JAMESON	1999	WASCO	2998	DOUBLE C
2	BLYTHE	1001	HALE J2	2000	SEMITRPC	2999	HISIERRA
3	DAVIS	1002	GOLDHILL	2001	CUYAMA	3000	BADGERCK
4	KNOB	1003	RICE	2002	3EMIDIO	3001	TEXSUNST
5	HASSYAMP	1004	CLSA CRS	2003	VALPREDO	3002	MARTELTP
6	MOENKOPI	1005	MAXWELL	2004	ROSE	3003	BIG_RVR_
7	NAVAJO	1006	CORTINA	2005	PACI_PIP	3004	MDWY 11T
8	N.GILA	1007	HARINTON	2006	LST HLLS	3005	MDWY 11M
9	N.GILA 4	1008	ARBUCKLE	2007	TECUYA	3006	MDWY 13T
10	MEAD	1009	DRAKE	2008	KNG_ELIS	3007	MDWY 13M
11	PARKER	1010	WILLIAMS	2009	GRAPEVNE	3008	Agnew
12	MEAD S	1011	DUNNIGAN	2010	STALLION	3009	Brokaw
13	N.GILA 3	1012	COLUSA	2011	STALIONJ	3010	CCA
14	AVE42	1013	CLSA JCT	2012	LEBEC	3011	Central
15	AVE58	1014	MERIDIAN	2013	EMDO JCT	3012	Fibergla
16	AVE58	1015	CORDELIA	2014	CASTAC	3013	Gianera
17	COACHELA	1016	CRD-JCT	2015	KELLEY	3014	Homestea
18	COACHELV	1017	WILKINS	2016	BRRNDA C	3015	Juliette
19	COACHELV	1018	CORD PMP	2017	BRRNDA A	3016	Kifer Re
20	COACHELV	1019	WLKSLJCT	2018	ANTELOPE	3017	Laf T1
21	COACHLA1	1020	DIST2047	2019	TWISSLMN	3018	Laf T2
22	COACHLA2	1021	PLFLDJCT	2020	TX_LOSHL	3019	Laf T3
23	COACHLA3	1022	WLLW SLJ	2021	CHEVLHLS	3020	Mathew

24	COACHLA4	1023	KNGHTSLJ	2022	SUNSET G	3021	Norman A
25	COLMAC	1024	VACA-DXN	2023	KERN 1	3022	Scott Re
26	DELRANCH	1025	WINTERS	2024	KERN 2	3023	Serra
27	DELRANCH	1026	PLAINFLD	2025	KERNCNYN	3024	Tasman
28	DPWR#3	1027	VACA-JT2	2026	RIOBRAVO	3025	Uranium
29	DPWR#3	1028	VACA-JT1	2027	DEXEL +	3026	Walsh
30	DROP3	1029	TRAVISJT	2028	KERNFRNT	3027	Zeno
31	DROP4	1030	DIXON	2029	OILDALE	3028	NRS 600
32	DROP4	1031	CAMPUS	2030	CHV-CYMR	3029	Gia100
33	DROP5	1032	DIXONCAN	2031	MIDSUN	3030	NRS 230k
BUS	Name	Bus	Name	Bus	Name	Bus	Name
34	EENERGY	1033	CACHSLJ1	2032	MIDSUN +	3031	PLCRVLT1
35	EENERGY	1034	GOLD HLL	2033	MT POSO	3032	PLCRVLT2
36	ELCENTRO	1035	VC DX11T	2034	CHLKCLF+	3033	DIMOND_2
37	ELCENTSW	1036	WADHAM	2035	KERNRDGE	3034	SHPRING1
38	ELSTEAMP	1037	WOODLAND	2036	TX MIDST	3035	CPM TAP
39	ELSTM 1	1038	RIV.DLTA	2037	SEKR	3036	SSS
40	RAMON	1039	CTY FAIR	2038	FRITOLAY	3037	Duane
41	RAMON92	1040	UC DAVIS	2039	SLR-TANN	3038	DVR A GT
42	ELSTM 2	1041	PEASE	2040	SLR_TANH	3039	DVR B GT
43	ELSTM 3	1042	E.MRYSVE	2041	CHEV.USA	3040	DVR A ST
44	ELSTM 4	1043	OLIVHRST	2042	PSE-LVOK	3041	DVR B Lo
45	ELSTM2-2	1044	BOGUE	2043	PSEMCKIT	3042	DVRPP 1M
46	EMESA1	1045	GLEAF TP	2044	DISCOVERY	3043	DVRPP 2M
47	EMESA2	1046	GLEAF 1	2045	NAVY 35R	3044	POT_SVC
48	HEBER SC	1047	E.NICOLS	2046	PSE-BEAR	3045	COSUMNE2
49	HEBER SC	1048	RIO OSO	2047	SN LNDRO	3046	COSUMNE3
50	HIGHLINE	1049	DRUM	2048	EDES	3047	COSUMNE4

51	HIGHLINE	1050	DTCH FL1	2049	EDS GRNT	3048	COSUMNE5
52	HOLTVILL	1051	DTCH FL2	2050	GRANT	3049	COSUMNE6
53	JJELMORE	1052	CHCGO PK	2051	EASTSHRE	3050	Cogen
54	JJELMORE	1053	BRUNSWCK	2052	MT EDEN	3051	MOSSL-CB
55	LEATHERS	1054	PLACER	2053	DUMBARTN	3052	BRNSWALT
56	LEATHERS	1055	HORSESHE	2054	NWRK 2 M	3053	TRSVQ+NW
57	MIDWAY X	1056	HIGGINS	2055	FREMNT	3054	CORT_D
58	MIDWAY X	1057	NEWCASTLE	2056	JARVIS	3055	BAF COG2
59	NILAND	1058	FLINT1	2057	NUMMI	3056	TKO
60	NILAND	1059	BELL PGE	2058	DMTAR_SL	3057	COWCRK
61	ORM11	1060	DRUM 1M	2059	JV BART	3058	TBL MTX1
62	ORM11G	1061	BRNSWCKP	2060	CRYOGEN	3059	CLMN FSH
63	ORM11M	1062	DRUM 2M	2061	NEWARK D	3060	NOTRDAME
64	ORM12	1063	ROCKLIN	2062	NUMI JCT	3061	BDLSWSTA
65	ORM1EG	1064	ELDORAD	2063	NEWARK E	3062	SHILOH
66	ORM1EM	1065	APPLE HL	2064	NEWARK F	3063	KIERNAN
67	ORM21	1066	PLCRVLB2	2065	SEAWEST	3064	CRABTREE
68	ORM2G	1067	PLCRVLB3	2066	VASCO	3065	MARSHALL
69	ORM2M	1068	DMND SPR	2067	USWP-WKR	3066	TAYLR
70	PERRY	1069	MIZOU_T2	2068	LIVERMRE	3067	RIPN_1
71	PILOTKNB	1070	MIZOU_T1	2069	ZONDWD	3068	RIPN_2
72	PILOTKNB	1071	CLRKSVLE	2070	RADUM	3069	RIPN
73	PILOTKNB	1072	CLRKSVLT	2071	VINEYARD	3070	WEC115
BUS	Name	Bus	Name	Bus	Name	Bus	Name
74	ROCKWOD1	1073	SHPRING	2072	KAISER	3071	WEC69
75	ROCKWOD2	1074	TAYLOR	2073	PARKS	3072	WEC1-CT
76	ROCKWOOD	1075	DIMOND_1	2074	USWP-FRK	3073	WEC3-ST
77	RTAP1-6	1076	SHPRING2	2075	SAN RAMN	3074	WEC2-CT

78	SALTSEA4	1077	PENRYN	2076	VASCJCT.	3075	NRS 300
79	SIGC	1078	DEL MAR	2077	ALTAMONT	3076	Gianera
80	VULCAN1	1079	SIERRAPI	2078	IUKA	3077	Gia200
81	VULCAN1	1080	CPM	2079	VALLECTS	3078	FRWWTAP
82	MNPLNT	1081	SPICAMIN	2080	SUNOL	3079	FRESNOWW
83	UNIT5	1082	GLEAF2	2081	DCTO JCT	3080	FRESNOWW
84	WPOWER#1	1083	YUBACITY	2082	NEWARK	3081	MALAGATP
85	UNIT5L	1084	CATLETT	2083	FLOWIND1	3082	KRCDP
86	WPOWER#2	1085	COLGATE	2084	VINEYARD	3083	KRCDPCT1
87	YUCCA	1086	NARRWS 1	2085	LPOSTAS	3084	KRCDPCT2
88	YUCCGT21	1087	NARRWS 2	2086	E DUBLIN	3085	MRT RCTR
89	CALIPAT	1088	SMRTSVLE	2087	CALMAT60	3086	TRAN230A
90	ERTH ENG	1089	NRRWS2TP	2088	PARKS TP	3087	TRAN230B
91	MAGMAP	1090	NRRWS1TP	2089	VINEYD_D	3088	CAROLD1
92	BRAVO	1091	YUBAGOLD	2090	LIVRMR_2	3089	CAROLD2
93	CLX92	1092	BRWNS VY	2091	LFC FIN+	3090	TRAN-60
94	WESTMRLN	1093	MRYSVLLE	2092	SEAWESTF	3091	OGLE JCT
95	CALIPAT	1094	ENCINAL	2093	WALKER+	3092	OGLE TAP
96	SIGC92	1095	HARTER	2094	ZOND SYS	3093	ULTR PWR
97	EARTHE1	1096	ENCL TAP	2095	FLOWDPTR	3094	ELCRTJ1
98	BRAWLEY	1097	YBA CTYJ	2096	USW FRIC	3095	ELCRTJ2
99	ADELANTO	1098	PEAS RG	2097	AMES BS1	3096	Northwes
100	CASTAI1G	1099	PEASE	2098	AMES BS2	3097	NWRK 11T
101	CASTAI2G	1100	LIVE OAK	2099	WHISMAN	3098	NWRK 7T
102	CASTAI4G	1101	ALMENDRA	2100	MT VIEW	3099	NWRK 9T
103	CASTAIC	1102	BARRY	2101	STELLING	3100	GATES11T
104	GLENDAL	1103	TUDOR	2102	WOLFE	3101	GATES11M
105	GRAMERC1	1104	E.NICOLS	2103	MNTA VSA	3102	KEKAWAK

106	GRAMERC2	1105	PLUMAS	2104	LCKHD J1	3103	SOLANOWP
107	HALLDALE	1106	BEALE_1	2105	MFT.FD J	3104	FRANTDM
108	HARB	1107	BEALE2J2	2106	MOFT.FLD	3105	T22_93
109	HAYNES	1108	WHEATLND	2107	LCKHD J2	3106	AIRWAYJ1
110	HAYNES1G	1109	WEST JCT	2108	LOCKHD 1	3107	AIRWAYJ2
111	OWENS UP	1110	CMP FRWT	2109	LOCKHD 2	3108	AIRWAYS
112	OWENSMID	1111	LINCOLN	2110	LAWRENCE	3109	MLLBTP97
113	OWENSCON	1112	CLMBA HL	2111	A.M.D	3110	LONETREE
BUS	Name	Bus	Name	Bus	Name	Bus	Name
114	MARKETPL	1113	PIKE CTY	2112	AMD JCT	3111	RVNSWD D
115	MCCULLGH	1114	ALLEGHNY	2113	PHILLIPS	3112	Laf300
116	MCCULLGH	1115	GRSS VLY	2114	PHLPS_JT	3113	NRS 500
117	MEAD	1116	CISCO GR	2115	BRITTN	3114	CLARIBEL
118	OLIVE	1117	CAPEHORN	2116	APP MAT	3115	MRAGA_3M
119	OLIVE 1	1118	ENVRO_HY	2117	LOS ALTS	3116	ENXCO
120	OLIVE 2	1119	SPAULDNG	2118	L.ALTS J	3117	JMDAMCX1
121	PP 1	1120	BOWMN TP	2119	LOYOLA	3118	JMDAMCX2
122	PP 1 G	1121	DRUM	2120	NRTHGRUM	3119	NWRK_7M
123	PP 2	1122	BONNIE N	2121	WSTNG JT	3120	NWRK_9M
124	PP 2 G	1123	ROLLINS	2122	MNTA VSA	3121	NWRK_11M
125	RINALDI	1124	WEMR SWS	2123	PRMNT J3	3122	BOTTLERK
126	RINALDI	1125	FORST HL	2124	PERMNNTE	3123	BOTTLERK
127	RIVER	1126	OXBOW	2125	PRMNT J1	3124	OAK-TAP1
128	SCATERGD	1127	MDDLE FK	2126	PRMNT J2	3125	OAK-TAP2
129	SCATERGD	1128	FRNCH MS	2127	LOS GATS	3126	REP
130	STJOHN	1129	HALSEY	2128	DIXON LD	3127	REP1
131	CNTURY	1130	AUBURN	2129	ZNKER J2	3128	REP2
132	CNTURY1	1131	PLACER	2130	ZNKER J1	3129	REP3

133	CNTURY2	1132	LIMESTNE	2131	ZANKER	3130	CANBY4
134	CNTURYLD	1133	ULTRA JT	2132	AGNEW J	3131	INTBST
135	WLMNTN1	1134	SPI-LINC	2133	AGNEW	3132	INTBCT
136	WLMNTN2	1135	ULTR-RCK	2134	MONTAGUE	3133	INTB
137	WLMNTNLD	1136	SPI JCT	2135	TRIMBLE	3134	IV GEN1
138	FAIRFAX	1137	BOWMN PH	2136	FMC	3135	IV GEN2
139	TOLUCA	1138	PLSNT GR	2137	SJ B E	3136	IV GEN3
140	TOLUCA	1139	MTN_QJCT	2138	FMC JCT	3137	IV-GEN
141	TOLUCA	1140	ATLANTIC	2139	SN JSE A	3138	ALPINE
142	VELASCO	1141	FORMICA	2140	SJ B F	3139	ASH
143	ATWATER	1142	HAYPRESS	2141	EL PATIO	3140	ASH TP
144	HOLYWD_E	1143	COLGATE1	2142	IBM-HR J	3141	AVCADOTP
145	HOLYWD1	1144	COLGATE2	2143	SWIFT	3142	AVOCADO
146	HOLYWD2	1145	DRUM 5	2144	MILPITAS	3143	B
147	HOLYWDLD	1146	MIDLFORK	2145	MCKEE	3144	B TP
148	NRTHRDGE	1147	RALSTON	2146	WAUKESHA	3145	BARRETT
149	OLYMPIC	1148	NEWCASTLE	2147	MABURY J	3146	BARRETTTP
150	OLYMPCLD	1149	CHI.PARK	2148	MABURY	3147	BATIQTOS
151	AIRPORT	1150	DTCHFLT1	2149	MARKHM J	3148	BATIQTTP
152	HARBOR	1151	NARROWS1	2150	MARKHAM	3149	BERNARDO
153	HARBOR	1152	NARROWS2	2151	EVRGRN 2	3150	BERNDOTP
BUS	Name	Bus	Name	Bus	Name	Bus	Name
154	TARZANA	1153	CMP.FARW	2152	STONE J	3151	BLDCRKTP
155	TARZANA	1154	SPAULDG	2153	GEN ELEC	3152	BOLDRCRK
156	SYLMARLA	1155	DEER CRK	2154	EVRGRN 1	3153	BOLVRDTP
157	TAP 1	1156	ROLLINSF	2155	IBM-CTLE	3154	BORDER
158	TAP 2	1157	HALSEY F	2156	EDENVALE	3155	BORDERTTP
159	SYLMAR1	1158	BOWMAN	2157	IBM-HRRS	3156	BORREGO

160	SYLMAR2	1159	APLHTAP2	2158	IBM-BALY	3157	BOULEVRD
161	VALLEY	1160	APLHTAP1	2159	EDNVL J1	3158	CABRILLO
162	VALLEY	1161	OXBOW F	2160	MTCALF D	3159	CABRLNVY
163	VICTORVL	1162	HELLHOLE	2161	MTCALF E	3160	CALAVRTP
164	VICTORVL	1163	HAYPRES+	2162	CYTE PMP	3161	CAMERON
165	SCATT2G	1164	GRNLEAF1	2163	EVRGRN J	3162	CANNON
166	RINALDI2	1165	GRNLEAF2	2164	MRGN HIL	3163	CAPSTRNO
167	ADELSVC	1166	YUBA CTY	2165	LLAGAS	3164	CARLTHTP
168	MKTPSVC	1167	SPILINCF	2166	EDNVL J3	3165	CARLTNHS
169	CRYSTAL	1168	ULTR RCK	2167	GILROY F	3166	CHCARITA
170	OWENS UP	1169	DTCHFLT2	2168	BAILY J3	3167	CHOLLAS
171	OWENSMID	1170	DRUM 1-2	2169	BAILY J1	3168	CLAIRMNT
172	OWENSCON	1171	DRUM 3-4	2170	BAILY J2	3169	CLARMTTP
173	BARRENRD	1172	FRNCH MD	2171	MORGN J1	3170	CORONADO
174	COTTONWD	1173	CHILIBAR	2172	MORGN J2	3171	CORONADO
175	HAYNES8G	1174	WISE	2173	MABURY	3172	CALPK_BD
176	HAYNES9G	1175	SILVERDO	2174	JENNINGS	3173	CALPK_BD
177	HAYNS10G	1176	MONTCLLO	2175	JENING J	3174	CALPK_EC
178	HOLYWD_F	1177	MNTCLOPH	2176	EVERGREN	3175	CALPK_EC
179	PTWTG	1178	PUEBLOJT	2177	EVRGRN J	3176	CALPK_ES
180	PCOLLEC	1179	PUEBLO	2178	SENER	3177	CALPK_ES
181	PT34_5	1180	IGNACIO	2179	SENER J	3178	CREELMAN
182	PT230	1181	LS GLLNS	2180	ALMADEN	3179	CRSTNTS
183	BURBANK	1182	SAN RAFL	2181	GLRY COG	3180	DEL MAR
184	LINCLN69	1183	SKGGS J1	2182	OLS-AGNE	3181	DELMARTP
185	OLIVE_69	1184	SKGGS J2	2183	SJ-SCL W	3182	DESCANSO
186	VALLEY69	1185	SKAGGS	2184	CATALYST	3183	DIVISION
187	LAKE1	1186	HGHWY J1	2185	GRN VLY1	3184	DIVISNGT

188	BURBANK1	1187	HIGHWAY	2186	GRN VLY2	3185	DOUBLET
189	TOLUCA69	1188	JCPMPJCT	2187	CMP EVRS	3186	DOUBLET
190	MAG_CT	1189	JMSCNPMP	2188	PAUL SWT	3187	DOUBLTTP
191	MAG_ST	1190	NTWR ALT	2189	ROB ROY	3188	DOUBLTTP
192	OLIVE#1	1191	MEYERS	2190	HOLLISTR	3189	DUNHILL
193	OLIVE#2	1192	NRTH TWR	2191	LGNTSSW1	3190	DUNHILTP
BUS	Name	Bus	Name	Bus	Name	Bus	Name
194	GLENDALE	1193	NTWRJCT2	2192	LGNTSSW2	3191	EASTGATE
195	COLUMBUS	1194	NTWRJCT1	2193	NTVD SW2	3192	EL CAJON
196	TROPICO	1195	MREIS JC	2194	NTVD SW1	3193	ELCAJNGT
197	MONTROSE	1196	CARQUINZ	2195	PRNDL J1	3194	ELLIOTT
198	WESTERN	1197	CRQNZTP2	2196	PRUNEDLE	3195	ENCINA
199	ROSSMOYN	1198	MRE IS-Q	2197	PRNDL J2	3196	ENCINA
200	KELLOGG	1199	ST.HELNA	2198	SALINAS2	3197	ENCINA 1
201	GRAYS_3	1200	CALISTGA	2199	SOLEDAD	3198	ENCINA 2
202	GRAYS_4	1201	TULUCAY	2200	SALINAS1	3199	ENCINA 3
203	GRAYS_5	1202	NAPA	2201	MOSLND E	3200	ENCINA 4
204	GRAY_8A	1203	BASALT	2202	MOSLND D	3201	ENCINA 5
205	GRAY_8BC	1204	BSLT TAP	2203	CSTRVLJ2	3202	ENCINAGT
206	GRAYS_9	1205	TULCY JT	2204	CSTRVLE	3203	ENCNITAS
207	AIRWAY_1	1206	IGNACO A	2205	CSTRVLJ1	3204	ESCNDIDO
208	AIRWAY_2	1207	IGNACO B	2206	DOLAN RD	3205	ESCNDIDO
209	AIRWAY_3	1208	IG JCT	2207	DOLAN J1	3206	ESCND050
210	TLOLIVE1	1209	NOVATO	2208	DOLAN J2	3207	ESCO
211	TLOLIVE2	1210	STAF_JCT	2209	DEL MNTE	3208	F
212	MAG_CT69	1211	STAFFORD	2210	SLDAD 4M	3209	FELCTATP
213	CAPON_69	1212	BOLINAS	2211	SLDAD 5M	3210	FELICITA
214	MAG_ST69	1213	OLEMA	2212	HOLST D	3211	FENTON

215	ROA-230	1214	TOCA_JCT	2213	BIG BASN	3212	FENTONTP
216	TJI-230	1215	WOODACRE	2214	BURNS J1	3213	FRIARS
217	FAULKNER	1216	TOCALOMA	2215	BURNS	3214	GARFIELD
218	LAUGHLIN	1217	HMLTN FD	2216	BURNS J2	3215	GENESEE
219	TOLSON	1218	HMLTNBFD	2217	LONE STR	3216	GLENCLIF
220	CRSTL2PS	1219	SAN RFLJ	2218	PT.MRT J	3217	GLNCLFTP
221	CRSTL3PS	1220	GREENBRE	2219	PT MRTTI	3218	GOALLINE
222	MERCHANT	1221	ALTO	2220	CRUSHER	3219	GRANITE
223	CRSTL N	1222	ALTOJT1	2221	GREN VLY	3220	HORNO
224	CAPTJACK	1223	ALTOJT2	2222	C.I.C.	3221	HORNO TP
225	DELTA	1224	SAUSALTO	2223	ERTA	3222	IMPRLBCH
226	MALIN	1225	MONTICLO	2224	CIC JCT	3223	IMPRLVLY
227	BULK PS1	1226	OLEUM	2225	WTSNVLE	3224	IMPRLVLY
228	BULK PS2	1227	VLYVWTP2	2226	ERTA JCT	3225	JAMACHA
229	SNPBLTP1	1228	CHRISTIE	2227	GRANT JT	3226	JAP MESA
230	VLYVWTP1	1229	SAN PBLO	2228	GRANT RK	3227	KEARNY
231	EDESTAP1	1230	PT PINLE	2229	AGRILINK	3228	KEARN3CD
232	FRUITVLE	1231	PPSTLTAP	2230	LGNTS J1	3229	KETTNER
233	EISENTP	1232	STD. OIL	2231	LGNSTAP	3230	KYOCERA
BUS	Name	Bus	Name	Bus	Name	Bus	Name
234	UNIONJCT	1233	VALLY VW	2232	GABILAN	3231	KYOCRATP
235	RNFROTP2	1234	EL CRRTO	2233	FTORD J1	3232	LA JOLLA
236	RNFROTP1	1235	RICHMOND	2234	SALINAS2	3233	LAGNA NL
237	TPMNTP2	1236	GRIZZLY2	2235	FTORD J2	3234	LASPULGS
238	TPMNTP1	1237	GRIZLYJ1	2236	SALINAS1	3235	LILAC
239	FRTLYTP	1238	PTPNLTAP	2237	BRNDA J1	3236	LOSCOCHS
240	POLPASPP	1239	SNPBLTP2	2238	BORONDA	3237	LOSCOCHS
241	BLUSTNPP	1240	GRIZLYJ2	2239	BRNDA J2	3238	LOVELAND

242	DEVLDNPP	1241	MRTNZJCT	2240	FORT ORD	3239	MAIN ST
243	BIOMSJCT	1242	CLARMNT	2241	MZNTA J2	3240	MAINST50
244	WSTLDJCT	1243	STATIN D	2242	MANZANTA	3241	MAINST51
245	GFFNJCT	1244	OAK C115	2243	MZNTA J1	3242	MARGARTA
246	AGRCJCT	1245	SCHNITZR	2244	DEL MNTE	3243	MDWLRKTP
247	SNJQTP	1246	STATIN L	2245	MONTEREY	3244	MELROSE
248	SNJQJCT	1247	STATIN X	2246	NAVY SCHL	3245	MELRSETP
249	DNUBAEGY	1248	STATIN J	2247	VIEJO	3246	MESA RIM
250	SNGRCOGN	1249	MARITIME	2248	HATTON	3247	MESAHGTS
251	SNGRJCT	1250	OWENSTAP	2249	VIEJO JT	3248	MIGUEL
252	DFS	1251	OWNBRKWY	2250	NAVY LAB	3249	MIGUEL
253	KNIGHTLD	1252	UNIN CHM	2251	LAURLS J	3250	MIGUEL
254	HYATT3	1253	CHRISTIE	2252	RSVTN RD	3251	MIGUEL
255	HYATT2	1254	PRT CSTA	2253	LAURELES	3252	MIGUEL
256	COTWD_F	1255	FRANKLIN	2254	OTTER	3253	MIGUELMP
257	BRIGTANO	1256	SEQUOIA	2255	FREXP JT	3254	MIGUELTP
258	WILLITSJ	1257	FRKLNALT	2256	FRSHXPRS	3255	MIRAMAR
259	LWRLAKEJ	1258	CRCKTCOG	2257	B.VSTA J	3256	MIRAMAR1
260	CACHE J2	1259	OAKLND 1	2258	BNA VSTA	3257	MIRAMRGT
261	CACHE J1	1260	OAKLND 2	2259	FIRESTNE	3258	MIRAMRTP
262	HGHLNDJ2	1261	OAKLND 3	2260	SPNCE J1	3259	MISSION
263	HGHLNDJ1	1262	OAKLND23	2261	SPNCE J2	3260	MISSION
264	REDBUDJ2	1263	OAK C12	2262	SPENCE	3261	MISSION
265	REDBUDJ1	1264	UNOCAL	2263	SNBRN JT	3262	MNSRATTP
266	LUCERNJ2	1265	UNION CH	2264	IND.ACRE	3263	MONSRATE
267	LUCERNJ1	1266	ChevGen1	2265	9 ST JCT	3264	MONTGMRY
268	STHELNJ1	1267	ChevGen2	2266	CMPHR J1	3265	MONTGYTP
269	STHELNJ2	1268	PITSBURG	2267	GONZALES	3266	MORHILTP

270	MTCLPHJ1	1269	KIRKER	2268	GNZLSJCT	3267	MOROHILL
271	MTCLPHJ2	1270	DOW TAP1	2269	CAMPHORA	3268	MURRAY
272	MNTCLOJ1	1271	DOW TAP2	2270	CMPHR J2	3269	N.GILA
273	MNTCLOJ2	1272	DOW MTR	2271	SOLEDAD	3270	NARROWS
BUS	Name	Bus	Name	Bus	Name	Bus	Name
274	SILVRDJ1	1273	PRAXAIR	2272	SEF TAP	3271	NATNLCTY
275	SILVRDJ2	1274	GWF#2 HS	2273	LOS CCHS	3272	NAVSTMTR
276	RINCONJ1	1275	GWF2 TAP	2274	LCCHS J1	3273	NOISLMTR
277	RINCONJ2	1276	CLAYTN	2275	LOS OSTS	3274	NORTHCTY
278	ER_FTNJT	1277	MEDW LNE	2276	LCCHS J2	3275	OCEANSDE
279	HYMPOMJT	1278	EBMUDGRY	2277	COBRN J1	3276	OCNSDETP
280	RDGE CBN	1279	LAKEWD-C	2278	COBRN J2	3277	OLD TOWN
281	AMES J1B	1280	LAKEWD-M	2279	KING CTY	3278	OLD TOWN
282	AMES J1A	1281	LK_REACT	2280	JOLON	3279	OTAY
283	AMEGTAP	1282	MARTNZ D	2281	COBURN	3280	OTAY TP
284	MTN_QUAR	1283	MARTNZ E	2282	BA FOOD1	3281	OTAYLAKE
285	TCY TER2	1284	BOLLMAN2	2283	BA FOOD2	3282	OTAYLKTP
286	TESLA 4M	1285	W.P.BART	2284	JOLON TP	3283	PACFCBCH
287	TESLA 2M	1286	CC SUB	2285	S ARDOJ1	3284	PALA
288	TESLA 2T	1287	DOMTAR	2286	S ARDOJ2	3285	PALOMAR
289	CHENYT	1288	CROWN Z	2287	TEXCO J1	3286	PARADISE
290	STONE	1289	SOBRANTE	2288	SAN ARDO	3287	PENDLETN
291	MARKH MJ2	1290	ALHAMBRA	2289	TEXCO J2	3288	PENSQTOS
292	MENLO G	1291	EST PRTL	2290	OILFLDS	3289	PENSQTOS
293	NVTO JCT	1292	MORAGA	2291	TEXACO	3290	PENSQTOS
294	NWK DIST	1293	COLSTJT1	2292	TEXCO J3	3291	PICO
295	WEBER 2	1294	COLSTJT2	2293	SARG CYN	3292	POINTLMA
296	WODBRG J	1295	KIRKTAP1	2294	SALN RVR	3293	POMERADO

297	INDSTR J	1296	KIRKTAP2	2295	SARGCN G	3294	POWAY
298	WINERY J	1297	LKWD_JCT	2296	SALNR GN	3295	PRCTRVLY
299	NEW HOPE	1298	LINDETP1	2297	BAF COG1	3296	R.CARMEL
300	MEYERTP2	1299	LINDETP2	2298	CIC COGN	3297	R.SNTAFE
301	MEYERTP1	1300	LINDEJCT	2299	SLDAD 5T	3298	R.SNTATP
302	CRQNZTP1	1301	BOLLMAN1	2300	PSWTSTCM	3299	RINCON
303	HGHWY J2	1302	IMHOFF_1	2301	M	3300	ROSCYNTP
304	ALHAMTP2	1303	IMHOFF_2	2302	FOOTHILL	3301	ROSE CYN
305	ALHAMTP1	1304	FIBRBJCT	2303	MORRO BY	3302	SAMPSON
306	TEXSUN2G	1305	FIBRJCT1	2304	SN LS OB	3303	SAMPSON
307	TEXSUN1G	1306	FIBRJCT2	2305	MESA_PGE	3304	SANLUSRY
308	TEX_SUN	1307	CC JCT	2306	S.M.ASSO	3305	SANLUSRY
309	LAPLM_G4	1308	CC SUB	2307	SISQUOC	3306	SANLUSRY
310	LAPLM_G3	1309	DU PONT	2308	GAREY	3307	SANMATEO
311	LAPLM_G2	1310	MARSH	2309	S.YNZ JT	3308	SANMRCOS
312	LAPLM_G1	1311	BRIONES	2310	SNTA MRA	3309	SANTYSBL
313	LAPALOMA	1312	BALFOUR	2311	DIVVIDE	3310	SANYSDRO
BUS	Name	Bus	Name	Bus	Name	Bus	Name
314	NORTECH	1313	BIXLER	2312	FAIRWAY	3311	SCRIPPS
315	PARADSE	1314	ANTIOCH	2313	BUELLTON	3312	SHADOWR
316	CR CANAL	1315	PITTSBRG	2314	LOMPCJ2	3313	SOUTHBAY
317	RASN JNT	1316	SHLL CHM	2315	OCEANO	3314	SOUTHBAY
318	JESSUP	1317	WLLW PSS	2316	UNION OL	3315	SOUTHBGT
319	LOMPCJ1	1318	SFPP CNC	2317	SURF JCT	3316	SOUTHBY1
320	TEMPL J2	1319	URICH	2318	SURF	3317	SOUTHBY2
321	BEALE_2	1320	STAUFFER	2319	PALMR	3318	SOUTHBY3
322	BEALE1J2	1321	PCBRICK	2320	ZACA	3319	SOUTHBY4
323	ROSSTAP2	1322	WILBRTAP	2321	SNTA YNZ	3320	SPRNGVLY

324	ROSSTAP1	1323	DUPNTJCT	2322	MANVILLE	3321	STREAMVW
325	AMES DST	1324	BALFRJCT	2323	CABRILLO	3322	STUART
326	ARVINJ1	1325	MDLRVRJT	2324	PURSMAJ1	3323	STUARTTP
327	ARVINJ2	1326	BXLR_TAP	2325	PURISIMA	3324	SUNYSDTP
328	STCKDLJ	1327	SHLLCHMT	2326	PURSMAJ2	3325	SUNYSIDE
329	TEVISJ2	1328	TAP GWF5	2327	GOLDTREE	3326	SWEETWTR
330	TEVISJ1	1329	PTSB 5	2328	TEMPLT7	3327	SWTWTRTP
331	WHTLNDAL	1330	PTSB 6	2329	TEMPL J	3328	SYCAMORE
332	HORSHE2	1331	C.COS 4	2330	CHOLAME	3329	SYCAMORE
333	NEWCSL2	1332	C.COS 5	2331	CHLME JT	3330	TALEGA
334	FLINT	1333	C.COS 6	2332	SAN MIGL	3331	TALEGA
335	HALE	1334	C.COS 7	2333	PSA RBLS	3332	TALEGA
336	KNTJALT	1335	MRAGA 1T	2334	ATASCDRO	3333	TALEGATP
337	DIST1500	1336	MRAGA 2T	2335	CACOS J1	3334	TELECYN
338	CACHSLJ2	1337	MRAGA 3T	2336	CACOS J2	3335	TOREYPNS
339	DIXON-J2	1338	GWF #1	2337	CAYUCOS	3336	TRABUCO
340	UCDAVSJ2	1339	GWF #2	2338	PERRY	3337	UCM
341	WILL JCT	1340	GWF #3	2339	CAMBRIA	3338	URBAN
342	WADHMJCT	1341	GWF #4	2340	BAYWOOD	3339	VALCNTR
343	WILSONAV	1342	GWF #5	2341	MUSTNG J	3340	WABASH
344	ARBALT	1343	CCCSD	2342	MUSTANG	3341	WARCYNTP
345	ARBJCT	1344	STAUFER	2343	SN LS OB	3342	WARENCYN
346	HUSTD	1345	SHELL 1	2344	DIVIDE	3343	WARNERS
347	WESCOT2	1346	SHELL 2	2345	VAFB SSA	3344	KEARNYLD
348	WESCOT1	1347	SHELL 3	2346	VAFB SSB	3345	KEARN2AB
349	MERIDJCT	1348	CROWN.Z.	2347	VAFB A-N	3346	KEARN2CD
350	PP STEEL	1349	TOSCO	2348	MOSSLND6	3347	KEARN3AB
351	LINC ALT	1350	FOSTER W	2349	MOSSLND7	3348	KEARNGT1

352	SUNMAID	1351	DOW CHEM	2350	MORRO 1	3349	KEAMDGT2
353	SCWAX	1352	DOWCHEM1	2351	MORRO 2	3350	KEAMDGT3
BUS	Name	Bus	Name	Bus	Name	Bus	Name
354	SCWAXJCT	1353	DOWCHEM2	2352	MORRO 3	3351	OMWD
355	AIRPROD	1354	DOWCHEM3	2353	MORRO 4	3352	CRESTWD
356	ULTPWRJ	1355	WINDMSTR	2354	DIABLO 1	3353	MMC_ES
357	LEE_JCT	1356	ALTAMONT	2355	DIABLO 2	3354	MMC_ES
358	LEARNER	1357	LARKIN D	2356	UNION OL	3355	MMC_OY
359	STKTN WW	1358	LARKIN E	2357	SO VAFB	3356	MMC_OY
360	TOSCO-PP	1359	LARKIN F	2358	ST MARIA	3357	LRKSP_BD
361	ALTA-CGE	1360	MISSON	2359	GAREY	3358	LRKSPBD1
362	SEBASTIA	1361	POTRERO	2360	Kifer Re	3359	LRKSPBD2
363	CAL CEDA	1362	HNTRS PT	2361	Scott Re	3360	ENCINATP
364	ZAMORA1	1363	BAYSHOR1	2362	CCA100	3361	SANTEE
365	KNIGHT1	1364	BAYSHOR2	2363	RICHMOND	3362	ARTESN
366	PSIERRA	1365	MARTIN C	2364	MEADOWVW	3363	TALEGA
367	CSCDE T	1366	SHAWROAD	2365	MILLWOOD	3364	GEN DYNM
368	CSCDE M	1367	MARTIN	2366	WIN&AMED	3365	GENDYNTP
369	SPI_AND1	1368	POTRERO3	2367	JELD-WEN	3366	MEF_MR1
370	WHEELBR1	1369	POTRERO4	2368	HONEYLAK	3367	KUMEYAAY
371	WHEELBR	1370	POTRERO5	2369	CHESTNUT	3368	PEN
372	TULCAY1	1371	POTRERO6	2370	WIN&AMDE	3369	PEN_CT1
373	PCLUMBER	1372	HNTRS P2	2371	JELD-WN	3370	PEN_CT2
374	BRDGV L T	1373	HNTRS P3	2372	HONEYLKE	3371	PEN_ST
375	BRDGV L M	1374	HNTRS P4	2373	INTAKE	3372	SYCAMORE
376	EUREKA A	1375	HNTRS P1	2374	OAKDLTID	3373	GRANITTP
377	UKIAH JT	1376	DALY CTY	2375	MOCCASIN	3374	BORREGO
378	MASON TP	1377	DLY CTYP	2376	WRNRVLLE	3375	KUMEYAAY

379	OLIVH J1	1378	SERRMNT E	2377	KIRKWD 1	3376	KUMEYAAY
380	E.MRY J1	1379	EST GRND	2378	KIRKWD 2	3377	PFC-AVC
381	HONC JT3	1380	UAL COGN	2379	KIRKWD 3	3378	GRNT HLL
382	OLIVH J3	1381	SFIA	2380	HOLM 1	3379	NEVBD501
383	E.MRY J2	1382	MILLBRAE	2381	HOLM 2	3380	NEVBD502
384	HONC JT1	1383	SFIA-MA	2382	MCSN CK1	3381	SUMMIT 3
385	CLOVISJ2	1384	SANMATEO	2383	MCSN CK2	3382	SUMMIT 1
386	CLOVISJ1	1385	BAY MDWS	2384	KES MP1	3383	SUMMIT 2
387	HILLSIDE	1386	BELMONT	2385	KES MP2	3384	ALAMT1 G
388	PIERCY	1387	BAIR	2386	KES MP3	3385	ALAMT2 G
389	CRBNA JC	1388	SHREDDER	2387	KESWICK	3386	ALAMT3 G
390	MONDAVI	1389	RVNSWD E	2388	TRY MP1	3387	ALAMT4 G
391	LODI AUX	1390	CLY LND2	2389	TRY MP2	3388	ALAMT5 G
392	PTSB 7	1391	CLY LND	2390	AIRPORTW	3389	ALMITOSE
393	ROUND MT	1392	SMATEO3M	2391	COTWDWAP	3390	ALMITOSW
BUS	Name	Bus	Name	Bus	Name	Bus	Name
394	TABLE MT	1393	SHREDJCT	2392	ELVERTAW	3391	ALMITOSW
395	OLINDA	1394	LONESTAR	2393	FOLSOM	3392	APPGEN1G
396	MAXWELL	1395	PACIFJCT	2394	FOLSOM	3393	APPGEN2G
397	VACA-DIX	1396	SNTH LNE	2395	FOLSOM1	3394	ARCO 1G
398	TRACY	1397	SN BRNOT	2396	FOLSOM2	3395	ARCO 2G
399	TESLA	1398	SNANDRES	2397	FOLSOM3	3396	ARCO 3G
400	METCALF	1399	MILLBRAE	2398	J.F.CARR	3397	ARCO 4G
401	MOSSLAND	1400	MLLBRETP	2399	J.F.CARR	3398	ARCO SC
402	LOSBANOS	1401	PACIFICA	2400	KESWICK2	3399	BARRE
403	GATES	1402	BURLNGME	2401	KESWICK3	3400	BLYTHESC
404	DIABLO	1403	SAN MATO	2402	KESWICK	3401	BRIGEN
405	MIDWAY	1404	BERESFRD	2403	KESWICK1	3402	CAMINO

406	RD MT 1M	1405	CAROLNDS	2404	LLNL	3403	CARBOGEN
407	TB MT 1M	1406	HILLSDL	2405	MELONE1	3404	CENTER S
408	VC DX11M	1407	HLLSDLJT	2406	MELONE2	3405	CHEVGEN1
409	L.BANS M	1408	CRYSTLSG	2407	MELONES	3406	CHEVGEN2
410	COTWD_E	1409	RALSTON	2408	OLINDAW	3407	CHINO
411	BRNY_FST	1410	ORACLE60	2409	ROSEVILL	3408	CHINO
412	GLENN	1411	SAN CRLS	2410	FIDDYMNT	3409	CIMGEN
413	LOGAN CR	1412	HLF MNBY	2411	FLANAGAN	3410	COLDGEN
414	PIT 1	1413	BAIR	2412	FLANAGAN	3411	DELAMO
415	SPI-BRNY	1414	REDWDTP1	2413	SHAST LK	3412	DELAMO
416	PIT 3	1415	REDWDTP2	2414	ROSEVLL1	3413	DELGEN
417	PIT 4	1416	REDWOOD	2415	ROSEVLL2	3414	ETIWAN7A
418	BLACK	1417	RAYCHEM	2416	FIDDYMNT	3415	AMERON
419	PIT 5 JT	1418	BLLE HVN	2417	SHASTA1	3416	EAGLEMTN
420	PIT 6	1419	BLHVNTTP1	2418	SHASTA2	3417	EAGLROCK
421	PIT 7	1420	BLHVNTTP2	2419	SHASTA3	3418	EL NIDO
422	PIT 7 JT	1421	CLY LNDG	2420	SHASTA4	3419	EL NIDO
423	PIT 4 JT	1422	LAS PLGS	2421	SHASTA5	3420	ELDORDO
424	PIT 6 JT	1423	EMRLD LE	2422	SHASTA	3421	ELDORDO
425	COVE_RD.	1424	WTRSHDTP	2423	SPRINGCR	3422	ELDORDO
426	PIT 7JT2	1425	WATRSBED	2424	TRACY YG	3423	ELLIS
427	ROUND MT	1426	JEFFERSN	2425	TRACYPP1	3424	ELSEG1 G
428	CARIBOU	1427	GLENWOOD	2426	TRACYPP2	3425	ELSEG2 G
429	CARBOU M	1428	S.R.I.	2427	TRCY PMP	3426	ELSEG3 G
430	BELDEN	1429	MENLO	2428	TRINTY12	3427	ELSEG4 G
431	RK C JT1	1430	MNLO JCT	2429	TRINITY	3428	ELSEGND0
432	BCKS CRK	1431	MNLOJCT2	2430	SPRINGCR	3429	MTNVIST1
BUS	Name	Bus	Name	Bus	Name	Bus	Name

433	ROCKCK 1	1432	STANFORD	2431	NIMBUS12	3430	MTNVIST2
434	ROCKCK 2	1433	WOODSIDE	2432	NIMBUS	3431	MTNVIST3
435	RK C JT2	1434	S.L.A.C.	2433	KNAUF	3432	MTNVIST4
436	CRESTA	1435	SMATO2SC	2434	LLNLAB	3433	ETIWANDA
437	POE	1436	SMATO3SC	2435	AIRPORTW	3434	ETIWANDA
438	TBL MT D	1437	SMATO1SC	2436	AIRPORT1	3435	GOLETA
439	TBL MT2M	1438	CARDINAL	2437	AIR JCT1	3436	GOLETA
440	TBL MT E	1439	UNTED CO	2438	AIR JCT2	3437	GOULD
441	TBL MT3M	1440	SRI INTL	2439	AIRPORT1	3438	GROWGEN
442	PALRMO M	1441	MELNS JA	2440	AIRPORT2	3439	HARBOR
443	PALERMO	1442	FROGTOWN	2441	BELTLINE	3440	HARBOR G
444	COLGATE	1443	CATARACT	2442	BELT1	3441	HILLGEN
445	RIO OSO	1444	STANISLS	2443	CANBY	3442	HINSON
446	ATLANTC	1445	AVENA	2444	CANBY1	3443	HINSON
447	GOLDHILL	1446	MANTECA	2445	CANBY2	3444	HUNT1 G
448	LAKE	1447	RPN JNCN	2446	CANBY3	3445	HUNT2 G
449	RALSTON	1448	VIERRA	2447	CLEAR CR	3446	HUNTGBCH
450	MIDLFORK	1449	RIPON	2448	COLLEGE	3447	HUNTGBCH
451	MDDLFK M	1450	CROSRDJT	2449	COLLEGE1	3448	ICEGEN
452	BRIGHTON	1451	CL AMMNA	2450	EAST RDG	3449	INLAND
453	CR1T3_18	1452	KSSN-JC1	2451	EASTRDG1	3450	JOHANNA
454	G14CRT15	1453	KASSON	2452	EUREKA	3451	LA FRESA
455	GEYSR12	1454	KSSN-JC2	2453	EUREKA1	3452	LA FRESA
456	GEYSR18	1455	OI GLASS	2454	GOODWAT	3453	LAGUBELL
457	GEYSR14	1456	SAFEWAY	2455	MOORE	3454	LAGUBELL
458	CR2T3_18	1457	TESLA	2456	MOORE1	3455	LBEACH
459	NCPA1	1458	LEPRINO	2457	MOORE2	3456	LBEACH1G
460	NCPATT2	1459	ELLS GTY	2458	OASIS RD	3457	LBEACH7G

461	G16T0_2	1460	TRACY JC	2459	OASIS1	3458	LBEACH8G
462	BEARCNYN	1461	TRACY	2460	OREGON	3459	LBEACH9G
463	WSFRDFLT	1462	HJ HEINZ	2461	OREGON1	3460	LCIENEGA
464	GEYSR16	1463	STCKTNJB	2462	QUARTZ H	3461	LITEHIPE
465	NCPA2	1464	STKTON B	2463	RDGCT 1	3462	LITEHIPE
466	G9CRT111	1465	STKTON A	2464	RDGCT 2	3463	LUGO
467	G13TT1_9	1466	STN COGN	2465	RDGCT 3	3464	LUGO
468	G13TT1_8	1467	LCKFRDJB	2466	RDGPOWER	3465	MAGUNDEN
469	SNTAFE	1468	LCKFRDJA	2467	RDGSTEAM	3466	MANDALAY
470	GEYSR13	1469	BELLOTA	2468	SULP CRK	3467	MANDLY1G
471	GEYSR20	1470	LOCKFORD	2469	SULP JCT	3468	MANDLY2G
472	SMUDGE01	1471	CAMANCHE	2470	SULP1	3469	MESA CAL
BUS	Name	Bus	Name	Bus	Name	Bus	Name
473	GEYSR17	1472	TH.E.DV.	2471	SULP2	3470	MIRALOMA
474	FULTON	1473	SPC JCT.	2472	TEXASSPR	3471	MIRALOMW
475	LAKEVILE	1474	SP CMPNY	2473	TEXASSP1	3472	MOBGEN
476	CROCKETT	1475	LLNL TAP	2474	WALDON	3473	MOHAV1CC
477	C&H	1476	USWP-PAT	2475	WALDON1	3474	MOHAV2CC
478	TULUCAY	1477	FAYETTE	2476	WALDON2	3475	MOHAVE
479	IGNACIO	1478	ALTENRGY	2477	LODI	3476	MOORPARK
480	CORTINA	1479	SLT SPRG	2478	CITY UKH	3477	MOORPARK
481	CRTNA M	1480	TIGR CRK	2479	CARTWRT	3478	OLINDA
482	VACA-DIX	1481	HERDLYN	2480	JENNY	3479	OMAR
483	EXXON_BH	1482	NEWARKS	2481	ALAMEDCT	3480	OMAR 1G
484	BAHIA	1483	WEST PNT	2482	PLO ALTO	3481	OMAR 2G
485	PARKWAY	1484	P.GRVEJ.	2483	LMPC-CTY	3482	OMAR 3G
486	PEABODY	1485	ELECTRAJ	2484	HELDSBRG	3483	OMAR 4G
487	USWP-RUS	1486	PNE GRVE	2485	BIGGS	3484	ORMOND

488	LOCKFORD	1487	VLLY SPS	2486	GRIDLEY	3485	ORMOND1G
489	TIGR CRK	1488	N BRANCH	2487	PLMS-SRA	3486	ORMOND2G
490	TIGR CKM	1489	CAL CMNT	2488	ROSEVLCT	3487	OXGEN
491	ELECTRA	1490	MARTELL	2489	INDUSTRL	3488	PADUA
492	VLLY SPS	1491	INE_TP	2490	SPICER	3489	PADUA
493	STAGG	1492	OLETA	2491	COLLRVL1	3490	PANDOL
494	BELLOTA	1493	AM FORST	2492	COLLRVL2	3491	PARDEE
495	BLLTA 1M	1494	CLAY	2493	NCPA1GY1	3492	PASTORIA
496	COLLRLVL	1495	INE PRSN	2494	NCPA1GY2	3493	PITCHGEN
497	WEBER	1496	I.NRGYJT	2495	NCPA2GY1	3494	PROCGEN
498	WARNERVL	1497	I.ENERGY	2496	NCPA2GY2	3495	PULPGEN
499	CC SUB	1498	PARDEE A	2497	STIG CC	3496	REDON5 G
500	C.COSTA	1499	PRDE JCT	2498	ROSEVCT1	3497	REDON6 G
501	PITSBG E	1500	N.HGN JT	2499	ROSEVCT2	3498	REDON7 G
502	TIDEWATR	1501	N.HOGAN	2500	ALMDACT1	3499	REDON8 G
503	SOBRANTE	1502	CORRAL	2501	ALMDACT2	3500	REDONDO
504	ROSSMOOR	1503	LINDEN	2502	LODI25CT	3501	RIOHONDO
505	MORAGA	1504	MRMN JCT	2503	NEWSPICE	3502	S.CLARA
506	MRAGA 1M	1505	MORMON	2504	COTTLE A	3503	S.CLARA
507	MRAGA 2M	1506	DANA	2505	COTTLE B	3504	S.ONOFR2
508	CASTROVL	1507	WEBER 1	2506	WALNT	3505	S.ONOFR3
509	SANRAMON	1508	SNTA FEA	2507	TUOLUMN	3506	S.ONOFRE
510	CV BART	1509	CARGILL	2508	PINEER	3507	SANBRDNO
511	E. SHORE	1510	SNTA FEB	2509	CRTEZ	3508	SANTIAGO
512	TASSAJAR	1511	JM	2510	HILMAR	3509	SANTIAGO
BUS	Name	Bus	Name	Bus	Name	Bus	Name
513	TES JCT	1512	LIPTON	2511	DONPEDRO	3510	SAUGUS
514	RESEARCH	1513	CHEROKEE	2512	ROEDING	3511	SERRANO

515	BRENTWOD	1514	WATERLOO	2513	INDSTRIL	3512	SERRANO
516	KELSO	1515	STCKTN A	2514	LA GRNGE	3513	SERRFGEN
517	USWP-RLF	1516	CHRTRWYS	2515	COLLEGE	3514	SIMPSON
518	ALTALAND	1517	HAZLTN J	2516	CERES	3515	SPRINGVL
519	WND MSTR	1518	E.STCKTN	2517	TUOLUMNE	3516	SYC CYN
520	ALTM MDW	1519	MONARCH	2518	HAWKINS	3517	SYCCYN1G
521	LS PSTAS	1520	OAK PARK	2519	GILSTRAP	3518	SYCCYN2G
522	USWP-JRW	1521	SUMIDEN	2520	HUGHSON	3519	SYCCYN3G
523	CAYETANO	1522	HARDING	2521	GEER	3520	SYCCYN4G
524	FLOWIND2	1523	STCKTNAR	2522	F STREET	3521	SYLMAR S
525	TRES VAQ	1524	ROB-LRNR	2523	MONTPELR	3522	TENNGEN1
526	EIGHT MI	1525	ROGH-RDY	2524	WESTPORT	3523	TENNGEN2
527	TESLA E	1526	CHANNEL	2525	WALNUT	3524	ULTRAGEN
528	TESLA D	1527	CHNNL JT	2526	FAIRGRND	3525	VALLEYSC
529	NEWARK D	1528	COG.NTNL	2527	DAWSON	3526	VESTAL
530	NEWARK E	1529	FRNCH CP	2528	DAWSN TP	3527	VESTAL
531	ADCC	1530	FRNCH CJ	2529	ALMOND	3528	VILLA PK
532	WESTLEY	1531	GRONMYER	2530	CROWSLND	3529	VINCENT
533	EMBRCDRD	1532	STAGG	2531	LA GTP1	3530	VINCENT
534	EMBRCDRE	1533	CNTRY CB	2532	LA GTP2	3531	WALNUT
535	MARTIN C	1534	UOP	2533	STURLOCK	3532	WALNUT
536	SANMATEO	1535	WSTLNESW	2534	COMMONS	3533	WILLAMET
537	SMATEO5M	1536	WESTLANE	2535	DONPDRO1	3534	VALLEYSC
538	SMATEO6M	1537	HAMMER	2536	DONPDRO2	3535	ALAMT6 G
539	RAVENSWD	1538	HMMR JCT	2537	DONPDRO4	3536	ALAMT7 G
540	SMATEO7M	1539	MORADAJT	2538	WALNT1CT	3537	ARCO 5G
541	MONTAVIS	1540	METTLER	2539	WALNT2CT	3538	ARCO 6G
542	SLACTAP2	1541	TERMNOUS	2540	LA GRNGE	3539	HUNT3 G

543	SLACTAP1	1542	NW HPE J	2541	DAWSON	3540	HUNT4 G
544	S.L.A.C.	1543	LOCKEFRD	2542	ALMONDCT	3541	HUNT5 G
545	JEFFERSN	1544	LOCKFRD1	2543	LA GRNLD	3542	LBEACH2G
546	SARATOGA	1545	VICTOR	2544	BUENAVJ1	3543	LBEACH3G
547	HICKS	1546	LODI	2545	BUENAVT1	3544	LBEACH4G
548	VASONA	1547	GENMILLS	2546	BUENAVJ2	3545	LBEACH5G
549	METCALF	1548	COLONY	2547	BUENAVT2	3546	LBEACH6G
550	MOSSLND2	1549	CLNY JCT	2548	DELTAPMP	3547	VALLEY4T
551	MOSSLND1	1550	LODI JCT	2549	DS AMIGO	3548	valley4i
552	COBURN	1551	WATRLJCT	2550	HYATT	3549	MIRLOM1T
BUS	Name	Bus	Name	Bus	Name	Bus	Name
553	LOSBANOS	1552	MSHR 60V	2551	SN LS PP	3550	mirlom1i
554	PANOCHE	1553	MANTECA	2552	THERMLTO	3551	MIRLOM3T
555	PNCHE 1M	1554	LOUISE	2553	THM JCT	3552	mirlom3i
556	STOREY 2	1555	MSSDLESW	2554	WHLR RJ1	3553	MIRLOM4T
557	STOREY 1	1556	CALVO	2555	WHLR RT1	3554	mirlom4i
558	WILSON	1557	LTHRP JT	2556	WHLR RJ2	3555	SERRAN1T
559	BORDEN	1558	KASSON	2557	WHLR RT2	3556	serran1i
560	GREGG	1559	BANTA	2558	WND GPJ1	3557	SERRAN2T
561	HELMS PP	1560	BNTA JCT	2559	WND GPT1	3558	serran2i
562	MCMULLN1	1561	LYOTH-SP	2560	WND GPJ2	3559	VINCEN1T
563	KEARNEY	1562	CARBONA	2561	WND GPT2	3560	vincen1i
564	HERNDON	1563	MNTCA JT	2562	THERMLT1	3561	LUGO 1T
565	FGRDN T1	1564	BNTA CRB	2563	THERMLT2	3562	lugo 1i
566	FIGRDN 1	1565	HERDLYN	2564	THERMLT3	3563	LUGO 2T
567	FGRDN T2	1566	B.BTHNY-	2565	THERMLT4	3564	lugo 2i
568	FIGRDN 2	1567	HRDLNJCT	2566	PINE FLT	3565	ELDOR 1T
569	ASHLAN	1568	SOUTH BY	2567	SANLUIS1	3566	eldor 1i

570	HAAS	1569	MDL_RIVR	2568	SANLUIS2	3567	ELLIS
571	BALCH3TP	1570	MCD_ISLE	2569	SANLUIS3	3568	CHEVMAIN
572	BALCH	1571	WEST SDE	2570	SANLUIS4	3569	CHEVMAIN
573	PINE FLT	1572	SALT SPS	2571	DOS AMG1	3570	SAUG TAP
574	HELM	1573	STAGG_5	2572	DOS AMG2	3571	BARRE
575	MC CALL	1574	BELLTA T	2573	DELTA E	3572	CAMINO
576	MCCALL1M	1575	TH.E.DV.	2574	DELTA D	3573	CENTER S
577	MCCALL2M	1576	SJ COGEN	2575	DELTA C	3574	EAGLEMTN
578	MCCALL3M	1577	SP CMPNY	2576	BUENAVS1	3575	EAGLROCK
579	HENTAP1	1578	ELECTRA	2577	BUENAVS2	3576	GOULD
580	HENTAP2	1579	CPC STCN	2578	WHLR RD1	3577	JOHANNA
581	HENRIETA	1580	I.ENERGY	2579	WHLR RD2	3578	LCIENEGA
582	HERNDN1M	1581	COG.NTNL	2580	WINDGAP1	3579	MESA CAL
583	HERNDN2M	1582	WEST PNT	2581	WINDGAP2	3580	MIRALOMA
584	GATES	1583	TIGR CRK	2582	WINDGAP3	3581	OLINDA
585	GATES 1M	1584	GEN.MILL	2583	WINDGAP4	3582	RECTOR
586	TEMPLETN	1585	COG.CAPT	2584	DELTA B	3583	RIOHONDO
587	MORROBAY	1586	KALINA	2585	DELTA A	3584	SANBRDNO
588	DIABLOCN	1587	USWP_#4	2586	HYATT 1	3585	SPRINGVL
589	MESA PGE	1588	USWP_#3	2587	HYATT 2	3586	VILLA PK
590	ARCO	1589	FLOWD3-6	2588	HYATT 3	3587	WARNETAP
591	STCKDLEA	1590	PATTERSN	2589	HYATT 4	3588	WARNE
592	STCKDLEB	1591	PRDE 1-3	2590	HYATT 5	3589	PISGAH
BUS	Name	Bus	Name	Bus	Name	Bus	Name
593	STCKDLJ1	1592	PARDE 2	2591	HYATT 6	3590	ELDOR 2T
594	STCKDLJ2	1593	CAMANCHE	2592	ELVERTAS	3591	eldor 2i
595	BKRSFDJ2	1594	DONNELLS	2593	HURLEY S	3592	MANDLY3G
596	KERN PP	1595	BRDSLY J	2594	RNCHSECO	3593	MANDALAY

597	BKRSFLDA	1596	BEARDSLY	2595	PARKER2M	3594	MIRLOM2T
598	BKRSFLDB	1597	SPRNG GP	2596	PRKR MID	3595	mirlom2i
599	MIDWAY	1598	SANDBAR	2597	PARKER1M	3596	VALLEY-S
600	SUNST	1599	SNDBR JT	2598	STNDFDM2	3597	RECTOR
601	SUMMIT	1600	SPRNG GJ	2599	CLAUS	3598	VERNON66
602	WHEELER	1601	MI-WUK	2600	MC CLURE	3599	MALBRG1G
603	HUMBOLDT	1602	CURTISS	2601	SNTA CRZ	3600	MALBRG2G
604	HMBLT TM	1603	FBERBORD	2602	STANDFRD	3601	MALBRG3G
605	HMBLDT B	1604	RCTRK J.	2603	HUNTWSTP	3602	RERC1G
606	LOW GAP1	1605	R.TRACK	2604	HERSHEY	3603	RERC2G
607	BRDGVLE	1606	CH.STNJT	2605	PARKER	3604	SPRINGEN
608	ORICK	1607	CH.STN	2606	STANDFRD	3605	BIG CRK1
609	BIG_LAGN	1608	PEORIA	2607	FINNEY	3606	BIG CRK2
610	TRINIDAD	1609	MELONES	2608	ROSEMORE	3607	BIG CRK3
611	ESSX JCT	1610	TULLOCH	2609	8TH ST	3608	BIG CRK4
612	JANCK TP	1611	MELNS JB	2610	PRESCOTT	3609	BIG CRK8
613	ARC_JT2X	1612	RVRBANK	2611	BRGGSMRE	3610	B CRK1-1
614	LP_FLKBD	1613	RVRBK J1	2612	ENSLEN	3611	B CRK1-2
615	JANS CRK	1614	RVRBK J2	2613	WOODROW	3612	B CRK2-1
616	ULTR_PWR	1615	RVRBK TP	2614	12TH ST	3613	B CRK2-2
617	BCHIPMIL	1616	VALLY HM	2615	SNTA RSA	3614	B CRK2-3
618	BLUE LKE	1617	SJ COGEN	2616	LAPHAM	3615	B CRK3-1
619	BCHIP_TP	1618	CPC STCN	2617	MARIPOS1	3616	B CRK3-2
620	SMPSNTAP	1619	MDSTO CN	2618	CLAUS	3617	B CRK3-3
621	ARCTAJT1	1620	SALDO TP	2619	OAKDALE	3618	B CRK 4
622	SIMPSON	1621	SALADO	2620	SYLVAN	3619	B CRK 8
623	ARCTAJT2	1622	SALADO J	2621	REINWAY	3620	MAMMOTH
624	ARCTA_J2	1623	MILLER	2622	LINCOLN	3621	MAMOTH1G

625	ARCATA	1624	MILER TP	2623	DN PDROM	3622	MAMOTH2G
626	FAIRHAVN	1625	TEICHERT	2624	PARADSE	3623	EASTWOOD
627	SIERA_PC	1626	INGRM C.	2625	SISK	3624	EASTWOOD
628	LP-SAMOA	1627	WESTLEY	2626	POUST	3625	PITMAN
629	FPC	1628	SALADO	2627	PRSC TTJT	3626	PORTAL
630	SIM_PULP	1629	PTRSNFRZ	2628	BNDS FLT	3627	PORTAL
631	HUMBOLDT	1630	PATTERSN	2629	ROSELLE	3628	HIDESERT
632	HARRIS	1631	STNSLSRP	2630	LADD	3629	HUNTBCH1
BUS	Name	Bus	Name	Bus	Name	Bus	Name
633	HARRISST	1632	CRWS LDJ	2631	RSMRE TP	3630	ANTELOPE
634	EUREKA	1633	GUSTN JT	2632	STOCK AV	3631	ANTELOPE
635	HMBLT JT	1634	NEWMAN	2633	FOXRIVER	3632	BAILEY
636	HMBLT BY	1635	MEDLIN J	2634	CLOUGH	3633	BAILEY
637	MPLE CRK	1636	CRWS LDG	2635	STODDARD	3634	VARWIND
638	RUSS RCH	1637	NWMN JCT	2636	WOODLMID	3635	ACTON SC
639	WILLWCRK	1638	GUSTINE	2637	CONEJO	3636	ANAVERDE
640	HOOPA	1639	CH.STN.	2638	DONPDRO3	3637	BREEZE
641	EEL RIVR	1640	STNSLSRP	2639	MCCLURE1	3638	CORUM
642	NEWBURG	1641	DONNELLS	2640	MCCLURE2	3639	CUMMINGS
643	CARLOTTA	1642	SANDBAR	2641	WOODLMID	3640	DEL SUR
644	RIO DELL	1643	STANISLS	2642	PARKER1T	3641	GORMAN
645	SWNS FLT	1644	BEARDSLY	2643	PARKER2T	3642	FRAZPARK
646	BRDGVLE	1645	TULLOCH	2644	STNDFR1L	3643	MONOLITH
647	FRUITLND	1646	SPRNG GP	2645	STNDFR2L	3644	LORAIN
648	FRT SWRD	1647	CHWCHLLA	2646	CAMINO S	3645	WALKERBN
649	GRBRVLE	1648	CERTAN T	2647	CAMPBELL	3646	HAVILAH
650	KEKAWAKA	1649	CERTTEED	2648	CARMICAL	3647	LANCSTR
651	FAIRHAVN	1650	ATWATER	2649	ELKGROVE	3648	LITTLERK

652	PAC.LUMB	1651	CERTANJ1	2650	ELVRTAX1	3649	NEENACH
653	HUMBOLDT	1652	CASTLE	2651	ELVRTAX2	3650	OASIS SC
654	ULTRAPWR	1653	CERTANJ2	2652	FOOTHILL	3651	PALMDALE
655	LP SAMOA	1654	CHWCGNJT	2653	HEDGE	3652	PIUTE
656	HMBLT TT	1655	CRESEY T	2654	JAYBIRD	3653	QUARTZHL
657	HMBOLDT1	1656	ATWATR J	2655	ORANGEVL	3654	REDMAN
658	HMBOLDT2	1657	EXCHEQUR	2656	POCKET	3655	SHUTTLE
659	MENDOCNO	1658	JRWD GEN	2657	PROCTER	3656	WILSONA
660	CALPELLA	1659	LE GRAND	2658	UNIONVLY	3657	CALCMENT
661	UKIAH	1660	LE GRNDJ	2659	WHITEROK	3658	GREATLKS
662	HPLND JT	1661	SHARON	2660	PROCTERI	3659	HELIJET
663	CLOVRDL	1662	SHARON T	2661	PROCTERJ	3660	LANPRI
664	MPE TAP	1663	OAKHURST	2662	EAST CTY	3661	ROCKAIR
665	MPE	1664	JR WOOD	2663	ELVERTAS	3662	TORTOISE
666	GEYERS56	1665	CORSGOLD	2664	HEDGE	3663	ROSAMOND
667	LUCERNE	1666	OAKH_JCT	2665	HURLEY	3664	WESTPAC
668	ERFT5_25	1667	LIVNGSTN	2666	MID CTY	3665	GOLDTOWN
669	EGLE RCK	1668	GALLO	2667	NORTHCTY	3666	KERNRVR
670	GEYSR11	1669	WILSON A	2668	SOUTHCTY	3667	TAP 66
671	REDBUD	1670	WILSON B	2669	STA. A	3668	TAP 65
672	INDIN VL	1671	EL CAPTN	2670	STA. B	3669	TAP 70
BUS	Name	Bus	Name	Bus	Name	Bus	Name
673	HGHLAND	1672	CRESSEY	2671	STA. D	3670	TAP 64
674	HOMSTKTP	1673	MERCED	2672	CARMICAL	3671	TAP 68
675	HOMEPROC	1674	MERCED M	2673	ELKGROV1	3672	TAP 69
676	HOMEGRND	1675	CHENY	2674	ELVERTA1	3673	TAP 63
677	FULTON	1676	NEWHALL	2675	ELVERTA2	3674	TAP 60
678	MONROE1	1677	DAIRYLND	2676	FOOTHIL1	3675	TAP 62

679	MONROE2	1678	MENDOTA	2677	HEDGE 1	3676	TAP 61
680	SNTA RSA	1679	PANOCHET	2678	HEDGE 3	3677	TAP 72
681	STNY PTP	1680	PAN2_TAP	2679	HURLEY 1	3678	TAP 73
682	STONY PT	1681	PANOCH	2680	HURLEY 2	3679	TAP 71
683	BELLVUE	1682	PANOCH	2681	JONESFRK	3680	TAP 86
684	PENNGRVE	1683	HAMMONDS	2682	LAKE 1	3681	TAP 85
685	RINCON	1684	DFSTP	2683	LOON LK	3682	TAP 84
686	CORONA	1685	ORO LOMA	2684	MCCLELLN	3683	TAP 83
687	LAKEVLLE	1686	LUIS_#3	2685	ORANGVL1	3684	TAP 82
688	FLTN JCT	1687	LUIS_#5	2686	ORANGVL2	3685	BOREL
689	SONOMA	1688	OXFORD	2687	POCKET 1	3686	ARBWIND
690	MNDCNO M	1689	EL NIDO	2688	POCKET 2	3687	ENCANWND
691	MENDOCNO	1690	WESIX	2689	ROBBS PK	3688	FLOWIND
692	PTTR VLY	1691	WESTLAND	2690	SRWTP	3689	DUTCHWND
693	WILLITS	1692	EXCHQRT	2691	UNIONVLY	3690	SOUTHWND
694	LYTNVLLE	1693	MADERAPR	2692	ELKGROV2	3691	NORTHWND
695	COVELO6	1694	ORO LOMA	2693	LAKE 2	3692	ZONDWIND
696	FRT BRGG	1695	MERCED	2694	EAST CTY	3693	MIDWIND
697	BIG RIVR	1696	LIVNGSTN	2695	MID CTY1	3694	MORWIND
698	ELK	1697	CANAL	2696	MID CTY2	3695	TAP 81
699	PNT ARNA	1698	CHEVPIPE	2697	NORTHCT1	3696	TAP 80
700	GARCIA	1699	SNTA NLA	2698	NORTHCT2	3697	TAP 79
701	GARCIA J	1700	LVNGSTNT	2699	SOUTHCTY	3698	TAP 78
702	PHILO	1701	LOS BANS	2700	STA. D 1	3699	TAP 75
703	PHLO JCT	1702	SNTA RTA	2701	STA. D 2	3700	TAP 74
704	MASONITE	1703	DOS PALS	2702	MID CTY3	3701	TAP 76
705	UPPR LKE	1704	ORTIGA	2703	UCDMC	3702	TAP 67
706	HARTLEY	1705	MRCYSPRS	2704	CAMINO 1	3703	TAP 77

707	CLER LKE	1706	ARBURUA	2705	CAMINO 2	3704	RITE AID
708	HPLND JT	1707	MC SWAIN	2706	CAMPBEL1	3705	CORRECT
709	KONOCI6	1708	MARIPOS2	2707	CAMPBEL2	3706	TAP 50
710	LOWR LKE	1709	MRCDFLLS	2708	JAYBIRD1	3707	TAP 51
711	MIDDLTWN	1710	EXCHEQUR	2709	JAYBIRD2	3708	TAP 52
712	EGLE RCK	1711	POSO J1	2710	JONESFRK	3709	TAP 90
BUS	Name	Bus	Name	Bus	Name	Bus	Name
713	GUALALA	1712	POSO J2	2711	LOON LK	3710	OAKWIND
714	ANNAPOLS	1713	CANANDGA	2712	MCCLELLN	3711	VICTOR
715	FORT RSS	1714	BONITA	2713	PROCTER1	3712	VICTOR
716	SLMN JCT	1715	GLASS	2714	PROCTER2	3713	APPLEVAL
717	SLMN CRK	1716	BER VLLY	2715	PROCTER3	3714	AQUEDUCT
718	MONTE RO	1717	BRCEBG J	2716	PROCTER4	3715	HESPERIA
719	WOHLER	1718	SAXONCRK	2717	ROBBS PK	3716	PHELAN
720	WHLR JCT	1719	INDN FLT	2718	SRWTPA	3717	ROADWAY
721	WHLR TAP	1720	YOSEMITE	2719	SRWTPB	3718	SAVAGE
722	MIRABEL	1721	MADERA	2720	UNIONVLY	3719	AFG IND
723	MIRBELTP	1722	TRIGO	2721	WHITERK1	3720	BLKMTN
724	TRNTN JT	1723	TRIGO J	2722	WHITERK2	3721	PLEUSS
725	TRNTN_JC	1724	BORDEN	2723	UCDMC	3722	SOPPORT
726	MOLINO	1725	SJNO2	2724	STA. A 1	3723	COTNWD
727	MLNO JCT	1726	CASSIDY	2725	STA. A 2	3724	TAP601
728	GYSRVLL	1727	EL PECO	2726	STA. A 3	3725	TAP602
729	CLVRDLJT	1728	FIREBAGH	2727	STA. A 4	3726	TAP603
730	GYSR 1-2	1729	TOMATAK	2728	STA. A 5	3727	TAP604
731	GYSRJCT1	1730	MENDOTA	2729	STA. A 6	3728	TAP605
732	GYSRJCT2	1731	BIOMASS	2730	STA. B	3729	TAP606
733	FCHMNT2	1732	WRGHT PP	2731	SNMA TAP	3730	TAP607

734	FULTON	1733	PCHCO PP	2732	SNMALDFL	3731	TAP608
735	HDSBGTP2	1734	INTL TUR	2733	OREGNTRL	3732	PERMANTE
736	FTCH MTN	1735	ONLL PMP	2734	OREGNTRL	3733	GOLDHILS
737	HDSBGTP1	1736	L.BANS T	2735	BRKR TP	3734	CIMA
738	FTCHMTNP	1737	EXCHQUER	2736	BRKRJCT	3735	CIMA
739	LAGUNA	1738	KERCKHOF	2737	UCD_TP2	3736	TAP817
740	COTATI	1739	PNCHE 1T	2738	BRKR SLG	3737	KRAMER
741	LAGUNATP	1740	MERCED T	2739	DST1001A	3738	KRAMER
742	MCDWLLSW	1741	ONEILPMP	2740	DST1001B	3739	BLM E7G
743	PETLMA C	1742	MCSWAIN	2741	DIST1001	3740	BLM E8G
744	PETC_JCT	1743	MCSWAINJ	2742	WOODJCT	3741	BLM W9G
745	PETLMA A	1744	MERCEDFL	2743	CPEHRNTP	3742	BLM EAST
746	LAKEVLLE	1745	JRWCOGEN	2744	COLFAXJT	3743	BLM WEST
747	LKVLE JT	1746	BIO PWR	2745	ROLLNSTP	3744	BORAX I
748	DUNBAR	1747	N.FORK E	2746	SHADYGLN	3745	BSPHYD26
749	SANTA FE	1748	INT.TURB	2747	COLGATEA	3746	BSPHYD34
750	BEAR CAN	1749	KERCKHOF	2748	CHLLNGEA	3747	CALGEN1G
751	WEST FOR	1750	SAXNCK L	2749	TAMARACK	3748	CALGEN2G
752	GEYSR5-6	1751	KAMM	2750	CISCOTAP	3749	CALGEN3G
BUS	Name	Bus	Name	Bus	Name	Bus	Name
753	GEYSER78	1752	CANTUA	2751	CMNCHETP	3750	ALTA 1G
754	GEYSER11	1753	SCHINDLR	2752	BLLTAJCT	3751	ALTA 2G
755	GEYSER12	1754	KERCKHF1	2753	OXFRDJCT	3752	COLWATER
756	GEYSER13	1755	KERCKHF2	2754	WSTLDJCT	3753	COLWATER
757	GEYSER14	1756	WWARD JT	2755	WSTLD1RA	3754	ALTA31GT
758	GEYSER16	1757	CLOVIS-1	2756	LUISJCT	3755	ALTA 3ST
759	GEYSER17	1758	CLOVIS-2	2757	AUBERRY	3756	ALTA41GT
760	GEYSER18	1759	SANGER	2758	SJ2GEN	3757	ALTA 4ST

761	GEYSER20	1760	LASPALMS	2759	SJ3GEN	3758	CONTROL
762	MENDCNTR	1761	MC CALL	2760	SJNO3	3759	CONTROL
763	SMUDGE01	1762	MALAGA	2761	NRTHFORK	3760	OXBOW B
764	POTTRVLY	1763	RANCHRS	2762	PNEDLE	3761	CSA DIAB
765	GEO.ENGY	1764	PPG	2763	PNDLJ1	3762	CSA DIAB
766	INDIAN V	1765	GATES	2764	PNDLJ2	3763	HOLGATE
767	GA PACIF	1766	REEDLEY	2765	UAL TAP	3764	INYO
768	SONMA LF	1767	WAHTOKE	2766	GILROY	3765	INYO
769	WILDWOOD	1768	GERAWAN	2767	OBANION	3766	INYO PS
770	TRINITY	1769	KINGS J1	2768	SUTTER1	3767	INYOKERN
771	PANRAMA	1770	KINGS J2	2769	SUTTER2	3768	KERRGEN
772	MALACHA1	1771	KNGSCOGN	2770	SUTTER3	3769	KERRMGEE
773	MALACHA2	1772	DANISHCM	2771	SUTTER	3770	ALTA32GT
774	JESSTAP	1773	PIEDRA 1	2772	MTHOUSE	3771	ALTA42GT
775	SMPSN-AN	1774	PIEDRA 2	2773	MONTP TP	3772	LUZ LSP
776	COTWDPGE	1775	BALCH	2774	JMSN JCT	3773	LUZ8 G
777	JESSUPJ1	1776	KNGSRVR1	2775	GLDTRJC1	3774	LUZ9 G
778	SPI_AND	1777	CAL AVE	2776	FTHILTP2	3775	MC GEN
779	CASCADE	1778	WST FRSO	2777	FTHILTP1	3776	MC GEN
780	SLYCREEK	1779	BARTON	2778	GLDTRJC2	3777	MOGEN
781	WODLF TP	1780	MANCHSTR	2779	FRWAYTP	3778	MOGEN G
782	FRBSTNTP	1781	HERNDON	2780	BELDENTP	3779	NAVY II
783	OWID	1782	WOODWARD	2781	JAMESN-A	3780	NAVYII4G
784	TBLM JCT	1783	BULLARD	2782	TRAVIS	3781	NAVYII5G
785	WYANDTTE	1784	KINGSBRG	2783	TRVS_HPT	3782	NAVYII6G
786	PALERMO	1785	CORCORAN	2784	BRNSWKTP	3783	OXBOW G1
787	HONCUT	1786	CHLDHOSP	2785	N.HGN DM	3784	OXBOW A
788	CARIBOU	1787	GAURD J1	2786	FRGTNTP1	3785	SEARLES

789	GRIZ JCT	1788	GAURD J2	2787	FRGTNTP2	3786	SEGS2
790	BUTTVLLY	1789	GRDN GLS	2788	AVENATP1	3787	SEGS 1G
791	GRIZZLY1	1790	KCOGNJCT	2789	AVENATP2	3788	SEGS 2G
792	BIGBENTP	1791	ALPAUGH	2790	VLYHMTP1	3789	SUNGEN
BUS	Name	Bus	Name	Bus	Name	Bus	Name
793	NORD 1	1792	GRDNGLS2	2791	VLYHMTP2	3790	SUNGEN3G
794	CHICOTP2	1793	CONTADNA	2792	TCHRT_T1	3791	SUNGEN4G
795	SYCAMORE	1794	HENRETTA	2793	STAGG_6	3792	SUNGEN5G
796	BUTTE	1795	WESTLNDs	2794	QUEBECTP	3793	SUNGEN6G
797	CHICO B	1796	WISHON	2795	QUEBEC	3794	SUNGEN7G
798	TBLE MTN	1797	RIVERROC	2796	RAINBWTP	3795	TORTILLA
799	NDAME J	1798	HRDWK TP	2797	RAINBW	3796	OXBOW B
800	CHICOTP1	1799	HARDWICK	2798	DEXZEL	3797	TAP701
801	BIG BEND	1800	GUERNSEY	2799	SANPAULA	3798	TAP702
802	WYANDJT2	1801	GUR3TPT	2800	NUMI TAP	3799	TAP703
803	WYANDJT1	1802	COPPRMNE	2801	WESTRN_D	3800	TAP704
804	MC ARTHR	1803	BIOLA	2802	LP_JCT	3801	TAP705
805	GROUSCRK	1804	BOWLES	2803	RIODLLTP	3802	TAP709
806	TRINITY	1805	GIFFEN	2804	SCOTIATP	3803	ROCKET
807	DGLS CTY	1806	SAN JOQN	2805	SCTIATP2	3804	RANDBSRG
808	HAYFORK	1807	HELM	2806	FLTN JT2	3805	EDWARDS
809	LEWISTON	1808	AGRICO	2807	PIT5JT2	3806	SOUTHBAS
810	FRNCHGLH	1809	TVY VLLY	2808	ELKCRKJT	3807	GALE
811	KESWICK	1810	KEARNEY	2809	KANAKAJT	3808	SHERWIN
812	BENTON	1811	OLDKERN	2810	TYLERJT	3809	TIEFORT
813	GIRVAN	1812	KERMAN	2811	CATLETJT	3810	DUNNSIDE
814	ANDERSON	1813	SANGER	2812	GLEAF2TP	3811	RUSH
815	WNTU PMS	1814	PARLIER	2813	SFWY_TP1	3812	LEE VINE

816	LOMS JCT	1815	REEDLEY	2814	SFWY_TP2	3813	BAKER
817	CASCADE	1816	DNUBAJCT	2815	OWENSTP1	3814	MTN PASS
818	STLLWATR	1817	AUBRYTP	2816	OWENSTP2	3815	LUZ8
819	MTN GATE	1818	DUNLAP	2817	AEC_TP1	3816	LUZ9
820	ANTLER	1819	STCRRL J	2818	AEC_TP2	3817	NAVYCOSO
821	PPL	1820	STONCRRL	2819	AEC_JCT	3818	CAL GEN
822	WHITMORE	1821	DINUBA	2820	AEC_300	3819	RUSH
823	TKO TAP	1822	OROSI	2821	TCHRT_T2	3820	POOLUWD
824	OLSEN JT	1823	CAMDEN	2822	TCHRTJCT	3821	SEARLES
825	CEDR CRK	1824	CMDN JCT	2823	AMFOR_SW	3822	CSA DIAB
826	CLOV TAP	1825	CARUTHRS	2824	TERMNS J	3823	DEVERS
827	DESCHUTS	1826	MUSLSLGH	2825	STAGG JT	3824	DEVERS T
828	COWCK TP	1827	LEPRINO	2826	N.ST_SW	3825	devers i
829	VOLTA	1828	LEMOORE	2827	LOUISJCT	3826	DEVERS
830	SOUTH	1829	LPRNO TP	2828	LMECCT2	3827	DEVERS
831	KILARC	1830	HNFRD SW	2829	LMECCT1	3828	MIRAGE
832	INSKIP	1831	CANDLEWK	2830	LMECST1	3829	MIRAGE
BUS	Name	Bus	Name	Bus	Name	Bus	Name
833	COLEMAN	1832	ORSI JCT	2831	LMEC	3830	TAP801
834	CLMN TAP	1833	SANDCRK	2832	BEALE2J1	3831	YUCCA
835	COTTONWD	1834	CORCORAN	2833	BEALE1J1	3832	HI DESER
836	CLMN JCT	1835	BSWLL TP	2834	WHTLND1	3833	TAP802
837	RED B JT	1836	ARMSTRNG	2835	TCY MP1	3834	TAP804
838	RED BLFF	1837	RESERVE	2836	CORNSWCH	3835	BANNING
839	TYLER	1838	ANGIOLA	2837	CAPAYJCT	3836	GARNET
840	DIRYVLE	1839	BOSWELL	2838	CAPYSWCH	3837	SANTA RO
841	RWSN J2	1840	HENRITTA	2839	DELEVAN	3838	EISENHOW
842	LP FB SP	1841	JCBSCRNR	2840	DEC PTSG	3839	FARREL

843	GERBER	1842	TLRE LKE	2841	DEC STG1	3840	CONCHO
844	LS MLNSJ	1843	AVENAL	2842	DEC CTG1	3841	THORNHIL
845	LS ML JT	1844	KETTLEMN	2843	DEC CTG2	3842	TAMARISK
846	VINA	1845	CHEVPLIN	2844	DEC CTG3	3843	INDIAN W
847	GRBR JCT	1846	GATES	2845	HIWD TAP	3844	TAP805
848	CORNING	1847	GATS2_TP	2846	HIGHWNDS	3845	CARODEAN
849	PIT 1	1848	AMSTG SW	2847	DUKE ML1	3846	INDIGO
850	HAT CRK1	1849	STRD JCT	2848	DUKMOSS1	3847	TAP821
851	HAT CRK2	1850	HURON	2849	DUKMOSS2	3848	DEVERS2T
852	HT CRKRG	1851	CALFLAX	2850	DUKMOSS3	3849	TAP820
853	BURNEY	1852	SCHLNDLR	2851	DUKMOSS4	3850	MARASCHI
854	BURNEYQF	1853	STROUD	2852	DUKMOSS5	3851	devers2i
855	TRES VIS	1854	PLSNTVLY	2853	DUKMOSS6	3852	MIRAGE E
856	PEACHTON	1855	VLY NTRN	2854	DUKE ML2	3853	BANWIND
857	BIGGSJCT	1856	COLNGA 2	2855	WALNT115	3854	VSTA
858	KLLY RDE	1857	TORNADO	2856	AUGUST	3855	VSTA
859	ELGN JCT	1858	COLNGA 1	2857	CRD_INTR	3856	VSTA
860	OROENEGY	1859	KNGLOBUS	2858	SLD ENRG	3857	HIGROVE
861	OROVILLE	1860	JACALITO	2859	NEO REDT	3858	RVCANAL1
862	LSNA PCC	1861	BDGR HLL	2860	NEO REDB	3859	RVCANAL2
863	APT ORVC	1862	ARCO	2861	CACHSTAP	3860	RVCANAL3
864	PALERMO	1863	DEVLS DN	2862	DIXON-J1	3861	RVCANAL4
865	BANGOR	1864	HELMS 1	2863	MAINE-PR	3862	PEPPER
866	DOBBINS	1865	HELMS 2	2864	BTAV-JCT	3863	CAL ELEC
867	CHALLNGE	1866	HELMS 3	2865	UCDAVSJ1	3864	HOMART
868	WESTWOOD	1867	AGRICO	2866	MAXTAP	3865	SHANDIN
869	HATLOSCK	1868	HAAS	2867	CHWCGN	3866	SANBRDNO
870	ULTR WSD	1869	BLCH 2-2	2868	CHOWCOGN	3867	MTNVIEW1

871	CHESTER	1870	BLCH 2-3	2869	TCY TER1	3868	MTNVIEW2
872	HMLTN BR	1871	KINGSRIV	2870	TCY MP2	3869	TAP902
BUS	Name	Bus	Name	Bus	Name	Bus	Name
873	BIG MDWS	1872	MCCALL1T	2871	TESLA 6M	3870	TAP901
874	HOWELLS	1873	MCCALL2T	2872	BOLLMAN	3871	MNTVIEW
875	GRS F JT	1874	MCCALL3T	2873	IMHOFF	3872	MNTV-CT1
876	GRYS FLT	1875	GATES 1T	2874	PEASETP	3873	MNTV-CT2
877	GANSNER	1876	BALCH 1	2875	STAGG-H	3874	MNTV-ST1
878	SPANSHCK	1877	HERNDN1T	2876	STAGG-F	3875	MNTV-CT3
879	EST QNCY	1878	HERNDN2T	2877	STAGG-D	3876	MNTV-CT4
880	SPI	1879	FRIANTDM	2878	STAGG-E	3877	MNTV-ST2
881	ELIZ TWN	1880	ULTR.PWR	2879	STAGG-J2	3878	DEVRSVC1
882	CARIBOU	1881	KINGSBUR	2880	DG_PAN1	3879	GOODRICH
883	DE SABLA	1882	SANGERCO	2881	GWF_GT1	3880	GOODRICH
884	BTTE CRK	1883	DINUBA E	2882	GWF_GT2	3881	LEWIS
885	CNTRVLLE	1884	GWF-PWR.	2883	GWF_HENR	3882	LEWIS
886	MCNE JCT	1885	CHV.COAL	2884	GWF_HEP1	3883	ANAHEIMG
887	CLARK RD	1886	COLNGAGN	2885	GWF_HEP2	3884	EAGLEMTN
888	DRHM JCA	1887	WISHON	2886	GWF_HEP	3885	GENE
889	CHICO A	1888	SMYRNA	2887	MADERA_G	3886	GENE BK1
890	BUTTE	1889	GOSE LKE	2888	WHD_GAT2	3887	GENE BK2
891	DRHM JCB	1890	SEMITRPC	2889	WHD_PAN2	3888	IRON MTN
892	ESQUON	1891	WSCOPRSN	2890	NRS 400	3889	J.HINDS
893	TBLE MTN	1892	SMTRPCWS	2891	LEPRNOFD	3890	GENE69 N
894	GLENN	1893	WESTPARK	2892	DRHMSW45	3891	GENE69 S
895	ORLND JT	1894	MCKIBBEN	2893	YCEC	3892	INTK69 N
896	ORLAND B	1895	CHARKA	2894	THM JCT2	3893	INTK69 S

897	ORL B JT	1896	FAMOSO	2895	COVERDTP	3894	EAGLEMP1
898	ELKCREEK	1897	LERDO	2896	MALACHA2	3895	EAGLEMP2
899	WILLOWS	1898	LRDO JCT	2897	CANAL TP	3896	GENE P1
900	CAPAY	1899	KERN OIL	2898	HORSHE1	3897	GENE P2
901	HMLTN JT	1900	DSCVRYTP	2899	FLINT2	3898	INTAKEP1
902	HAMILTON	1901	RASMUSEN	2900	NEWCSL1	3899	INTAKEP2
903	HEADGATE	1902	KRN OL J	2901	WEBER016	3900	IRONMTP1
904	ANITA	1903	PTRL JCT	2902	PITSBG D	3901	IRONMTP2
905	JACINTO	1904	LIVE OAK	2903	SRGNT JT	3902	JHINDSP1
906	TB MT 1T	1905	PSE-3	2904	K1-JCT	3903	JHINDSP2
907	TBL MT3T	1906	COLUMBUS	2905	RDGCT4	3904	ETI MWD
908	MALCHA	1907	BEAR TAP	2906	LS ESTRS	3905	ETI MWDC
909	PIT 4	1908	MAGUDN J	2907	LS ESTRS	3906	ESRP MWD
910	JBBLACK1	1909	MAGUNDEN	2908	ELKHIL_G	3907	ESRP P1
911	JBBLACK2	1910	GRIMWAYJ	2909	ELKHIL1G	3908	ESRP P2
912	PIT 6 U1	1911	BOLTHSE	2910	ELKHIL2G	3909	ESRP P3
BUS	Name	Bus	Name	Bus	Name	Bus	Name
913	PIT 6 U2	1912	GRIMWAY	2911	ELKHIL3G	3910	HARBORG4
914	PIT 7 U1	1913	STOCKDLE	2912	WOODMID2	3911	HARBOR13
915	PIT 7 U2	1914	SEMITRPJ	2913	GWFTTRACY	3912	DVLCYN12
916	BUTTVLLY	1915	GODN_BER	2914	GWFTRCY1	3913	DVLCYN34
917	CRBU 4-5	1916	GANSO	2915	GWFTRCY2	3914	DVLCYN3G
918	BELDEN	1917	TUPMAN	2916	TESLA C	3915	DVLCYN4G
919	ROCK CK1	1918	KERN PWR	2917	ELDRADO1	3916	EDMON1AP
920	ROCK CK2	1919	TEVIS	2918	ELDRADO2	3917	EDMON2AP
921	POE 1	1920	WHEELER	2919	DG_VADIX	3918	EDMON3AP
922	POE 2	1921	LAMONT	2920	ELPT_SJ1	3919	EDMON4AP
923	WOODLEAF	1922	RIO BRVO	2921	ELPT_SJ2	3920	EDMON5AP

924	RD MT 1T	1923	RENFRO	2922	waksha j	3921	EDMON6AP
925	BRNYFRST	1924	KRNSHRT1	2923	NATOMAS	3922	EDMON7AP
926	SMPSN-AN	1925	KRNSHRT2	2924	NATOMAS	3923	EDMON8AP
927	PIT 3	1926	SHAFTER	2925	COSUMNE1	3924	EDMONSTN
928	PIT 5 U1	1927	KERN 1 M	2926	COSUMNE1	3925	OSO A P
929	PIT 5 U2	1928	KERN 2 M	2927	COSUMNE2	3926	OSO B P
930	CRBOU2-3	1929	MIDWAY	2928	COSUMNE3	3927	PEARBLSM
931	CRBU 1	1930	RIOBRVTM	2929	FRUTLDJT	3928	PEARBMAP
932	CRESTA	1931	MIDKRNJN	2930	FTSWRDJT	3929	PEARBMBP
933	FORBSTWN	1932	TAFT	2931	KCTYPKER	3930	PEARBMCP
934	PIT 1 U1	1933	FELLOWS	2932	VACA-CB	3931	PEARBMDP
935	BCKS CRK	1934	CYMRIC	2933	CHICO JT	3932	OSO
936	VOLTA1-2	1935	TEXCO_NM	2934	ANTLP JC	3933	TAP806
937	SOUTH G	1936	TEXCO_NM	2935	TX-LOST	3934	TAP807
938	KILRC1-2	1937	CAWELO C	2936	RASMSNTP	3935	TAP808
939	HAMIL.BR	1938	UNIVRSTY	2937	DISCOVER	3936	TAP809
940	SLY.CR.	1939	NORCO	2938	CALWATER	3937	TAP811
941	KELLYRDG	1940	COLESLEV	2939	CALWTRTP	3938	TAP812
942	TOAD TWN	1941	KERNRDGE	2940	BEAR MTN	3939	TAP813
943	CNTRVL12	1942	TEMBLOR	2941	LARKIN 1	3940	TAP814
944	BLCKBUTT	1943	CARRIZO	2942	LARKIN 2	3941	TERAWND
945	CSC HYDR	1944	KERNWATR	2943	HALE2	3942	CAPWIND
946	HATCHET+	1945	MORGAN	2944	UNIVRSTY	3943	BUCKWND
947	CEDR FL+	1946	MIDSET	2945	WFRES J2	3944	ALTWIND
948	WEBR FL+	1947	BELRIDGE	2946	NORCO_TA	3945	RENWIND
949	OLSEN +4	1948	ARVIN_ED	2947	SEMI_TAP	3946	TRANWND
950	DEADWOOD	1949	ROSEDAL	2948	SNTAMRTP	3947	SEAWIND
951	HATLOST+	1950	TX_ROSDL	2949	UNOCAL2	3948	PANAERO

952	FORKBUTT	1951	POSO MT	2950	SHELLJ1	3949	TAP816
BUS	Name	Bus	Name	Bus	Name	Bus	Name
953	CLOVER	1952	VEDDER	2951	SHELLJ2	3950	TAP819
954	SPI-BURN	1953	FRITO LY	2952	NDUBLIN	3951	TAP818
955	SPI-HAYF	1954	WESTPLAT	2953	SNTH TP1	3952	VENWIND
956	PAC.ENGY	1955	NAVY 35R	2954	SNTH TP2	3953	SANWIND
957	OROVLE	1956	BLACKWLL	2955	SNTH JCT	3954	ALAMO SC
958	PO POWER	1957	CARNERAS	2956	LAMBIE	3955	DVLCYN1G
959	PE.WWOOD	1958	CELERON	2957	LAMBGT1	3956	DVLCYN2G
960	COLLINS	1959	MCKTTRCK	2958	GOOSEHGT	3957	MHV SPHN
961	SPI-QUCY	1960	NORTHMWY	2959	CREEDGT1	3958	WARNE1
962	DE SABL A	1961	MDWY_P_S	2960	FREC TAP	3959	WARNE2
963	GRIZZLYG	1962	TAFT A	2961	FREC	3960	ALAMO SC
964	HAT CRK1	1963	TAFT A_J	2962	CAL MEC	3961	VIEJOSC
965	HAT CRK2	1964	MARICOPA	2963	MEC CTG1	3962	VIEJO66
966	COLEMAN	1965	MOCO_JCT	2964	MEC CTG2	3963	MIRALOME
967	INSKIP	1966	GARDNER	2965	MEC STG1	3964	TAP998
968	CORTINA	1967	BRY_PTLM	2966	GILROYTP	3965	HIDEDST1
969	PUTH CRK	1968	BSCL_PLD	2967	GILROYPK	3966	HIDEDCT3
970	AMERIGAS	1969	COPUS	2968	GROYPKR1	3967	HIDEDCT2
971	CORDELLT	1970	TEMBLOR	2969	GROYPKR2	3968	HIDEDCT1
972	CORDELIA	1971	LAKEVIEW	2970	GROYPKR3	3969	ELLWOOD
973	MOBILCHE	1972	WHEELER	2971	RVECTP	3970	PASADNA1
974	WDLND_BM	1973	TEJON	2972	RVEC	3971	PASADNA2
975	KNIGHT2	1974	SN BRNRD	2973	RVEC_GEN	3972	BRODWYSC
976	WODLNDJ1	1975	SAN EMDO	2974	COSUMNE4	3973	LAKEGEN
977	WODLNDJ2	1976	MAGNDN J	2975	COSUMNE5	3974	WINTEC6
978	ZAMORA2	1977	ARVIN	2976	COSUMNE6	3975	WINTEC6

979	WOODLD	1978	WEEDPTCH	2977	MINNIEAR	3976	WINTEC4
980	ZAMORA	1979	KRN CNYN	2978	BANGS	3977	PSTRIA
981	MADISON	1980	RIOBRVQF	2979	TX-LOSTH	3978	PSTRIAG1
982	POST	1981	BAKRSFLD	2980	WEC	3979	PSTRIAG2
983	DPWT_TP2	1982	EISEN	2981	WOLFSKIL	3980	PSTRIAS1
984	DPWTR_TP	1983	MAGUNDEN	2982	LAMMERS	3981	PSTRIAG3
985	UCD_TP1	1984	OLD RIVR	2983	SANGR3T	3982	PSTRIAS2
986	BRIGHTN	1985	PANAMA	2984	CP LECEF	3983	SEAWEST
987	W.SCRMNO	1986	CARNATIO	2985	LECEFTAP	3984	WHITEWTR
988	DEEPWATR	1987	GRMWY_SM	2986	LECEFGT1	3985	WINTEC8
989	DAVIS	1988	WELLFILD	2987	LECEFGT2	3986	WINTECX2
990	HUNT	1989	KERN PW1	2988	LECEFGT3	3987	WINTECX1
991	GRAND IS	1990	MOCO	2989	LECEFGT4	3988	ALTAMSA4
992	HALE J1	1991	CADET	2990	FT_BRGD1	3989	CABAZON
BUS	Name	Bus	Name	Bus	Name	Bus	Name
993	SCHMLBCH	1992	KERN PW2	2991	FT_BRGD2	3990	MIDWIND
994	VACA-DIX	1993	TX_BV_HL	2992	ELK_D	3991	SOUTHWND
995	VACAVLL1	1994	ELK HLLS	2993	PHILO_D	3992	NORTHWND
996	VACAVLL2	1995	KRN OL J	2994	PNT_AREN	3993	ZONDWND1
997	VCVLE2J	1996	FAMOSO	2995	GYSR78TP	3994	ZONDWND2
998	VCVLE1J	1997	CAWELO B	2996	G9CRT2_9	3995	BREEZE1
999	SUISUN	1998	MC FRLND	2997	KCTY_TAP	3996	BREEZE2